The Association of Professional Women Engineers of Nigeria

APWEN

JOURNAL OF ENGINEERING, SCIENCE AND TECHNOLOGY

Volume 6, Issue 1 – December 2022

ISSN: 2714-2396

https://www.apwen.org/apwen-journal

APWEN Journal of Engineering, Science, and Technology

Volume 6, Issue 1. 2022

Publication of the Association of Professional Women Engineers of Nigeria

Managing Editor: Engr. Adiat Ibironke Arogundade Ph.D MNSE
adiat.arogundade@uniabuja.edu.ng

Editor-in-Chief: Engr. Yetunde M. Aladeitan Ph.D FNSE
technical-secretary@apwen.org

APWEN PRESIDENT: Engr. Elizabeth Etherigho Ph.D FNSE
elizabeth.eterigho@apwen.org

APWEN JOURNAL EDITORIAL BOARD

APWEN JOURNAL EDITORIAL ADVISORY BOARD

ISSN: 2714-2396

Published by APWEN Journals,
SUITE 5, GROUND FLOOR, NATIONAL ENGINEERING CENTER,
1, ENGINEERING CLOSE, OFF IDOWU TAYLOR STREET,
VICTORIA ISLAND LAGOS

Printed by APWEN Press

Journal of Engineering, Science, and Technology
ISSN: 2714-2396 | Volume 6, Issue 1

Table of Content of Published Articles

Journal of Engineering, Science, and Technology
ISSN: 2714-2396 | Volume 6, Issue 1

Green synthesis of zinc oxide nanoparticles (ZnONPs) from cassava leaf (Manihot *esculenta*) and its application as a corrosion inhibitor for mild steel in 1M hydrochloric acid

A.O. Okewale[1] and B.H Akpeji[2]
Department of Chemical Engineering, Federal University of Petroleum Resources, PMB 1221, Effurun, Delta State, Nigeria.[2]Department of Chemistry, Federal University of Petroleum Resources, PMB 1221, Effurun, Delta State, Nigeria.
Corresponding author: A.O.Okewale, Department of Chemical Engineering, Federal University of Petroleum Resources,Okewale.akindele@fupre.edu.ng Tel: +2348069365637

Abstract
Corrosion inhibition behaviour of metallic and semiconductor of Zinc Oxide Nanoparticles ZnONPs synthesized through biological means has been extensively reported. This work focuses on the synthesis of zinc oxide nanoparticles from cassava leaf (CL-ZnONPs) and has investigated its efficiency as corrosion inhibitor on mild steel in 1M HCl. The optical and structural properties of the resulting zinc oxide nanoparticles were studied using; UV-visible spectroscopy, Tauc's plot and Fourier transform Infrared spectroscopy (FTIR). The UV–Vis spectra of the zinc oxide nanoparticles showed typical absorption peaks around 371nm due to its large excitation binding energy at room temperature. The FTIR spectra affirmed the presence of –OH, C=C, N=C=S, and C=O functional groups.Gravimetric method was used to study the mild steel corrosion process with a view to evaluating inhibition efficiency of the zinc oxide nanoparticles in 1M HCl. The effects of inhibitor concentration and immersion time were studied at 303 K. The results showed that the efficiency of inhibition increased with immersion time but decreased with inhibitor concentration. The maximum inhibition efficiency was obtained at 120hours (t_{max}) with inhibitor concentration of 100ppm. It was revealed that the mild steel surface is susceptible to acidic corrosion, thus, an increase inconcentration of inhibitor and immersion time significantly influenced the pattern of corrosion.
Keywords: Nanoparticles, CL-ZnO NPs, Cassava Leaf (*Manihot esculenta*), Bio-synthesis, Inhibition efficiency.

Introduction
Recent advancements have been utterly significant in refining, development and implementation of techniques and strategies in metal corrosion management. Nanotechnology has as well ushered in a supporting, innovative and technological standpoint in this regard. In general, nanotechnology involves the atomic manipulation of matter to synthesize new structures, materials, systems, catalysts and devices that show new phenomena and characteristics. Nanotechnology offers the possibility of enhancing the inherent corrosion resistance, extending service life, reducing downtimes and overall performance of process equipment in ways that are cost effective and environmentally benign.
Nanoparticles have been the main focus of the majority of research into nanotechnology, which is largely due to the ease at which they can be prepared and manipulated [1], described the nanoparticle as being capable of bridging the gap between bulk materials and atomic or molecular structures. [2], defined the nanoscale as a theurgic point on the dimensional scale, where the properties of a material in the nanoscale would grossly deviate from that of those

materials at larger scales. [3], proposed the "quantum size effect" as a phenomenon created by the enhanced ratio of surface area to volume of particles as they exist in nanoscale. [4], noted that the enhanced ratio of surface area to volume, interfacial and surface chemistry were capable of giving materials in nanoscale more advantage in chemical reactions such as in catalysis.
According to [5], the physical and chemical methods of nanoparticle synthesis were very much conventional; yet, both methods came with a number of limitations such as the use of toxic compounds, highly endothermic reactions with a high demand for pressure and time as well. [6], in a study explained that the ability to transform inorganic metal ions to metal nanoparticles in biological organisms including humans was possible via the reductive capabilities of the proteins and metabolites present in the organisms. Although, they argued that using plants as a source of nanoparticle synthesis was of an advantage over other biological systems, as plants are readily available with a less tedious and cost effective biogenic synthesis procedure.Metal and metal oxide nanoparticles tend to exhibit interesting chemical properties due to their particle size and surface density. Physical, chemical and biological methods in the synthesis of nanostructured oxides all considers ZnO NPS to exhibit wide band gap (~3.4eV) and large exciton binding energy (60meV) which is responsible for wide range of applications especially in; nano-optoelectronics, transistors, nano-piezoelectronics, sensors and UV-detection. It is on this background that the authors were motivated to synthesize the zinc oxide cassava leaf nanoparticles and also tested its corrosion inhibition potential on mild steel surface in acidic medium with a view to establishing the mode of adsorption process, and its thermodynamic parameter at 303 K.

Materials and Methods

Reagents

Cassava Leaves (*Manihot esculenta*), Zinc Acetate dihydrate, Sodium Hydroxide, Hydrochloric acid, Ethanol, Acetone.

Materials

Mild steel, Whatman filter paper,magnetic stirrers, test tubes, petri-dishes, silicon carbide abrasive paper of various grit sizes, analytical weighing balance($\pm 0.0001\ g$ accuracy), beakers with sizes between 100-1000ml holding capacity, desiccators, centrifuge, industrial blender,and drying oven (LD-201-E Vision Scientific).The Coupons were dimension into 40 mm × 20 mm × 2 mm and cleaned with abrasive paper. A hole of 0.1 cm was drilled on each of the coupon before polishing so as to help in its suspension in acid medium.

Method

2.1 Extraction and Phytochemical Screening of Cassava Leaf

The procedure of extraction and phytochemical screening was performed in accordance with the processes laid out by [7; 8]. The screening of the extract was carried out to identify the main groups of active chemical constituents present in the extract by their colour reaction. The presence of saponins, alkaloids, terpenes, flavonoids, glycosides, reducing sugars and tannins were tested for by simple qualitative and quantitative methods.

2.2 Green synthesis of ZnONPs from Cassava Leaf (*Manihot esculenta)*

2.2.1 Preparation of Plant Extract

The Cassava (*M. esculenta*) leaves were collected from farmers within Iterigbi community in Delta State, Nigeria. The leaves were washed several times with double distilled water to remove any debris or particulates carried along during collection of leaves and then air-dried at room temperature for 72 hours. The Cassava leaves were afterwards pulverized with a standard electric blender and sieved using a Laboratory Test sieve with aperture of 600microns. Dried pulverized leaves of 2g was used in preparing the aqueous extract in 500 ml distilled water and heated at 80 °C for about 1hr. The extracting mixture displayed a colour change in its aqueous solution from watery to yellow. The extract was separated by filtration, using the Whatman^{TM} filter paper and stored in Polyethylene Terephthalate (PET) bottles in order to be used for further synthesis of ZnO nanoparticles.

2.2.2 Preparation of 0.01M Zinc Acetate

The analytical grade Zinc Acetate used in this synthesis was procured from Rovet Scientific Laboratories Benin, Nigeria. 0.01M solution of Zinc Acetate ($Zn(CH3COO)_2.2H_2O$) was prepared by the dissolution of 2.195g Zinc Acetate in 1000ml distilled water.

2.2.3 Preparation of 1M NaOH

Similarly, 1M solution of Sodium Hydroxide (NaOH) was prepared by weighing 40g of NaOH pellets and subsequently dissolved in 1000 ml distilled water.

2.2.4 Preparation of 1M HCI

The molar strength of HCl stock was determined using equation 1 below;

$$Molar\ strength\ of\ HCl\ stock = \frac{Percentage\ purity\ of\ HCl \times Specific\ gravity\ of\ HCl \times 10}{Molecular\ Weight\ of\ HCl} \quad (1)$$

Where percentage purity of HCl = 37 %, specific gravity of HCl = 1.08 g/cm^3, and molecular weight of HCl = 36.46 g/mol. Inserting these values in equation (1) above the resulting molar strength value of 11.269 M was obtained. Making use of serial dilution formula as indicated in equation (2) below;

$$C_1V_1 = C_2V_2 \quad (2)$$

Where, C_1 = Concentration of stock HCl (11.269 M), V_1 = Volume required from the stock, C_2 = Concentration required for preparation (1 M), and V_2 is the volume required for preparation of 1 M which is 1 L or 1000 mL. Therefore, 88.7 mL of HCl was measured from the stock bottle and was poured into 1000 mL volumetric flask previously containing some quantity of distilled water. After which, the solution was made up to the mark with distilled water.

2.2.5 Synthesis of Zinc Oxide Nps from Cassava Leaf (GLZnONps)

The procedure of extraction and synthesis was in accordance to the methods of [9, 10] with slight modifications.In this synthesis procedure, 50ml of the aqueous extract of Cassava leaves (*M. esculenta*) and 100ml of 0.01M zinc acetate solution were mixed together with 25ml of 1M NaOH solution that was added drop-wise. The resulting mixture was then mixed by continuously stirring on a magnetic stirrer at a temperature of 70^{o}C for 3hours. During this reaction time, the colour of the colloidal solution gradually changed from yellow to a cream-coloured solution which suggest an increased rate of bio-reduction of the Zinc Acetate and the formation of Zinc Hydroxide ($Zn(OH)_2$) precipitate.

2.2.6 Purification of ZnO Nps

The $Zn(OH)_2$ formed as precipitate was purified by washing with distilled water and then centrifuged at 5000rpm. The supernatant formed was discarded leaving a pure white precipitate of ZnO NPs which was dried in an LD-201-E Vision Scientific Drying oven at 70°C for 2hrs in order to obtain the desired ZnO Nanoparticles. The procedures are summarized below using a process flow diagram as depicted in Figure 1.

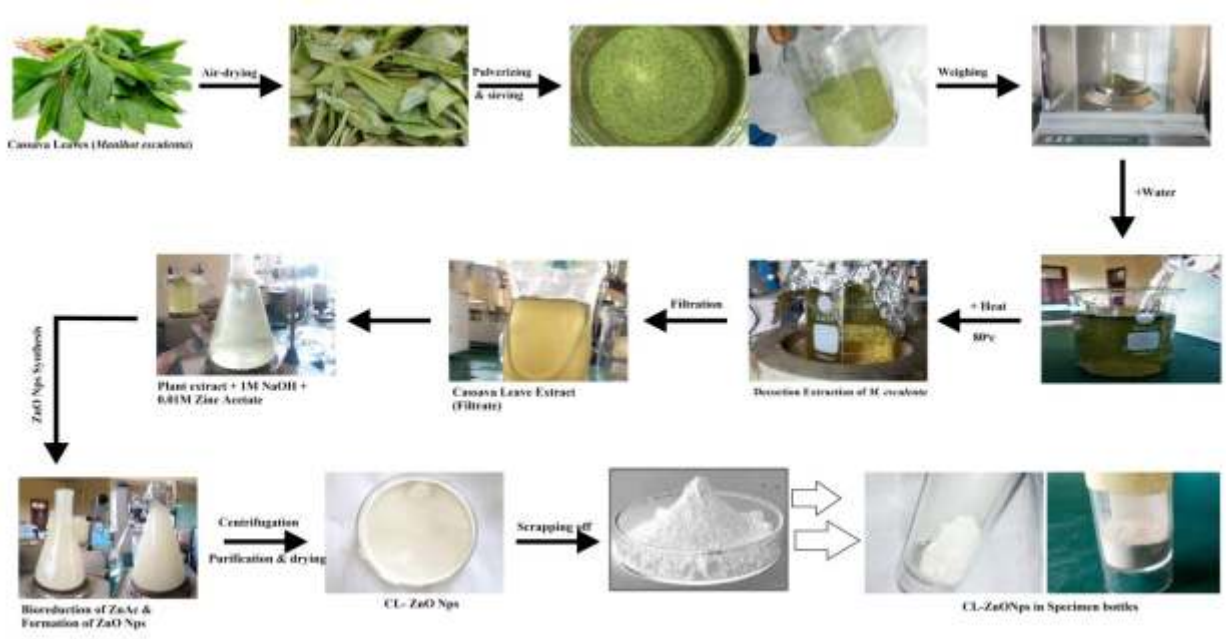

Figure 1: Process flow diagram for the synthesis of Zno nanoparticle from cassava leaf

2.2.7 Corrosion Weight Loss Method

Weight loss measurements were applied to evaluate the efficiency of the synthesized Nano particle (inhibitor), both in the presence and absence of different concentrations of ZnO-NPs. The mild steel metal were immersed for a total of 120hours, with each setup containing 100ppm, 200ppm, 300ppm and a blank (control) removed and weighed after every 24hours to ascertain the subsequent weight loss of the metal. The experimental setup was designed to test the corrosion inhibitory potentials of ZnO NPs from day1 to day5, at 303K.

Results and Discussion

3.1 UV-Vis Spectroscopy

The optical absorption of the ZnONPs as shown in Figure 2 was monitored using UV-Vis spectroscopy. The band was observed between 320 – 500nm of wavelengths, identified as the surface plasmon resonance band. The shape of the band indicated a uniform scattering of the zinc oxide nanoparticles due to the excitation of valence electrons within the nanomaterial. The absorption peak was observed at 371nm [1, 11] reported similar results in their findings.

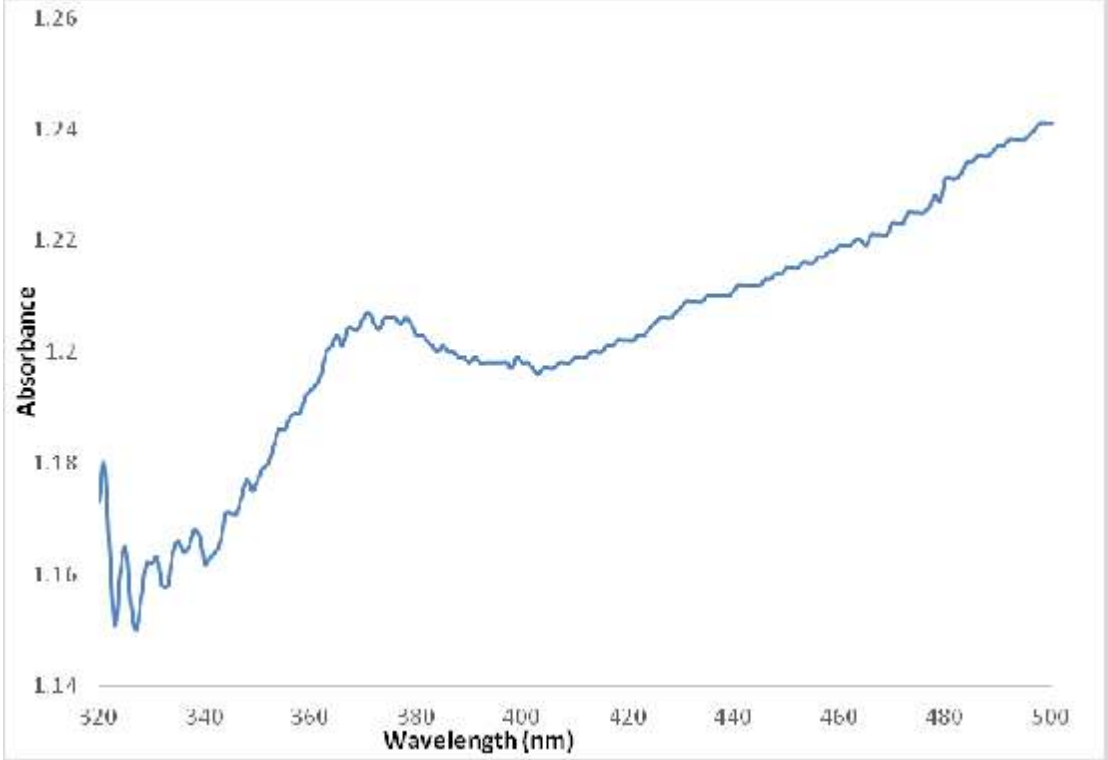

Figure 2: UV-Vis Spectroscopy of CLZnO Nps

3.2 Tauc's Plot (Energy band gap)

The band energy of the synthesized zinc oxide nanoparticle (ZnO NPs) was obtained at E_g=3.3 eV as shown in Figure 3. This provides information about electronic transitions occurring in the material. For semiconductors,the band gap in the absorption spectrum corresponds to the point at which absorption begins to increase from the baseline, since this indicates the minimum amount of energy required for a photon to excite an electron across the band gap and thus be absorbed in the semiconductor material [12]. Fitting a tangent would depend on the shape of the absorption spectrum and according to [12], the procedure is often subjective and may result in error with significant value. Since spectra are typically reported in units corresponding to the wavelength of light rather than its energy, the conversion between wavelength (nm) and band gap energy (eV) units was achieved by the equations 3 – 5 below: [13]

$$\alpha h\nu \; \alpha \; (h\nu - E_g)^n \qquad (3)$$

For direct transition where $n = \frac{1}{2}$

Thus;

$$(\alpha h\nu)^2 = (2.303 \times Abs \times E_g) \qquad (4)$$

Where; Abs = Absorbance and E_g= Band Energy, is given as equation 3;

$$E_g = \frac{hc}{\lambda} = \frac{1239.8}{\lambda}(eV \times nm) \qquad (5)$$

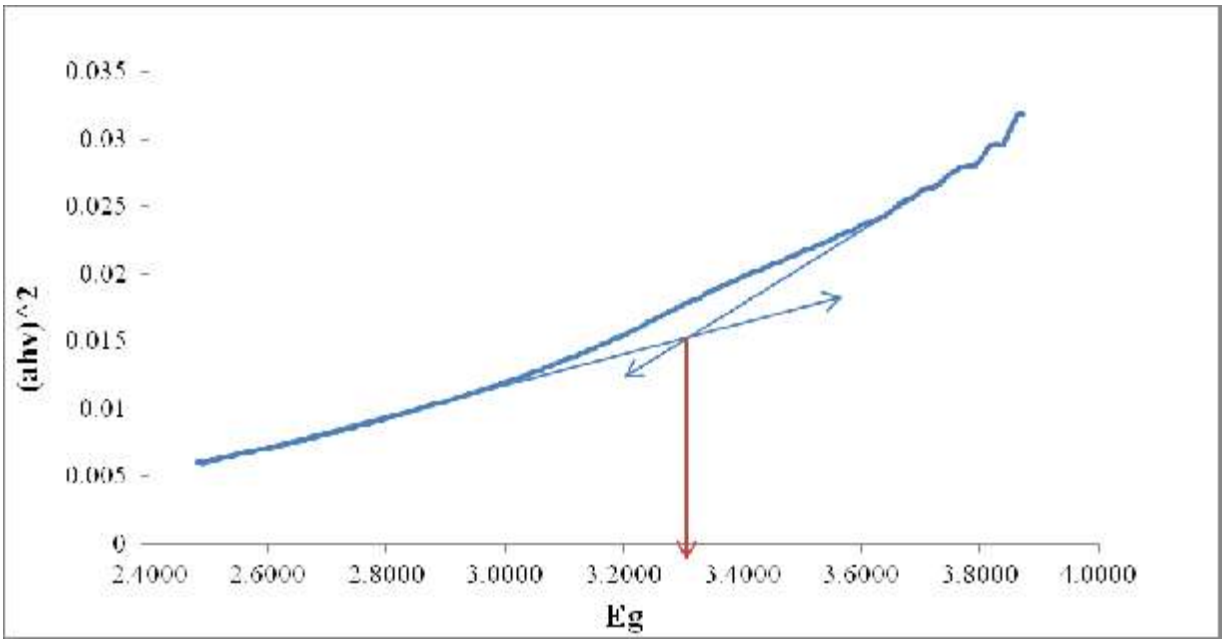

Figure 3: Tauc's plot for CI-ZnO Nps

3.3 Fourier Transform Infra-red Analysis (FTIR)

Figure 4 depict the FTIR result of the ZnONPs. This FTIR gives information on the vibration and rotational modes of motion of a molecule in line with the functional group present in the material and hence an important technique for identification and characterization of a substance. Absorptionpeak 1408.9 cm^{-1} which falls within the range of 1100 - 1600 cm^{-1}indicates Zn – OH bending mode thus corroborating the work of [14]. The peaks of absorption revealed at this wavelength 3380.8cm^{-1}, and 1982.98cm^{-1} showed the presence of –OH, and C=O functional group respectively. The broad band at 2109.7 cm^{-1} indicates bioactive thiamine N=C=S, while the region in the band 1640 cm^{-1} is due to the presence of C=N and C=O bonds.These functional groups indicated are relevant to corrosion inhibitor in the corrosion chemistry. In the work of [15], 756 and 431 cm^{-1} broad bands were used to indicate the presence of Zinc oxide nanoparticle but the band region 890.8 cm^{-1} observed suggest as well the presence of Zinc oxide nanoparticle formation since this value is closer to 887 cm^{-1} reported by [16], as ZnO absorption stretching mode.

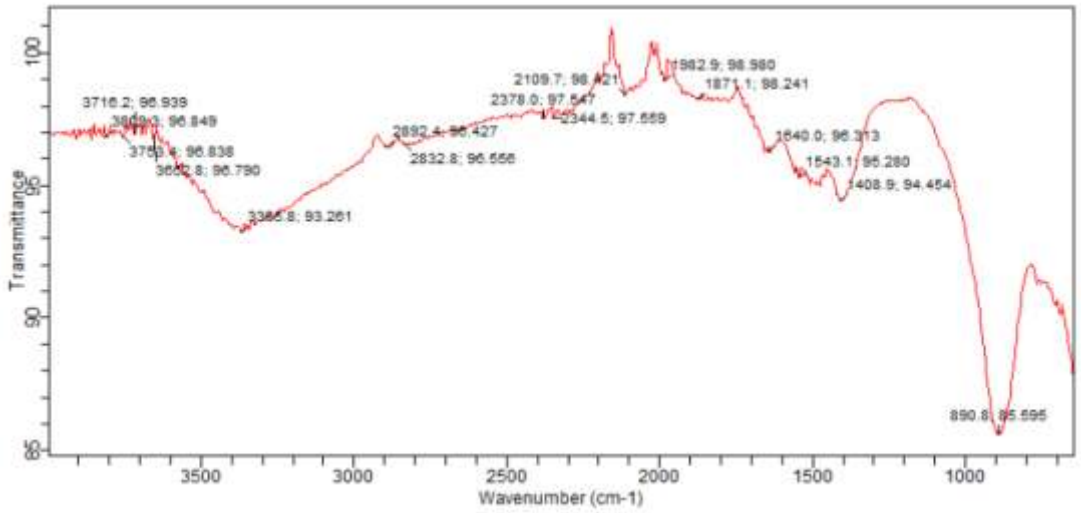

Figure 4: Fourier Infra-red (FTIR) of the CL-ZnO Nps

3.4 Corrosion Potential of ZnONPs (Weight loss)

Figures 5a and 5b showed the weight loss of mild steel in 1.0M HCl in the presence and absence of varying inhibitor concentrations with time of immersion. Figure 5a indicated that the weight loss of mild steel increases progressively as time increases with respect to the inhibitor concentration. From Figure 5b, it is seen that the weight loss decreases as inhibitor concentration increases with exposure time. This may be due to the fact that with increased inhibitor concentration, larger number of molecules of the zinc oxide nanoparticle is adsorbed onto the surface of the mild steel coupon, and the increased adsorption is facilitated by the particle size of the inhibitor, resulting in an increased surface area coverage on mild steel in corrosive medium thereby making it very difficult for the electrolytic solution to further attack the metallic surface. The rate of corrosion decreases with increased in inhibitor concentrations but increases with time as observed. The mild steel corrosion process in acidic medium can be attributed to the presence of OH^-, O_2^+, H^+, and Cl^-. The weight loss in absence of the inhibitor was much significant compared to the weight loss in the presence of the inhibitor. The result thus confirms an inverse proportionality between concentration of ZnONPs and weight loss.

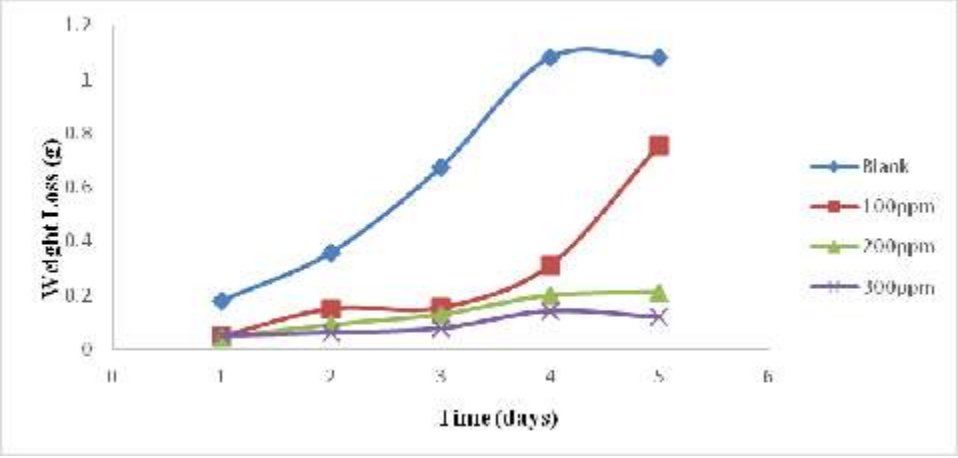

Figure 5a: Weight loss with time for Inhibitor Concentration

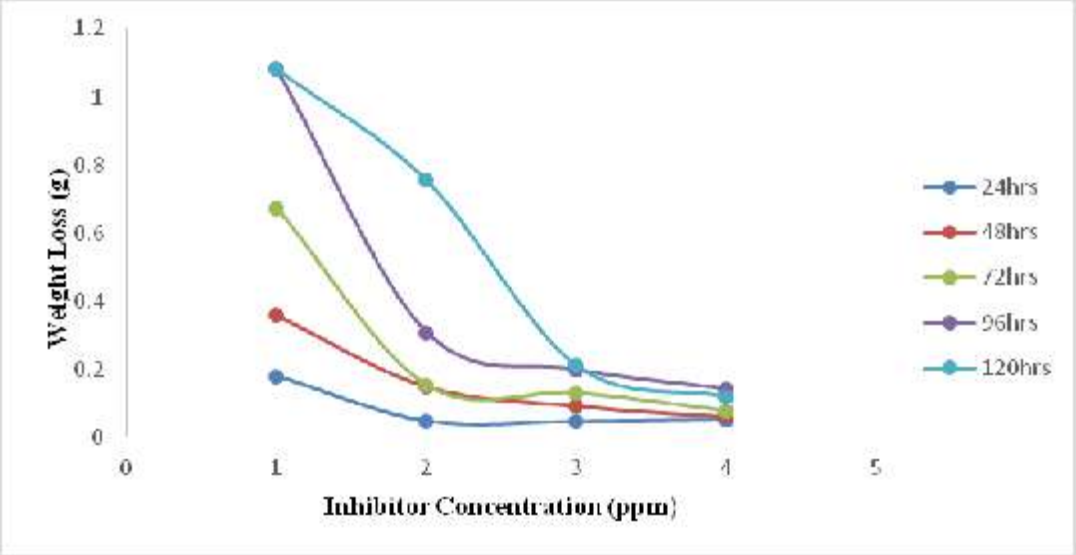

Figure 5b: Weight loss with Inhibitor Concentration at different exposure time.

Corrosion rate (CR) Analysis
The rate of corrosion was determined using equation 6 below;

$$\text{corrosion rate(mpy)} = \frac{kW}{ATD} (6)$$

Where, k is a constant with value as 87.6mpy, W is the weight loss (mg), A is the cross sectional area, T is the time (hr), D is the density of mild steel (g/cm^3). The corrosion rate of mild steel in 1.0M HClin the presence and absence of varying inhibitor concentrations is shown in Figure 6a, this indicates that the corrosion rate decreases with increase in inhibitor concentration from a maximum value of 0.0014 mmpy to 0.00018 mmpy on day 5. This phenomenon is largely attributed to certain physical properties of the Zinc oxide nanoparticles such as; particle size and surface density. These properties facilitated a quantum effect otherwise not experienced in bulk ZnONPs with increased in inhibitor concentration, the zinc oxide nanoparticles get adsorbed onto active sites on the surface of the mild steel coupon, and by virtue of its particle size within the nanoscale region, increased adsorption is continuously facilitated, making it difficult for the acidic medium to further attack the metallic surface. From Figure 6b, it shows the variation of corrosion rate with time for different inhibitor concentrations. Without any inhibitor concentration (blank), it was observed that the corrosion rate occurred distinctively at higher values compared to the inhibitor containing electrolytes. At 72hours on Blank, the corrosion rate reached its maximum and further exposure to the electrolyte resulted in decreasing values. Thus, it can observed that the ZnO NPs tries to literally decrease the distance between the points of initial and maximum corrosion rates, such that the metallic surface experience minimal effects of corrosion rate. Figure 6 also indicated that with increasing inhibitor concentration, the corrosion rate decreases.

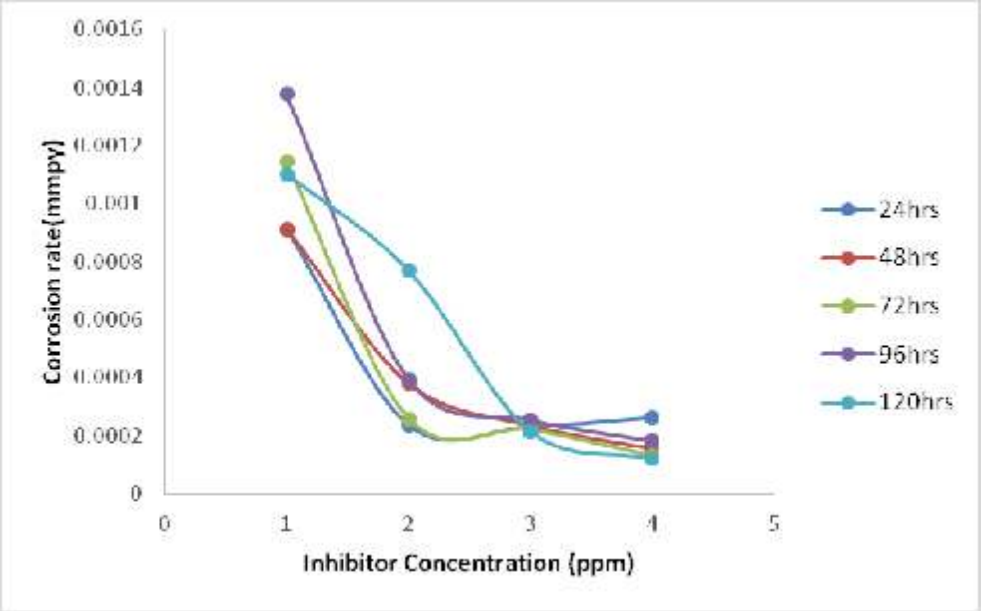

Figure 6a: Variation of Corrosion rate with Inhibitor Concentration at different exposure time.

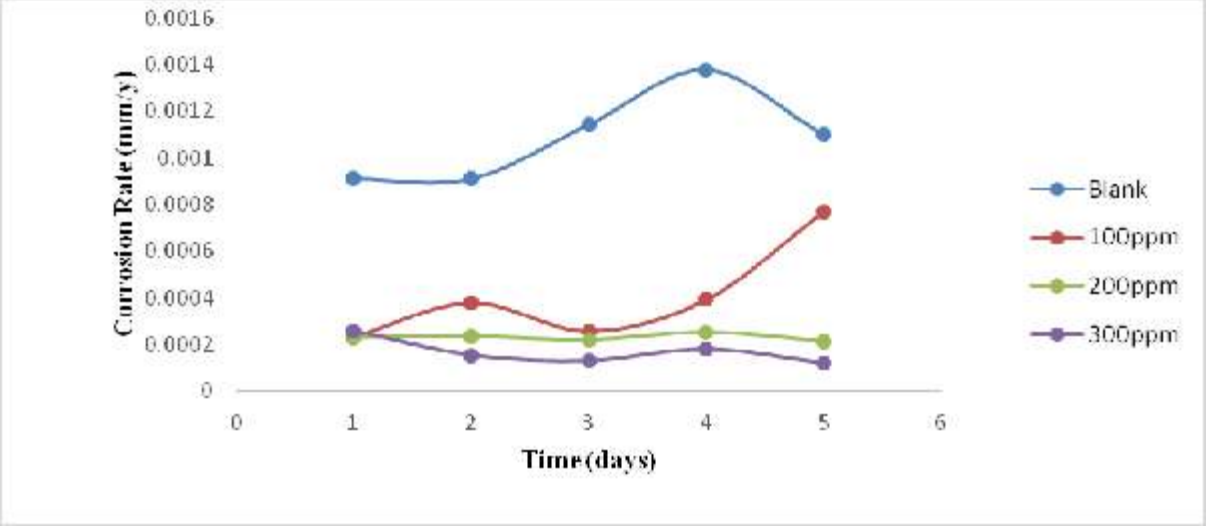

Figure 6b: Variation of Corrosion rate with time for different concentrations of ZnO NPs.

Surface Coverage and Inhibition Efficiency Analysis

Both surface coverage and inhibition efficiency was calculated using equations 7 and 8 respective;y;

$$\text{Surface coverage}(\theta) = \frac{W_A - W_P}{W_A} (7)$$

Where; W_A is Weight loss in the absence of inhibitor (g),W_P is Weight loss in the presence of inhibitor (g)

$$Inhibition\ \text{Efficiency}\ (\%) = \frac{W_A - W_P}{W_A} \times 100 (8)$$

Where, W_1 is the weight loss in the absence of inhibitor(g), W_2 is the weight loss in the presence of inhibitor (g).

The surface coverage and inhibition efficiency of zinc oxide nanoparticles on mild steel in 1.0M HCl in the presence and absence of varying inhibitor concentrations is seen in Figures 7a and 7b.This indicated that the surface coverage and inhibition efficiency decreases with increase in inhibitor concentrations while both surface coverage and inhibition efficiency decreased with increase in inhibitor concentration but as time progresses their values increased as well. 100ppm of the zinc oxide nanoparticles represented the least concentration, but at 120 hours of exposure time, it experienced the highest values of surface coverage and inhibition efficiency.

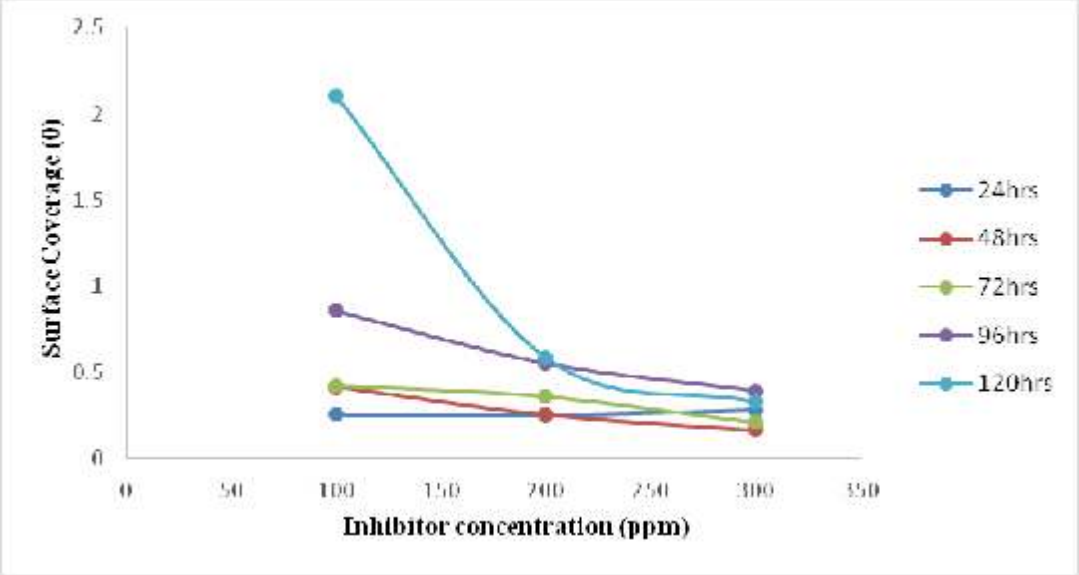

Figure 7a: Variation of Surface coverage with inhibitor concentration at different time interval

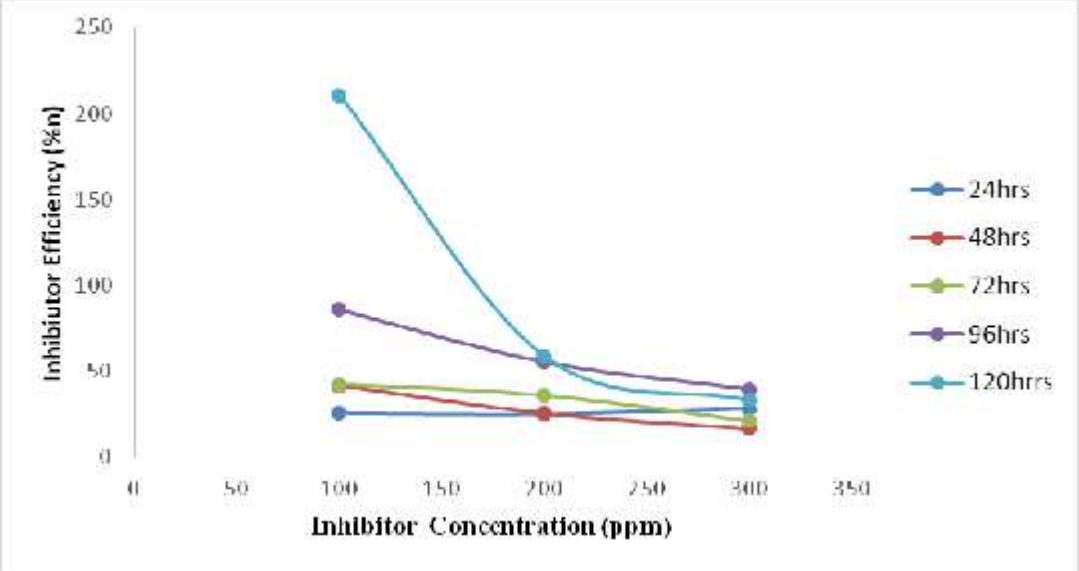

Figure 7b: Variation of Inhibitor Efficiency (%) with Inhibitor Concentration (ppm)

Conclusion

Cassava leaf Zinc oxide Nanoparticle (CL-ZnONPs) was synthesized and used as a corrosion inhibitor on mild steel in acidic medium in this study. Gravimetric method was employed in the weight loss analysis. The effects of contact time, and cassava leaf Nanoparticle concentrations on the corrosion rate, inhibition efficiency, surface coverage, and weight loss of mild steel were determined. Presence of Nitrogen, Oxygen, Carbon, and Sulphur atoms in the functional group of tannins, phenols, flavonoids, and saponins as secondary metabolites of the cassava leaf extract, facilitated the bio-reduction of Zinc acetate into ZnO NPs which makes it to be a good inhibitor on mild steel. The FTIR analysis also proved the presence of these heteroatoms that is responsible for the formation of protective layer on the metal surface. The inhibition efficiency was observed to increase with exposure time and decrease as inhibitor concentrations is increase. The band energy of the synthesized zinc oxide nanoparticle (ZnO NPs) was obtained at E_g=3.3 eV. Corrosion rate of the mild steel decrease with increase in inhibitor concentration from a maximum value of 0.0014 mmpy to 0.00018 mmpy.

REFERENCES

[1]. Vishwakarma, K., (2018), Green Synthesis of ZnO Nanoparticles using Abrus Precatorius Seed Extract and their Characterization, Thesis submitted to the Department of life science, Rouekela, India.

[2]. Subramanian, R., Abdullah, M., and Sadikun, A., (2012), A bitter plant with sweet future? A comprehensive review of an oriental medicinal plant: Andrographis paniculata, Phytochemistry Reviews, 11(1), DoI:10.1007/s11101-011-9219-z

[3]. Dabbs, D.M. and I.A. Aksay, (2000), Self-assembled ceramics produced by complex–fluid templation, Annual Rev. Physical Chem. 51, 601–622.

[4]. Nasrollahzadeh, M., Sajadi, S. M., Sajjadi, M., and Issaabadi, Z., (2019), An Introduction to Nanotechnology, In Interface Science and Technology, 1st Ed., Vol., 28, Elsevier Ltd, ISBN: 9780128135860, https://doi.org/10.1016/B978-0-12-813586-0.00001-8

[5].Herlekar, M., Barve, S., and Kumar, R., (2014), Plant-Mediated Green Synthesis of Iron Nanoparticles, Journal of Nanoparticles, Volume 2014, https://doi.org/10.1155/2014/140614.

[6].Chaudhuri, S. K., and Malodia, L. (2017), Biosynthesis of zinc oxide nanoparticles using leaf extract of *Calotropis gigantea*: characterization and its evaluation on tree seedling growth in nursery stage, Applied Nanoscience, 7, 501 – 512.

[7]. Balamurugan, V., Sheerin, F. M. A., and Sreenithi, V., (2019), A guide to phytochemical analysis, International Journal of Advance Research and Innovative Ideas in Education, 5, 236-245.

[8]. Odeja, O., Obi, G., Ene Ogwuche, C., Elemike, E. E., and Oderinlo, Y., (2015), Phytochemical screening antioxidant and antimicrobial activities of senna occidentalis (L) leaves extract, Journal of clinical phytoscience, 2 – 6.

[9]. Haque, M. J., Bellah, M. M., Hassan, M. R., and Rahman, S., (2020), Synthesis of ZnO nanoparticles by two different methods and comparison of their structural, antibacterial, photocatalytic and optical properties, Iop, Nano express, 1, 010007, https://doi.org/10.1088/2632-959x/ab7a43.

[10].Elemike, E. E., Damian, O., Anthony, C. E., Sonde, C. U., and Ehiri, R. C., (2017), Green Synthesis of Ag/Ag2O Nanoparticles Using Aqueous Leaf Extract of Eupatorium odoratum and Its Antimicrobial and Mosquito Larvicidal Activities, Molecules, 22(5): 674, DOI:**10.3390/molecules22050674**.

[11].Shabnam, F., Jamzad, M., and Hassan, K. F., (2019), Green synthesis of zinc oxide nanoparticles: a comparison, Green chemistry letters and reviews, 12(1): 19 – 24.

[12].Chen, Z., and Jaramillo, T. F., (2017), The Use of UV-visible Spectroscopy to Measure the Band gap of a Semiconductor, Edited by Bruce Brunschwig, Department of Chemical Engineering, Stanford University.

[13]. Tauc, J., (1972), Optical Properties of Solids," Abeles, North Holland, Amsterdam.

[14].Das, J., Evans, I. R., and Khushalani, D., (2009), "Zinc Glycolate: A Precursor to ZnO," Inorganic Chemistry, Vol. 48, No. 8, 2009, 3508-3510. doi:10.1021/ic900067

[15]. Al-Senani, G. M., (2020), Synthesis of ZnO-NPs using a Convolvulus arvensis leaf extract and
proving its efficiency as an inhibitor of carbon steel corrosion, Materials, 13(4), 890 https://doi.org/10.3390/ma13040890.

[16]. Nakamoto, K., (1997), Infrared spectra of inorganic and coordination compounds, Wiley, New York.

Journal of Engineering, Science, and Technology
ISSN: 2714-2396 | Volume 6, Issue 1

FT-IR AND GC-MS CHARACTERIZATION OF CRUDE OIL AND BIODIESEL FROM KHAYA SENEGALENSIS SEEDS.

Zamani D. Ishaya[1, a], Samuel Joseph[1], and Hauwa Ndaji[1].

[1] Department of Mechanical Engineering, Ahmadu Bello University, Zaria, Kaduna State, Nigeria.
[a] Corresponding E-mail: waidungiz@gmail.com

ABSTRACT. Globally, for energy sufficiency, incentives are put in place to drive more sustainable alternative energy sources that are renewable and eco- friendly. Biodiesels production from varied feedstocks and application in engines are encouraged due to the fuel higher lubrication quality, excellent combustion properties and low greenhouse gas emission. Khaya senegalensis seeds, a nonedible, readily available feedstock was used to extract its bio-oil. This research explored the seeds oil feasibility as biodiesel, so the crude oil was pretreated by esterification and trans-esterified to biodiesel. The specific objectives of this research were to establish the specific chemical characteristics - compositions, the essential components, the percentiles, and the quantitative transformation of desired components from the crude oil to the biodiesel as processed from Khaya senegalensis seeds. The crude and biodiesel oils produced were characterized using Fourier Transform Infrared (FT-IR) set at scanning range of 650 to 4000 cm-[1] and Gas Chromatography - Mass Spectrometry (GC-MS)-QO2010 Shimadzu Japan machines. The evolution of the results from the FT-IR test on the Khaya senegalensis crude oil to biodiesel oil, indicates that the functional groups increased from 10 to 11, with the addition of C=C weak stretch (alkene) at the wavelength of 1654 cm^{-1}. The GC-MS analyses confirmed that the predominant fatty acid is Oleic acid having 43.81 % by area, other esters are Nonadecanoic acid and Hexadecanoic acid. Also, the GC-MS validates the transesterification from 10 chemical compounds in the crude oil to 12 chemical compounds in the biodiesel oil. The major compounds found were fatty acids methyl esters as required for biodiesel. The natural occurring and transformed esters accounted for 95.39 % of total mass spectral area. Oleic acid ($C_{18}H_{34}O_2$) has the largest mass spectra area of 43.81 % that elute at retention time of 18.170 minutes.

Keywords: Renewable energy, Khaya senegalensis, crude oil, Biodiesel oil, Fatty acids, Esters.

1.0 INTRODUCTION

In recent times, efforts have been directed towards inventing sustainable alternative energy sources that are renewable and eco- friendly. Biodiesel has great potential; it is a renewable energy resource and can serve as alternate to conventional fossil fuels.It has a higher lubrication quality and low greenhouse gas emission [1]. Biodiesel is a fuel obtained from plant oil and is characteristically similar to petro-diesel, but it is non-toxic, renewable, sustainable, and environmentally harmless [2, 3]. Biodiesel is biodegradable. It is also used as aviation fuel, and when used in diesel engines, it presents excellent combustion properties due to its low sulfur and aromatic content, and high cetane number [4], [5]. Non-edible and microbial oil such as Khaya senegalensis, from nonedible feedstock are used in the production of biodiesel [6, 7, 8]. Most biodiesel production in the world is from edible oils, which either currently or in the future would lead to a food shortage that may create a global disparity in the food market [9]. Therefore, the use of non-edible oils such as from Khaya

senegalensis has been recommended for this purpose to avoid the food-versus-fuel crisis within the country.

The established pathways for biodiesel production are pyrolysis (thermal cracking), microemulsion, transesterification, and blending processes [10], of which transesterification is the most adopted industrial method. This is due to its simple process route and its viscosity lowering potential [2, 11].

Transesterification is the reaction of triglycerides in oil or fat and alcohol in the presence of a catalyst (either an enzyme or a base or an acid) to form alkyl esters [2, 4, 12]. It is the most common method of biodiesel production from any oil resources, where triglycerides are converted into fatty acid esters through interchange of alkoxy moiety using homogeneous (acid and alkaline) or heterogeneous catalysts [13 – 14]. Homogeneous catalysts are widely used for biodiesel due to their excellent catalytic activity with faster and higher yield conversions under mild reaction condition [15]. Transesterification process plays an important role in the biodiesel production as it greatly influences higher yields and cost of production. The operating conditions like, catalyst type, temperature, methanol amount, and reaction time are significantly attributed to biodiesel production [2, 3, 16, 17].

Ogwuche [18]characterized the leaves of Pandanus Candalabrum using FT-IR and GC-MS analyses. The results showed that Kaur-16-ene was the most abundant component with 84.62 % percentage abundance. Carboxylic, alkenes and renes functional group were identified at 2958.08 cm^{-1}, 1598.10 cm^{-1} and 1457.68 cm^{-1} wavenumber respectively. Odo [19]carried out FT-IR and GC-MS analyses on Brenania brieyi root extract. The results showed the presence of pentadecanoic acid (17.04 %), 9, 12-hexadecanoic acid (10.18 %), 9-Octadecanoic acid (60.53 %) in methanol extract, and hexadecanoic acid (11.29 %), 9-Octadecanoic acid (54.85%), 9, 12-Octadecanoic (3.90 %) in chloroform extracts. Kavipriya[20] used FT-IR and GC-MS to analyze the leaf extract of Cassia Alata. The FT-IR results showed sulfates, sulfonamides, sulfones, aromatic, alkane, alkenes, nitrile, and amide functional groups. The GC-MS results showed 1-Butanol, 3-methyl-1,6-Anhydro-beta-D-glucopyranose, Oxirane, and Oleic acid. Also Bolade [21] carried out FT-IR and GC-MS analyses on Canna indica. The FT-IR results showed presence of aromatic O-H stretch (3300cm^{-1}) and aromatic C=C stretch (1451 and 1640 cm^{-1}). The GC-MS result showed presence of di-alpha-tocopherol.

In this research work, production of biodiesel from khaya senegalensis with methanol through homogeneous catalyzed transesterification was reported. The quality of the purified biodiesel obtained in optimal conditions was characterized by FT-IR and GC–MS. Khaya senegalensis was investigated in this research due to regional availability, and limited previous studies on this subject was conducted on the feedstock. Principally, this research established the chemical characteristics - compositions, the essential components, the percentiles, and the quantitative transformation of desired components from the crude oil to the biodiesel as processed from Khaya senegalensis.

2.0 MATERIALS AND METHODS

2.1 Collection of Samples

Khaya senegalensis originate from tropical Africa, Madagascar. Khaya senegalensis is a flowering plant in the family Meliaceae, of the Angiosperms group in the Sapindales order. Khaya senegalensis is a medium size, deep root drought resistant tree, often buttressed at the base. The barks of the tree changes from dark grey to a grey-brown pigment at maturity. Its leaves are arranged in a spiral formation of 4-6 pairs without terminal leaf. The tree has deciduousevergreen leaves. It has white, sweet-scented flowers and the matured fruit is globose, four or five-valved woody capsule of 4–6 cm diameter, containing numerous winged seeds. The tree can also grow well in subtropical conditions.

The key material for this characterization is the Khaya senegalensis winged seed kernels collected in Kagoro and environs of Kaura Local government area of Kaduna State in Nigeria. The oil was extracted from the seed kernels using mechanical expeller press, where the yield varies from 14 % to 43 % by weight [2, 4, 16]. This implies that crude oil from this feedstock has high commercial viability for biodiesel production. Other materials used in this research are analytical grades solutions of methanol (CH_3OH), propan-2-ol (C_3H_7OH), sulphuric acid (H_2SO_4), 0.1 Mole sodium hydroxide (NaOH) pellets and 0.1 Mole potassium hydroxide (KOH) pellets as the major reagents employed for this experiment

2.2 Preparation of Biodiesel

Part of the methods of the characterization includes the biodiesel production, which involves pretreatment method of the oil, followed by the transesterification method. The procedure was to use 10.0 g of the extracted oil added to 240.0 g of propan-2-ol. The mixture was titrated using 0.1 Mole of potassium hydroxide and a blank titration was conducted. The FFA value and acid value (AV) of the oil were evaluated using Equations 1 and 2. The process cycle was repeated until the AV value of ≥ 0.5 % was achieved [16].

$$\text{Free Fatty Acid (FFA)} = \frac{\text{KOH Titre Value x Molarity of KOH x Molar Mass of KOH}}{\text{Mass of oil}} \quad (1)$$

% FFA = (v x 0.1 M x 56.1 g /mol) / 10.0g Where, v is the titre value.

$$\text{Acid Value (A.V.)} = \frac{\text{\% FFA}}{2} \quad (2)$$

Normally, the stoichiometric reaction requires a mole of oil (Triglyceride) and three moles of alcohol (Methanol) as expressed in Equation 3.

$$\underset{\text{Triglyceride}}{R\text{-}CO\text{-}OR'} + \underset{\text{Alcohol}}{R''\text{-}OH} \xrightleftharpoons{H^+ \text{ or } R''O^-} \underset{\text{Methyl Esters}}{R\text{-}CO\text{-}OR''} + \underset{\text{Glycerol}}{R'\text{-}OH} \quad (3)$$

The transesterification was conducted using 240 g of the esterified oil with 52.08 g of methanol for an oil to alcohol molecular mass ratio of 1:6 in excess times two, and 1.8 g (0.75 % m/m of oil) of NaOH as catalyst loaded times three the normal weight, for 1-hour at 60 °C to produce the Khaya senegalensis biodiesel. Similar process may be conducted for biodiesel production at higher oil to methanol ratios.

The required reagents used were methanol (CH_3OH), sulphuric acid (H_2SO_4), 0.1M potassium hydroxide (KOH) pellets, propan-2-ol (C_3H_7OH) and sodium hydroxide (NaOH) pellets. The reagents were of analytical grade (Assay 99.5 %) manufactured by BHD Chemical Ltd, Polle, England, and sourced from Cardinal Nig. Ltd, Kwagila in Zaria, Nigeria and were used as received.

2.3 Fourier Transform Infrared (FT-IR) Spectroscopy

Agilent technologies FT-IR Spectrophotometer was used to take the infrared spectrum of samples. Potassium bromide disc method was used to obtain the IR spectra of samples. 650 to 4000 cm^{-1} scanning range was used. In this research, functional groups were identified in the crude oil and biodiesel samples using the FT-IR spectra.

2.4 Gas Chromatography-Mass Spectrometry (GC-MS)

GC-MS-QO2010 Shimadzu Japan was used in the analysis. A fused silica column, filled with Elite-5MS (95 % dimethylpolysiloxane 5 % biphenyl, 30 m × 0.25 mm ID × 250 μm df). Helium as carrier gas flowing constantly at 1 mL/min was used to separate the components. Temperature of injector was set at 250 °C for the chromatographic run. The extract (1 μL) was injected into the instrument and the temperature was 70 °C (0 min); followed by 280 °C at the rate of 10 °C min^{-1}; and 280 °C, where it was kept for 5 minutes. The mass detector conditions were set at transfer line temperature at 250 °C; ion source temperature of 200 °C; and ionization mode electron impact of 70

eV, a scan time of 0.5 seconds and scan interval of 0.1 seconds respectively. In this research, compounds were detected in the crude oil, its biodiesel, and their respective quantities with GC-MS spectrometer.

2.5 Compounds Identification

National Institute Standard and Technology (NIST) was used as a reference to compare and interpret the results. Compounds were identified according to molecular mass, structure, and fragments. The unknown components spectrum was compared with that of the NIST library, and the closest match is taken.

3.0 RESULTS AND DISCUSSION

3.1 Fourier Transform Infrared Spectroscopy (FT-IR) Analysis

3.1.1 Crude Khaya senegalensis oil

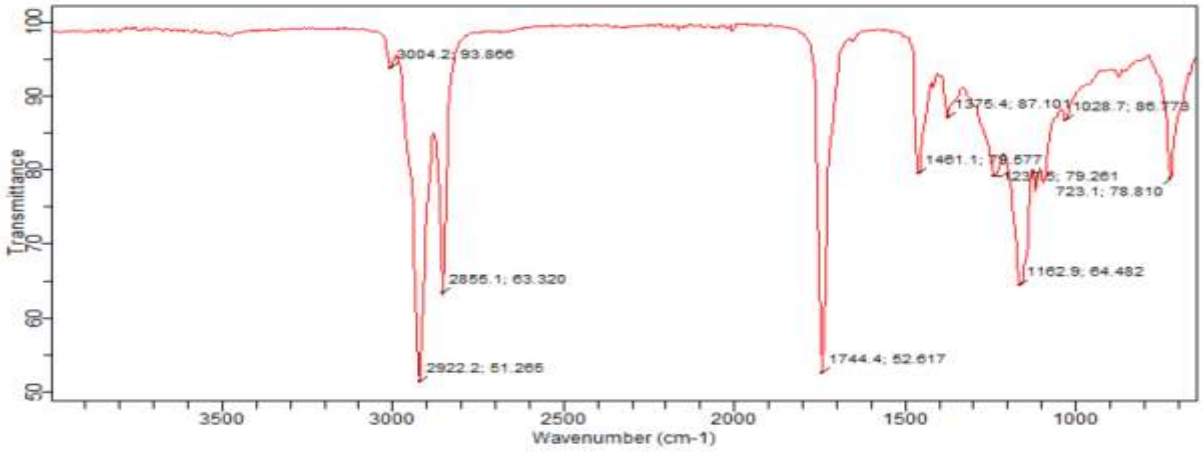

Fig. 1. FT-IR spectra of crude Khaya senegalensis oil.

Table 1. Functional groups in crude Khaya senegalensis oil.

S/N	Wavelength (cm^{-1})	Functional group
1	**3004**	**=C-H weak stretch (alkene)**
2	**2922, 2855**	**C-H strong stretch (alkanes)**
3	**1744**	**C=O strong stretch (alkanoic & ester)**
4	**1461**	**C-H medium stretch (terminal alkane bend)**
5	**1375**	**C-O weak stretch (alkanoic)**
6	**1103-1236**	**C-O medium stretch, (esters)**
7	**1028**	**C-O-C weak stretch (alkanoate)**
8	**723**	**C=C-H medium stretch (alkene bending)**

Tulashie [22] assigned 3000 cm^{-1} to -CH bond, 2853.09 and 2922.27 cm^{-1} to $–CH_2$ stretching vibrations, 1741.91 cm^{-1} to –C=O bond stretching, 1436.22 cm^{-1} to $–CH_3$ asymmetric stretching and 1196.28 cm^{-1} due to O-CH_3 stretching. In the present research, as indicated in Fig. 1 and Table 1; =C-H bond was observed at 3004 cm^{-1}, C-H bond at 2855-2922 cm^{-1}, C=O at 1744 cm^{-1}, C-H terminal alkane bond at 1461 cm^{-1} and C-O-C at 1028 cm^{-1}. Cheah [23] assigned peaks at 1059 cm^{-1} to C-O stretching, 2900 cm^{-1} to alkane C-H stretching, 1700 cm^{-1} to ester C=O stretching, 1650 cm^{-1} due to alkene C=C stretching. Similarly, Mohammed [24] identified 2853.78 cm^{-1} as methyl C-H group, and 1741.78 cm^{-1} as ester. The research identified C-O ester group at 1103-1236 cm^{-1}, C-O

carboxylic group at 1375 cm^{-1} and C-H bend at 723 cm^{-1}. This research is consistent with [22, 23, 24].

Based on the FT-IR result in Fig.1 in the research, it was observed that: alkanes, alkenes, carboxylic and esters functional groups were present in Khaya Senegalensis crude oil. The alkanes and alkenes functional groups were due to the presence of long fatty acid chain in the triglyceride compound. The chain usually consists of saturated and unsaturated sites. The carboxylic functional group indicates suitable site for transesterification reaction to occur. The carboxylic group is normally attached to the end of the long fatty acid chain away from the triglyceride backbone. The ester functional group was due to naturally occurring esters in plant oils.

3.1.2 Khaya Senegalensis Biodiesel

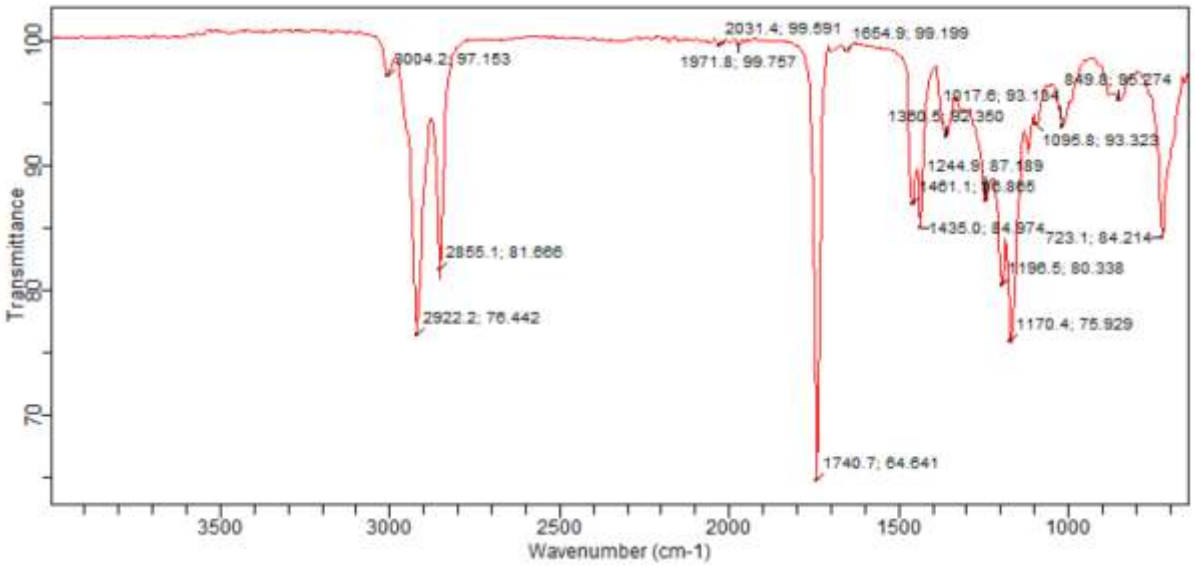

Fig. 1. FT-IR spectra of Khaya senegalensis biodiesel.

Table 2. Functional groups in Khaya senegalensis biodiesel.

S/N	Wavelength (cm^{-1})	Functional group
1	**3004**	**=C-H weak stretch (alkene)**
2	**2922, 2855**	**C-H strongh stretch (alkanes)**
3	**1744**	**C=O strongh stretch (alkanoic & ester)**
4	**1654**	**C=C weak stretch (alkene)**
5	**1461, 1435**	**C-H medium stretch (terminal alkane bend)**
6	**1380**	**C-O weak stretch (alkanoic)**
7	**1170-1244**	**C-O medium stretch, (esters)**
8	**1095**	**C-O-C weak stretch (alkanoate)**
9	**723-850**	**C=C-H medium stretch (alkene bending)**

Dass [26]observed that 1744.4, 1461.1, 1237.6, 1162.9 and 723.1 cm^{-1} were marched to C=O, C=C, C-O, C-C stretch, and C-H bending respectively in a biodiesel produced from Mahogany fruit shell. Alhassan [24] Attributed 1709, 1248 and 1611 cm^{-1} to C=O, C-O and C=C groups respectively. In this research as indicated in Fig. 2 and Table 2, C-H bond was identified at 2855-2922 cm^{-1}, C=O at 1744 cm^{-1}, C=C at 1654 cm^{-1}, C-H terminal alkane bond at 1435-1461 cm^{-1},

C-O at 1380 cm^{-1}, C-O-C at 1095 cm^{-1} and =C-H bending at 723-850 cm^{-1}. The present functional grouping in this research are in agreement with other research works [25 - 26].

Based on the FT-IR result in Fig. 2 in the research, it was observed that: alkanes, alkenes, alkanoic, and esters functional groups are clearly visible in the Khaya senegalensis biodiesel. The alkanes and alkenes functional groups were due to the presence of long fatty acid chain and mono-unsaturation in the fatty acid chain attached to the ester end in the biodiesel. The presence of alkanes implies the biodiesel will have high energy content and short ignition delay, but it will be faced with low pour and cloud point. Alkenes/mono-unsaturation presence implies the biodiesel will have good fluidity property, even though it will have to deal with oxidation instability and lower heating value. The long fatty acid chain will support high heating value and short ignition delay for the biodiesel, but it will contribute to high viscosity challenges. Due to the transesterification reaction, the long fatty acid chain has been detached from the triglyceride backbone to form the fatty acid methyl esters (FAME). The presence of esters in the biodiesel indicates good fuel properties like low viscosity, improved pour and cloud points, more energy per unit volume. Esters also implies the alkanoic functional group in the crude oil have undergone transesterification reaction. The remaining carboxylic group in the biodiesel may indicate incomplete transesterification reaction and results in high total acid number of the biodiesel.

3.2 Gas Chromatography-Mass Spectrometry (GC-MS) Analysis

3.2.1 Crude Khaya senegalensis oil

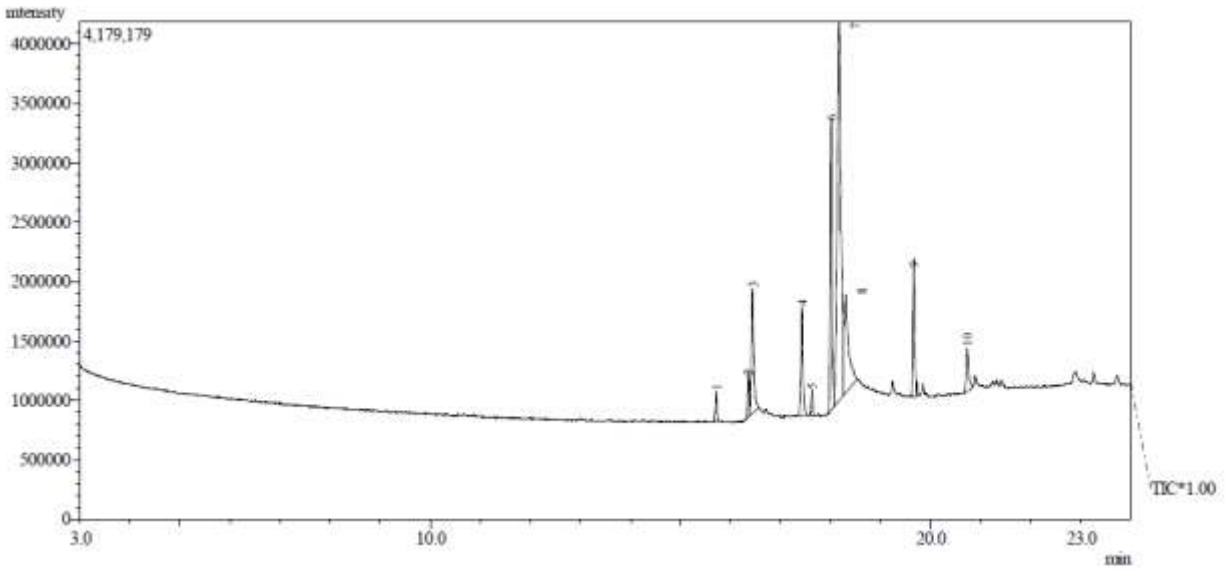

Fig. 3. GC-MS spectra of crude Khaya senegalensis oil.

Table 3. Compounds present in crude Khaya senegalensis.

*PK	*RT	Area %	Library - ID*	Formula
1	**15.713**	**1.41**	**Methyl 6-methyl heptanoate**	**$C_9H_{18}O_2$**
2	**16.357**	**1.98**	**Hexadecanoic acid, ethyl ester**	**$C_{18}H_{36}O_2$**
3	**16.440**	**9.05**	**Hexadecanoic acid**	**$C_{16}H_{32}O_2$**
4	**17.427**	**6.45**	**11-Octadecenoic acid, methyl ester**	**$C_{19}H_{36}O_2$**
5	**17.628**	**1.23**	**Methyl 8-hydroxyoctanoate**	**$C_9H_{18}O_3$**
6	**18.013**	**14.79**	**9-Octadecenoic acid, ethyl ester**	**$C_{20}H_{38}O_2$**

7	**18.170**	**43.81**	**Oleic acid**	**$C_{18}H_{34}O_2$**
8	**18.304**	**11.54**	**Nonadecanoic acid**	**$C_{19}H_{38}O_2$**
9	**19.665**	**6.60**	**cis-Oleic acid**	**$C_{18}H_{34}O_2$**
10	**19.665**	**3.15**	**10-Undecenal**	**$C_{11}H_{20}O$**

*PK= Peak, RT = Retention Time, ID = Identification.

The GC-MS analysis of crude Khaya senegalensis oil showed presence of 10 compounds as shown from the 10 Peaks (PK) in Fig. 3 and the data in Table 3. It was observed that major compounds were fatty acids, natural occurring esters and accounted for 95.39 % of total mass spectral area. Major compounds include: Oleic acid ($C_{18}H_{34}O_2$) at retention time of 18.170 min occupying the largest mass spectra area of 43.81 %, 9-Octadecenoic acid, ethyl ester ($C_{20}H_{38}O_2$) at retention time of 18.013 min with a mass spectra area of 14.79 %, Nonadecanoic acid ($C_{19}H_{38}O_2$) at retention time of 18.304 min with a mass spectra area of 11.54 %, Hexadecanoic acid ($C_{16}H_{32}O_2$) at retention time of 16.440 min occupying 9.05 % mass spectra area, 11-Octadecenoic acid, methyl ester ($C_{19}H_{36}O_2$) at retention time of 17.427 min with a mass spectra area of 6.45 %, cis-Oleic acid ($C_{18}H_{34}O_2$) at retention time of 19.665 min with a mass spectra area of 6.60 %, 10-Undecenal ($C_{11}H_{20}O$) at retention time of 20.727 min occupying 3.15 % mass spectra area.

The GC-MS result indicates that Oleic acid is the predominant fatty acid present in the crude Khaya senegalensis oil. The Oleic acid is a monounsaturated fatty acid with 18 carbon atoms. Mono-unsaturation implies the intended biodiesel will have good fluidity property. The long fatty acid chain will contribute high heating value and short ignition delay for the intended biodiesel. The presence of fatty acids indicates possible conversion to fatty acids methyl esters (FAME) that possesses good fuel properties.

3.2.2 Khaya senegalensis biodiesel

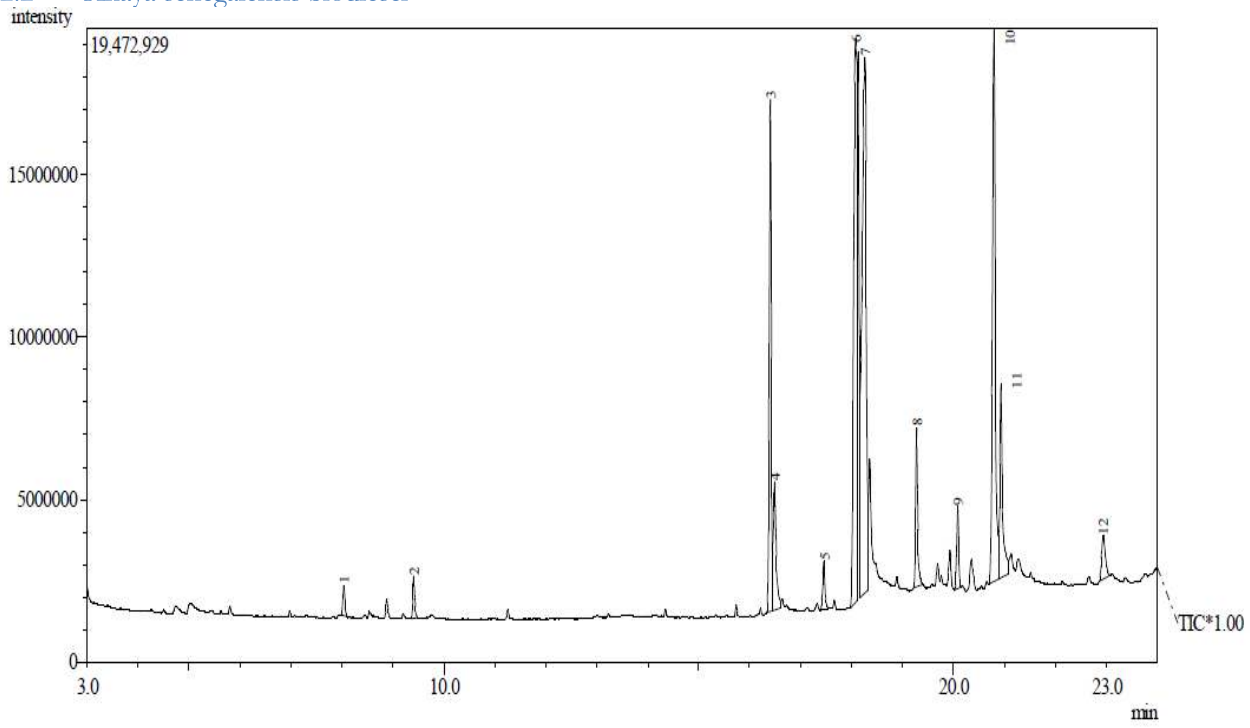

Fig. 4: GC-MS spectra of Khaya senegalensis biodiesel.

Table 4: Compounds present in Khaya senegalensis biodiesel.

*PK	*RT	Area %	Library - ID*	Formula
1	**8.037**	**0.65**	**2-Decenal, (E)**	**$C_{10}H_{18}O$**
2	**9.412**	**0.93**	**2-Undecenal**	**$C_{10}H_{20}O$**
3	**16.406**	**12.05**	**Hexadecanoic acid, ethyl ester**	**$C_{18}H_{36}O_2$**
4	**16.494**	**4.26**	**Palmitic acid**	**$C_{16}H_{32}O_2$**
5	**17.455**	**1.29**	**11-Octadecenoic acid, methyl ester**	**$C_{19}H_{36}O_2$**
6	**18.076**	**22.00**	**9-Octadecenoic acid, ethyl ester**	**$C_{20}H_{38}O_2$**
7	**18.267**	**26.50**	**Stearic acid, ethyl ester**	**$C_{20}H_{40}O_2$**
8	**19.275**	**3.66**	**2-Butyloctanol alcohol**	**$C_{12}H_{26}O$**
9	**20.080**	**1.82**	**Oleic acid**	**$C_{18}H_{34}O_2$**
10	**20.793**	**18.80**	**9-octadecenal**	**$C_{18}H_{34}O$**
11	**20.928**	**6.09**	**Stearyl vinyl ether**	**$C_{20}H_{40}O$**
12	**22.937**	**1.93**	**Oleic acid, 2-hydroxyethyl ester**	**$C_{20}H_{38}O_3$**

*PK= Peak, RT = Retention Time, ID = Identification.

The GC-MS analysis of the Khaya senegalensis biodiesel showed presence of 12 compounds as indicated from the 12 Peaks (PK) in Fig. 4 and the details in Table 4. It was observed that major compounds were esters, small fatty acids and accounted for 71.9 % of total mass spectral area. These compounds include: Stearic acid, ethyl ester ($C_{20}H_{40}O_2$) at retention time of 26.50 min occupying the largest mass spectra area of 26.50 %, 9-Octadecenoic acid, ethyl ester ($C_{20}H_{38}O_2$) at retention time (RT) of 18.1 min with a mass spectra area of 22.0 %, 9-octadecenal ($C_{18}H_{34}O$) at retention time of 20.8 min with a mass spectra area 18.80 %, Hexadecanoic acid, ethyl ester ($C_{18}H_{36}O_2$) at retention time 16.4 min occupying 12.05 % mass spectra area, Stearyl vinyl ether ($C_{20}H_{40}O$) at retention time of 20.9 min with a mass spectra area of 6.09 %, Palmitic acid ($C_{16}H_{32}O_2$) at retention time of 16.5 min with a mass spectra area of 4.26 %, 2-Butyloctanol alcohol ($C_{12}H_{26}O$) at retention time of 19.3 min occupying 3.66 % mass spectra area. Dass[26]reported 9-octadecenoic acid (Z), methyl ester at 7.678 RT, Hexadecanoic acid (Z) methyl ester at 13.790 RT, 12-Octadecenoic acid (Z), methyl ester at 15.425 RT and Oleic acid, 3-hydroxypropyl ester at 15.723 RT for a biodiesel produced from Mahogany fruit shells.

The GC-MS results indicates that the transesterification reaction has greatly reduced the percentage area of the Oleic acid in the crude oil from 43.81 % to 1.82 % in the biodiesel, with the formation of more esters. This implies the biodiesel will have low total acid number and good fuel properties such as high energy per unit volume, low viscosity, and short ignition delay. The percentage of esters increases 9-Octadecenoic, ethyl ester from 14.79 % to 22.0 % area, Hexadecanoic acid, ethyl ester from 1.98 % to 12.05 % area. New product like Stearic acid, ethyl ester occupying 26.50 % area was formed. The presence of fatty acid methyl esters (FAME) indicates successful transesterification reaction and good fuel properties. Biodiesels are the esters of fatty acids.

4.0 CONCLUSIONS

In this research, FT-IR and GC-MS characterization of crude oil and biodiesel oil from Khaya senegalensis seeds as investigated, establishes its chemical conformity as biodiesel fuel. Also, the following conclusions are drawn from the results:

1. The FT-IR analyses of the crude Khaya Senegalensis oil showed the presence of alkanes, alkenes, alkanoic and esters functional groups. The GC-MS analyses confirmed the presence of fatty acids having most of the functional groups identified in the FT-IR. The predominant fatty acid was Oleic acid having 43.81 % area. Others are Nonadecanoic acid and Hexadecanoic acid. The fatty acids are the reactive species in the oil for transesterification reaction to occur when reacted with alcohol.

2. The FT-IR analyses of Khaya Senegalensis biodiesel indicates that the functional groups increased from 10 to 11, with the addition of C=C weak stretch (alkene) at the wavelength of 1654 cm^{-1}. The alkanoic functional group in the crude oil underwent transesterification reaction.
3. The GC-MS analyses validates the transformation from 10 chemical compounds in the crude oil to 12 chemical compounds in the biodiesel oil. The major compounds were fatty acids, naturally occurring and transformed esters that accounted for 95.39 % of total mass spectral area. Oleic acid ($C_{18}H_{34}O_2$) has the largest mass spectra area of 43.81 %, elute at retention time of 18.170 min.
4. Other predominant FAME was Stearic acid, ethyl ester having 26.50 % area. More esters products with lower percent are 9-Octadecenoic acid, ethyl ester, Hexadecanoic acid, ethyl ester. The FAME are identified as biodiesel molecules.

ACKNOWLEDGEMENT.
The authors acknowledge the support of the Laboratories for the provision of the equipment used in conducting these experiments at the National Research Institute for Chemical Technology (NARICT), Zaria, Department of Chemistry and Department of Mechanical Engineering, Ahmadu Bello University, Zaria. Nigeria. Special thanks to Professor G.Y. Pam for his time and assistance in this research.

REFERENCES

[1] Elango, R. K., Sathiasivan, K., Muthukumaran, C., Thangavelu, V., Rajesh, M. and Tamilarasan, K. (2019). Transesterification of castor oil for biodiesel production: Process optimization and characterization. *Microchemical Journal, 145*, 1162–1168. doi:10.1016/j.microc.2018.12.039.

[2] Ishaya Z. D., Pam G.Y., Kulla D.M., Ngbale E. O. (2017). Non-Conventional Feedstock for Biodiesel Production for a Diversified Economy: Canarium Schweinfurtii and Thevetia Peruviana Seed oils Case**.** *Proceeding of Nigerian Society of Engineers (NSE) Conference on Diversification of Nigerian Economy: Engineering Perspective* at Chida Event Centre, Utako - Abuja 20th – 24th November 2017 (Technical Book of Abstracts Pg 10 and 50).

[3] Olagbende, O. H., Falowo, O. A., Latinwo, L. M. and Betiku, E. (2021). Esterification of Khaya senegalensis seed oil with a solid heterogeneous acid catalyst: Modeling, optimization, kinetic and thermodynamic studies. *Cleaner Engineering and Technology, 4, 100200.* doi:10.1016/j.clet.2021.100200.

[4] Yahuza I., **Ishaya Z. D.,** Dandakouta H. (2013).A Review of Ethanol-Diesel Blend as a Fuel in Compression-Ignition Engine.*Proceeding of the 3rd National Engineering Conference and Annual General Meeting of the Automotive Engineers Institute* at the NUT Conference Hotel, Kaduna, 26th – 27th September 2013.Pg 17 – 27.

[5] Chaudhary P., Verma A., Kumar S. and Gupta, V. K. (2018). Experimental design and optimization ofcastor oil transesterification process by response surface methodology. *Biofuels 9*:7-17.

[6] Bateni H. and Karimi K. (2016). Biodiesel production from castor plant integrating ethanol production via a biorefinery approach. *Chem Eng Res Des. 107*: 4-12.

[7] Sukkasi, S., Chollacoop, N., Ellis, W., Grimley, S. and Jai-In, S. (2010). Challenges and considerations for planning toward sustainable biodiesel development in developing countries: Lessons from the Greater Mekong Subregion. *Renew Sustain Energ Rev 14*: 3100-7.

[8] Dai, Y. M., Chen, K.T. and Chen, C. C. (2014). Study of the microwave lipid extraction from microalgae for biodiesel production. *Chem Eng J 250*: 267-73.

[9] Falowo, O.A., Ojumu, T.V., Pereao, O. and Betiku, E. (2020). Sustainable biodiesel synthesis from honne-rubber-neem oil blend with a novel mesoporous base catalyst synthesized from a mixture of three agrowastes. *Catalysts 10* (2), 190. doi: 10.3390/catal10020190.

[10] Olagbende, H.O., Aransiola, E.F., Ogunsina, B.S., Sanda, O. and Shonibare, D. (2016). Modification of a fixed bed reactor system for pyrolytic conversion of royalpoinciana pods into alternative fuels. *Int. J. Renew. Energy Resour. 6* (4),1350–1360.

[11] Juan, J.C., Kartika, D.A., Wu, T.Y. and Hin, T.-Y.Y. (2011). Biodiesel production from jatropha oil by catalytic and non-catalytic approaches: an overview. *Bioresour. Technol. 102* (2), 452–460. doi: 10.1016/j.biortech.2010.09.093.

[12] Olatundun, E.A., Borokini, O.O. and Betiku, E. (2020). Cocoa pod husk-plantain peel blend as a novel green heterogeneous catalyst for renewable and sustainable honne oil biodiesel synthesis: a case of biowastes-to-wealth. *Renew. Energy 166*, 163–175. doi: 10.1016/j.renene.2020.11.131.

[13] Baskar, G., Gurugulladevi, A., Nishanthini, T., Aiswarya, R. and Tamilarasan, K. (2017). Optimization and kinetics of biodiesel production from Mahua oil using manganese doped zinc oxide nanocatalyst. *Renew Energ. 103*: 641-6.

[14] Dai, Y. M., Wang, Y. F. and Chen C.C. (2018). Synthesis and characterization of magnetic LiFe5O8-LiFeO2as a solid basic catalyst for biodiesel production. *Catal Commun 106*: pp.20-4.

[15] Roschat, W., Phewphong, S., Thangthong, A., Moonsin, P., Yoosuk, B., Kaewpuang, T. and Promarak, V. (2018). Catalytic performance enhancement of CaO by hydration-dehydration process for biodiesel production at room temperature. *Energ Convers Manage 165*:1-7.

[16] Ishaya, Z. D., Pam, G.Y., Kulla, D. M., Jumare, A. I. (2020). "Fatty Acid Alkyl Esters Profiles of African Mahogany Biodiesel Produced at 0.25% NaOH Catalyst Concentration and Varied Molar Ratios". *African Journal of Renewable and Alternative Energy (AJRAE). 2020. Vol. 5 No. 1: 32 – 40.* (ISSN: 2006 0394). June 2020. A publication of Renewable and Alternative Energy Society of Nigeria (RAESON).

[17] Muthukumaran, C., Praniesh, R., Navamani, P., Swathi, R., Sharmila, G., and Kumar, N. M. (2017). Process optimization and kinetic modeling of biodiesel production using non-edible Madhuca indica oil. *Fuel 195*:217-25.

[18] Ogwuche C. E., Edema M. O. (2020). *GC-MS and FTIR characterization of essential oil from the fresh leaves of Pandanus candalabrum obtained from Bayelsa state, Nigeria*. Nigerian Journal of Chemical Research *25*(1).

[19] Odo, F., Ezeanyika, U. S., Ogugua, N., Joshua, E., & Okagu, U. (2017). *FTIR and GC-MS Spectroscopic Analysis of Methanol and Chloroform Extracts of Brenania brieyi Root Bark*. *5*(2013), 44–54.

[20] Kavipriya, K., Chandran, M., & Estuningtyas, A. R. I. (2018). *FTIR and GCMS Analysis of Bioactive Phytocompounds in Methonalic Leaf Extract of Cassia Alata Are Mangiferin and Mangiferin-Containing Plant Extracts Helpful for Iron- Loaded Transfusion-Dependent and Non-Transfusion-Dependent Thalassaemia Patients ?11*(1), 141–147.

[21] Bolade O. P., Akinsiku A. A., Adeyemi A. O. Jolayemi G. E., Williams A. B., Benson N. U. (2019). *Qualitative analysis, total phenolic content, FT-IR and GC-MS characterisation of Canna indica : bioreducing agent for nanoparticles synthesis Qualitative analysis , total phenolic content , FT-IR and GC-MS characterisation of Canna indica : bioreducing agent for nanoparticles synthesis.* https://doi.org/10.1088/1742-6596/1299/1/012135.

[22] Tulashie, S. K., Kalita, P., Kotoka, F., Segbefia, O. K., & Quarshie, L. (2018). Biodiesel production from Shea Butter: a suitable alternative fuel to premix fuel. *Materialia*. https://doi.org/10.1016/j.mtla.2018.08.038.

[23] Cheah, M. Y., Ong, H. C., Zulkifli, N. W. M., Masjuki, H. H., & Salleh, A. (2020). Physicochemical and tribological properties of microalgae oil as biolubricant for hydrogen-powered engine. *International Journal of Hydrogen Energy*, *45*(42), 22364–22381. https://doi.org/10.1016/j.ijhydene.2019.11.020.

[24] Mohammed, I. A., Sadiq, M. M., Aberuagba, F., Olurinde, A. O., & Obamina, R. (2015). *SYNTHESIS AND CHARACTERIZATION OF TRIMETHYLOLPROPANE-BASED Proceedings of the 45 th Annual Conference of NSChE , 5 th Nov – 7 th Nov ., 2015 , Warri , Nigeria P 024 Synthesis and Characterization of Trimethylolpropane-Based Biolubricants from Castor Oil D. November.*

[25] Alhassan, A. J., Muhammad, I. U., Sule, M. S., Wudil, A. M., & Imam, A. A. (2017). *Characterization and Anti-diabetic Activity of Dihydrophenantherene Isolated from Khaya senegalensis Stem Bark*. *17*(2), 1–17. https://doi.org/10.9734/ARRB/2017/35908.

[26] Dass P. M., Louis H., Alheri A., Amos P. I., Bifam M., Ago M. A. (2018). *Production of Biodiesel Oil from Desert Dates (Balanites aegyptiaca) Seeds Oil Using a Hetrogeneous Catalyst Produced from Mahogany (Khaya senegalensis) Fruit Shells*. Analytical Chemistry: An indian Journal *18*(1), 1–12.

Journal of Engineering, Science, and Technology
ISSN: 2714-2396 | Volume 6, Issue 1

DESIGN AND DEVELOPMENT OF A HYBRID SOLAR POWER TRAINER EQUIPMENT

Mustapha S. A.[1]*and Mahmud J. O.[1]
[1]NASENI Solar Energy Limited, Karshi, Abuja
Email: mustapha.sarafadeen@nsel.naseni.gov.ng*

ABSTRACT
The dearth of effective and indigenous manpower is a critical challenge facing the solar power industry in Nigeria. Several solar power training conducted lack well-structured hands-on practical scheme due to lack of appropriate equipment for the trainees. Therefore, this research work reports the design and development of a Hybrid Solar Power Trainer (HSPT) equipment using locally sourced materials. Double Diamond model was adopted where related research works were reviewed and then analyzed to have a well-defined goal leading to the design, development and implementation processes. The constructed HSPT equipment is detachable for ease of mobility. It also has the capability of simulating a typical household electrical wiring that is powered either by the grid supply/generator/solar power system or in their hybrid configuration for the purpose of teaching practical. The developed trainer was tested both on load and no load and generates stable outputs. The results of the tests show that the equipment can generate up to 894.6Wph, storage energy of 160Ah and can be used to conduct training for 12 hours at 65% depth of discharge before restoring state of charge. The quality of learning received by seventy-five trainees using the HSPT and assessed by five field expert was rated 90.55% and the quality and relevance of materials used was rated 92.25% making it to have high learning impact. This work will contribute to the improvement of the needed technical know-how in the solar power industry which will consequently increase confidence in the adoption of solar power technology in Nigeria.
Keywords: Solar Power Trainer, Electricity, Learning, Renewable energy

1.0 Introduction

Electricity is a very vital component for the development of socio-economic and technological activity of a nation. The epileptic electricity situation in Nigeria is such that the electricity demand far outweighs the supply which is causing hindrance to the nation's development[1]. Over the years, Nigeria has been very optimistic to solve the electricity challenge for the country which led to the drafting of various policies and strategies to achieve adequate and sustainable electricity for all through improvement in the energy mix [2][3]. Meanwhile, for the country to adequately match electricity supply to the rising demand there is need for investment in power generation infrastructure to attain 297,900MW by adding 11,686MW per year for 22 consecutive years [4]. Some of the realistic ways of achieving this feat is by decentralizing electricity generation, propagate the adoption of renewable energy for electricity generation and encourage distributed generation [5][6]. Researchers have proposed solar photovoltaic (PV) technology as a viable alternative source of electricity generation in Nigeria due to its abundance [7][8].
However, the dearth of adequate local human capacity in term of competence of the designers, installers, maintainers and other stakeholders of solar power systems in the solar energy industry in Nigeria is one of the identified challenges to the adoption of the technology [9].This calls for the need to develop capacity in the industry via qualitative training in orderfor Nigeria not to continuously rely on foreign technologies to ameliorate her challenges as seen in many sectors [10]. Although, several solar power training centers have sprung up, many of them lack well-structured practical scheme but rely more on theories. This calls for the need to adequately boost

the local human capacity required in the industry using locally developed infrastructures to conduct training tailored to follow the principles of instructional design as stated in [11][12].
This research work therefore aimed at further investigating the challenges to the adoption of solar power system relating to human capacity and reporting the design and development of a Hybrid Solar Power Trainer (HSPT) that is constructed with locally sourced materials for training purposes. The HSPT is a mobile and detachable equipment that consists of the basic components required for the design and installation of solar power system such as solar panels, charge controllers, inverters, storage batteries, electrical distribution board, electrical appliances and electrical tools used for a typical household electrical wiring. The HSPT is divided into three chambers. The load chamber contains the electrical loads such as bulbs and fans with their respective regulators as well as socket outlets. The power chamber is where the charge controllers, inverters, electrical distribution board and switch gear are fitted. The third chamber is the base chamber which houses the battery bank, electrical tools box, battery tester, a battery and inverter system to simulate hybrid connection to fuel powered generator. The HSPT affords learners to practically execute typical electrical wiring connections while learning off-grid and hybrid solar power systems. The use of the HSPT during training on solar power will improve the capacity to take jobs in the industry as well as improve the confidence in the adoption of solar power in Nigeria. The scope of this work is limited to trainer equipment.
This paper is divided into six sections; section one introduces the work while sections two and three present the literature review and material and methods respectively. Section four highlights the tests carried out as well as the discussion of the obtained results. Section five presents the conclusion.

2.0 Literature Review

In this section, review of related literatures is presented. Several research works by the authors in [13][14][15] highlighted numerous motivating factors that encourage the adoption of solar power system such as: stability of electricity supply, cost effectiveness in the long run as well as convenience in usage when compared to fossil fuel powered generators. However, some other factors have been serving as barrier factors hindering the adoption of solar power systems. Some of these barrier factors are presented in the research works by authors in[16][17][18] such as: high initial cost of installation of solar power systems, unregulated influx of substandard solar power products and inadequate required technical know-how in the industry. Meanwhile, in order to improve the solar power industry, one of the major areas in the solar PV value chain is training for improved required technical know-how [19]. Although, on the issue of technical know-how, different capacity building activities have sprung up in the solar power industry both online and physical organized by different organizations and training centres, the practical sessions however require upgrade [20]. Quality training is regarded as vital because human capital development is an inevitable needed tool if Nigeria must succeed in its effort to boost her citizens and the nation's laid down National Development Plan (NDP)[21][22].
In order to improve the needed technical know-how in the solar power system industry, researchers have designed and developed trainer kits and equipment of different operation conditions and limitations. In a research work by the authors in [23], sun simulator is used to direct light rays towards a 10Wp solar panel output from which measurement and data evaluation can be taken to study the current-voltage characteristics at various solar radiation. The development of solar educational training kit by the authors in [24] is designed for elementary studies on the use of solar cells as the basis for solar energy conversion to electricity. In a research presentation by [25], a solar PV power trainer was developed to be used as educational

instrument in laboratory. It was designed for the purpose of investigating performance evaluation of balance of systems (BOS) and effects of environmental factors on solar PV modules at different tilt angles. The instrument will improve knowledge of trainees on the characteristics of BOS at different climatic conditions. In a critical review of commercially available trainer and experimental kits meant for teaching renewable energies by [26], products used by universities to teach solar energy and designed by solar energy trainers producers such as EDIBON, Lab-Volt, De Lorenzo and Hampden were reviewed. In a related work by authors in [27], learning kit was designed for training on solar power system with power generating capacity of 22.74W and estimated energy of 136WH. After the tests, the system was rated 89.59% for the quality training acquired using the kit used while it was scored 87.5% for the quality and relevance of materials used.

The review indicated that many of the trainers are for experimental purposes which are used to investigate balance of system (BOS) responses to solar radiation intensity. Others who are used to study the electrical wiring and configurations of solar panels and BOS are plug and play which are short of physical real life wiring and components experience for trainees.Also, they did not consider the use of the instrument to train on practical installations of solar PV power system for residential or commercial applications. Hence the need for a trainer which has the capability of being used for real life connections of solar power system and electrical wiring. This therefore led to this research work.

3.0 Material and Methods

In order to address the problems discovered in the reviewed literature, the Double Diamond Model (or the 4Ds model) of design thinking as presented in Figure 1 was used as the adopted methodology.

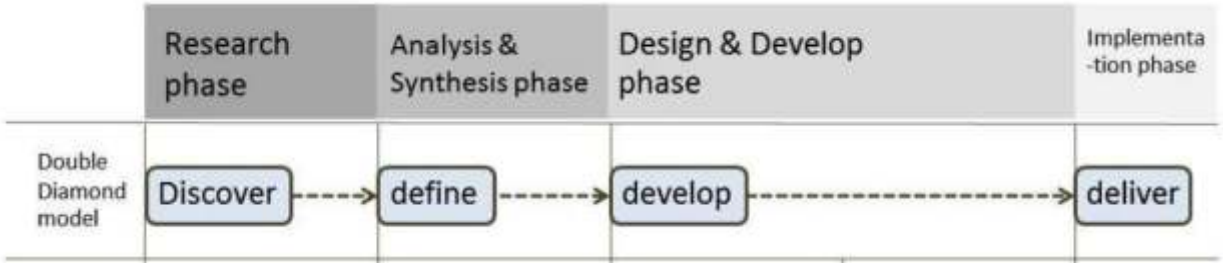

Figure 1: TheDouble Diamond Model Methodology [28]

The model consists of four steps which correspond to four phases of design thinking process as follows:

i. Discover (Research phase): The first step carried out was to identify the challenges in the solar power system industry through literature review in order to set research problem. This step afforded the opportunity to better discover variety of challenges demanding solutions while understanding them through various research opinions.

ii. Define (Analysis and Synthesis phase): The second step carried out in the methodology was to analyze the reviewed literature for the purpose of streamlining the investigation to a well-defined problem and precise goal. In this case, the development of a robust solar power trainer equipment to improve quality of technical know-how in the solar power industry.

iii. Develop (Design and Develop phase): In this step, brainstorming was done via discussions with five experienced solar power trainers on the needs assessment and different challenges being faced during training for effective training activities. This informed the design considerations: components availability in local market, compactness, detachability for mobility and use of mini modified

inverters, mini 12V/40Ah batteries, NSEL 80W solar panels as well as using locally available aluminum and light wood for the framework. In the design of the solar power trainer, the following were also carried out:

- The electrical load consist of two numbers of 12W bulbs and two numbers of 30W mini fans while socket outlets only indicate via LED making it to consume negligible power making the total load of 84W. It was estimated that the HSPT should be able to have battery backup time up to 12 training hours on full load at 0.8% efficiency and 65% depth of discharge (DOD). Also, the number of 80W solar panels is expected to restore the state of charge of the used batteries in 6 solar hours. This information was used as inputs to form the basis for sizing the HSPT as follows.
- The HSPT system sizing was calculated using equations (i) – (v) as stated in [29]:

$$System\ Energy = Total\ load\ x\ Usage\ hours \quad \text{(i)}$$
$$= 84W\ x\ 12h$$
$$= 1{,}008Wh$$

$$Number\ of\ batteries = \frac{System\ energy}{\text{Battery voltage x Battery capacity x DOD x Battery efficiency}} \quad \text{(ii)}$$
$$= \frac{1{,}008Wh}{\text{12V x 40Ah x 0.65 x 0.8}}$$
$$= \mathbf{4.03} \approx \text{ 4 batteries of 40Ah each are required}$$

The fifth battery is only used to demonstrate the connection of a fossil fuel generator in hybrid configuration.

$$Number\ of\ solar\ panels = \frac{System\ energy}{\text{Solar hours x solar panel power rating}} \quad \text{(iii)}$$
$$= \frac{1{,}008Wh}{\text{6h x 80W}}$$
$$= \mathbf{2.1} \approx \text{ 2 solar panels of 80W are required}$$

Considering 25% added tolerance;

$$Inverter\ capacity = Total\ load\ x\ 1.25 \quad \text{(iv)}$$
$$= 84W\ x\ 1.25$$
$$= 105\text{W inverter capacity is required}$$

However, due to availability, 1000W mini modified inverter was chosen

Similarly, considering 25% added tolerance;

$$Charge\ controller\ capacity = Total\ solar\ panel\ short\ circuit\ current\ x\ 1.25 \quad \text{(v)}$$
$$= 5\ x\ 2\ x\ 1.25$$
$$= 12.5\text{A charge controller current capacity is required}$$

Due to availability, 20A charge controller current capacity was considered.

- Using the sizing of each component in terms of space and after each component have been positioned in sketch, the HSPT was then drawn in 3D using AutoCAD as presented in Figure 2 with its dimensions as shown in Table 1.

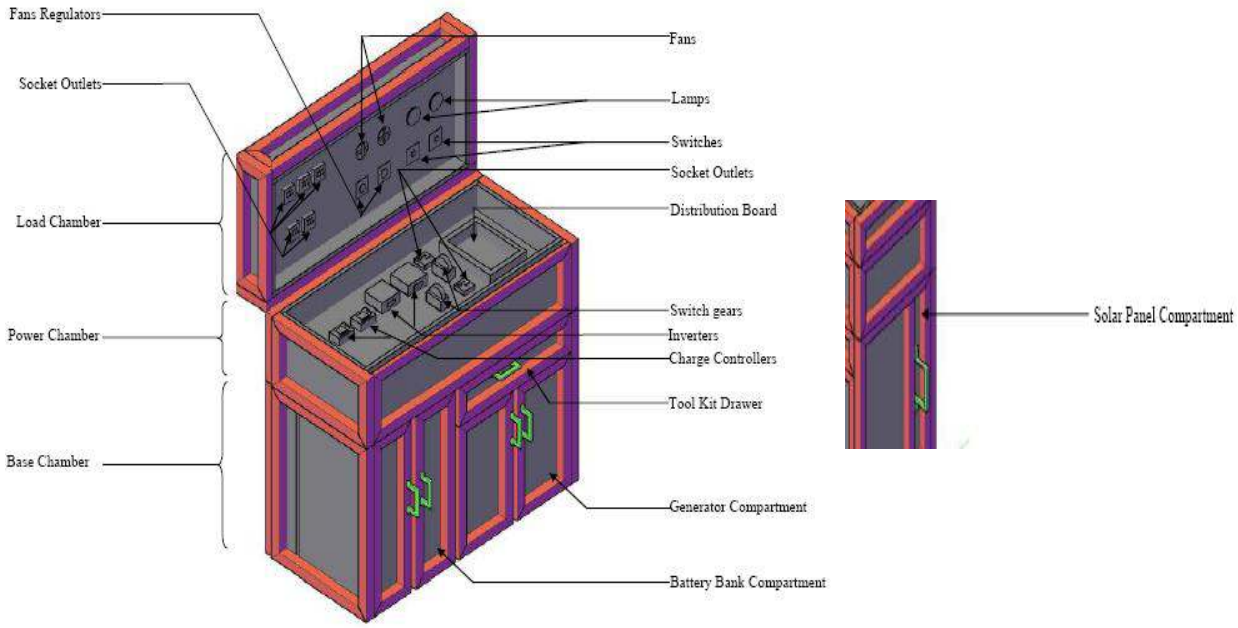

Figure 2: 3D Diagram of the HSPT

Table 1: Dimensions of the HSPT

Compartment	Length (m)	Breadth (m)	Height (m)
Load chamber	1.25	0.6	0.15
Power chamber	1.25	0.6	0.25
Base chamber	1.25	0.6	0.6

- The circuit diagram on how the electrical wiring will be carried out was then developed as shown in Figure 3. This shows how the solar panels are connected to the battery bank via the charge controllers, the inverter connection to the battery bank and supplying the electrical loads through the electrical distribution board. It also shows how the electricity supplies from mains and fossil fuel generator are hybridized to power the loads via a switch gear.

Journal of Engineering, Science, and Technology
ISSN: 2714-2396 | Volume 6, Issue 1

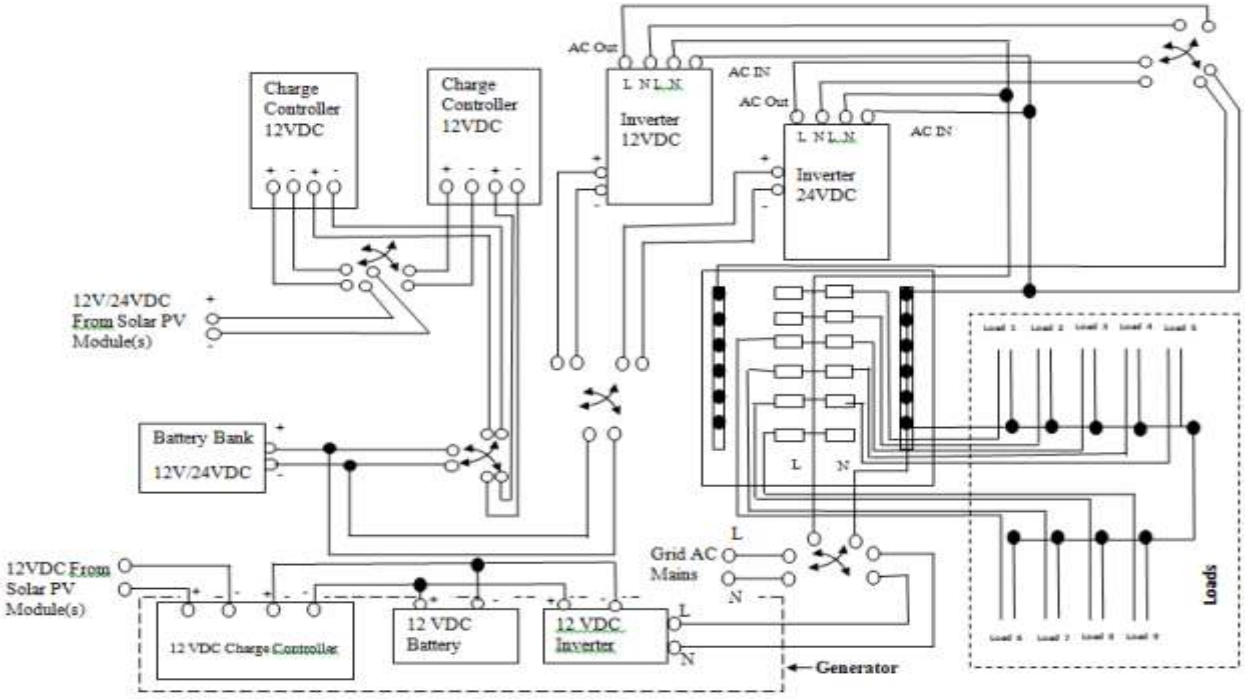

Figure 3: Electrical wiring of the HSPT

iv. Deliver (Implementation phase): This step in the methodology was the construction of the HSTP whereby the design stage was being implemented as shown in Figure 4. Figure 4A depicts the complete view of the outside structure of the HSPTwith the frames of the chambers made of aluminum bars embedded with plywood. Figure 4B shows the load chamber where the electrical loads and the power chamber where the charge controllers, inverters and electrical distribution board are fixed. Figure C shows the base chamber where the set of batteries are contained and the simulated generator system. Testing of the final equipment was carried out as presented in the following section.

A

B

C

Figure 4: Implemented HSPT

4.0 Results and Discussion

Upon completion of the construction, the HSPT was put to test and the result is presented in Table 2. The test was to determine the output functionality of the solar panels, inverter and the battery bank.

Table 2: Test results of the HSPT

	Solar panel			Inverter output					Battery	
				no load		on full load			on full load	
Temp. (°C)	Irradiance (W/m²)	Short circuit current (A)	Open circuit voltage (V)	Current (A)	Voltage (V)	Current (A)	Voltage (V)	Freq. (Hz)	Duration (H)	Voltage (V)
31	902	3.99	18	0	230	0.367	230	50	0	12.9
31	971	4	18.5	0	230	0.367	229	50	3	12.5
32	1001	4.2	18.5	0	230	0.367	229	50	6	12.42
32	1000	4.2	18.5	0	230	0.367	228.9	50	9	12.34
31	870	3.98	18	0	230	0.367	229	50	12	12.26

The result of the outdoor test of the solar panels in Table 2 shows that the two solar panels can generate up to an average of 149.1Wp (at 4.074A/18.3V each) and 894.6Wph in 6 hours/day at an average irradiance of 948.8W/m^2 and 31°C which is 93.2% of the solar panels power rating of a total 160Wp at standard test condition (STC). This indicates that the solar panels function optimally. Also, the inverter outputs were tested both on no load and on full load conditions. The result of the test shows that the output voltage, current and frequency of the inverter are averagely stable with only 0.43% in voltage drop on full load. Hence, the inverter system is appropriately functional. Similarly, the battery bank which has total energy storage of 160Ah was tested on full load for 12 hours as designed. The results show that after 12 hours, the battery still has 12.26V state of charge which is significantly good to elongate battery life.

Furthermore, the HSPT equipment was used to train seventy-five youth in Nigeria and assessed by five training experts. The HSPT equipment was rated an average of 90.55% in term of the quality of learning received and 92.25% in term of the quality and relevance of materials. The evaluation values shows that the learning outputs through the use of the HSPT are in the category of high feasibility with the capability of increasing trainees' learning significantly as in the work of [30]. This shows that based on the performance metrics above, the HSPT performs by 0.96% and 4.75% respectively better when compared to the work of the authors in [27].

5.0 Conclusion

Inadequate required skills for installers and designers of solar power systems as well as improperly structured practical sessions during training are some of the challenges facing the solar power industry in Nigeria. The design and development of a mobile and detachable solar power trainer that encompasses all basic components needed during installation of solar power systems to a typical residence and other related areas became imperative and executed in this work. The developed trainer equipment was tested and found to have daily outdoor generating capacity of 894.6Wph and storage energy of 104Ah at 65% depth of discharge when used to conduct training for 12 hours. The quality of learning received was rated 90.55% and the quality and relevance of materials used was rated 92.25%. This shows that the impact of the use of the equipment for training is highly significant which will improve the quality of human capacity in the solar power industry.

REFERENCES

[1] J. O. Mahmud and S. A. Mustapha, "Opportunities for Engineers in the Solar Energy Value Chain," in *1st NSE Minna Branch National Conference* , Minna, 2021.

[2] Central Bank of Nigeria, "Annual Report 2016," Central Bank of Nigeria, Abuja, 2016.

[3] Ministry of Budget and National Planning, "Economic Recovery and Growth Plan 2017 - 2020," Federal Republic of Nigeria, Abuja, 2017.

[4] A. S. Sambo, "Matching Electricity Supply with Demand in Nigeria," International Association for Energy Economics, 2008.

[5] S. A. Benson, E. C. Ashigwuike and J. K. Ogunjuyigbe, "Assessing the Benefits and Challenges of Distributed Generation in Nigeria Power Distribution Network," *Internationa Journal on Data Science and Technology,* vol. 1, no. 5, pp. 8-13, 2019.

[6] O. Bamisile, Q. Huang, P. Ayanmbire, P. O. K. Anane, S. Abbasoglu and W. Hu, "Analysis of Solar PV and Wind Power Penetration into Nigeria Electricity System," *IEEE,* pp. 1-5, 2020.

[7] A. Babajide and M. C. Brito, "Powering the Commercial Sector in Nigeria Using Urban Swarm Solar Electrification," *Sustainability,* pp. 1-19, 2020.

[8] H. O. Njoku and O. M. Omeke, "Potentials and Financial Viability of Solar Photovoltaic Power Generation in Nigeria for Greenhouse Gas Emissions Mitigation," *Clear Technologies and Environmental Policy,* pp. 1 12, 2020.

[9] J. O. Mahmud, "Improving Agro Community Commercial Farming Sustainability through Deployment of Renewable Energy," in *11th ICEPSOP*, Abuja, 2020.

[10] A. E. Eze, U. H. Okpara and C. V. Madichie, "Impact of Foreign Aid on Economic Growth in Nigeria," *Socialscientia Journal of the Social Sciences and Humanities,* vol. 1, no. 5, pp. 52-64, 2020.

[11] R. M. Gagne and L. J. Briggs, "Principle of Instructional Design," *Holt, Rinehart Winston,* 1974.

[12] J. Sweller, "Instructional Design," *Encyclopedia of Evolutionary Psychological Science* pp. 4159-4163, 2021.

[13] L. Olatomiwa, S. Mekhilef, A. S. N. Huda and O. S. Ohunakin, "Economic Evaluation of Hybrid Energy Systems for Rural Electrification in Six Geo-Political Zones of Nigeria," *Renewable Energy,* pp. 435 446, 2015.

[14] A. I. Ugulu, "Barriers and Motivations for Solar Photovoltaic (PV) Adoption in Urban Nigeria," *International Journal of Sustainable Energy Planning and Management,* vol. 21, pp. 19-34, 2019.

[15] D. Akinyele, O. Babatunde, C. Monyei, L. Olatomiwa, A. Okediji, D. Ighraywe, O. Abiodun, M. Onasanya and K. Temikotan, "Possibility of Solar Thermal Power Generation Technologies in Nigeria: Challenges and Policy Directions,"*Renewable Energy,* pp. 24-41, 2019.

[16] C. G. Ozoegwi, C. A. Mgbemene and P. A. Ozor, "The Status of Solar Energy Integration and Policy in Nigeria," *Renewable and Sustainable Energy Reviews,* no. 70, pp. 467-471, 2017.

[17] M. Yaqoot, P. P. Diwan and T. C. Kandpal, "Review of Barriers to the Dissemination of Decentralized Renewable Energy Systems," *Renewable and Sustainable Energy Review* pp. 477-490, 2016.

[18] A. S. Barau, A. H. Abubakar and A. I. Kiyawa, "Not There Yet: Mapping Inhibitions to Solar Energy Utilisation by Households in African Informal Urban Neighbourhoods," *Sustainability,* pp. 1- 14, 2020.

[19] M. D. Udayakumar, G. Anushree and A. Manjunathan, "The Impact of Advanced Technological Developments on solar PV Value Chain," *Materials Today,* pp. 1- 6, 2019.

[20] W. Arowolo, P. Blechinger, C. Cader and Y. Perez, "Seeking Workable Solutions to the Electrification Challenges in Nigeria: Miniggrid, Reverse Auctions and Institutional Adaptation," *Energy Strategy Reviews,* vol. 23, pp. 114-141, 2019.

[21] J. O. Mahmud, S. A. Mustapha and K. J. Mezue, "Renewable Energy Transition: A Panacea to the Ravaging Effects of Climate Change in Nigeria," Abuja, 2022.

[22] A. O. Johnson, "Human Capital Development and Economic Growth in Nigeria," *European Journal of Business and Management,* vol. 3, no. 9, pp. 29- 38, 2011.

[23] S. Statkic, N. Arsic, Z. Milkic and A. Cukaric, "Photovoltaic Laboratory Trainer in Student Educations for Renewable Energy Sources," in *7th International Scientific Conferer Technics and Informatics in Education*, Serbia, 2018.

[24] S. S. S. Ranjit, S. A. Anas, S. K. Subramaniam, C. F. Tan and S. H. Chuah, "Development of Solar Educational Training Kit," *International Journal of Engineering and Innovat Technology (IJEIT),* vol. 2, no. 3, pp. 25- 29, 2012.

[25] D. S. Dolan, L. Friedman and J. T. T. Huff, "Solar Trainer for Laboratory Photovoltaic Systems Education," in *2012 North American Power Symposium (NAPS)*, Champaign, IL, USA, 2012.

[26] W. Sun, B. Kramer, Z. Li and J. Stuart, "A Review of the Commercial Trainers and Experiment Kits for Teaching Renewable Energy Manufacturing," in *Proceedings of Tl 2014 IAJC/ISAM Joint International Conference*, Orlando, Florida, 2014.

[27] M. Ali, A. J. S. Wardhana, A. S. Damarwan, Muhfizaturrahman, Yuniarti and W. S. Bagas, "Design and Implementation of Trainer Kit for Hybrid On-Grid Solar Power Generation System," in *Journal of Physics: Conference Series*, 2020.

[28] V. Suwankarjank and Y. Rugwongwan, "Design Thinking Model in Design Education for Thai Product Design Student," *Review of International Geographical Education (RIGE* vol. 3, no. 11, pp. 787-796, 2021.

[29] Electrical Technology, "Electrical Technology," 2013. [Online]. Available: https://www.electricaltechnology.org/2013/05/a-complete-note-on-solar-panel.html. [Accessed 22 07 2022].

[30] H. Wang, F. Yang and X. Xing, "Evaluation Method of Physical Education Teaching and Training Quality Based on Deep Learning," *Computational Intelligence and Neuroscier* pp. 1-9, 2022.

Journal of Engineering, Science, and Technology
ISSN: 2714-2396 | Volume 6, Issue 1

Experimental Determination and Analysis of Harmonic Characteristics of Domestics Electric Lamps

***Ojo A.J[1], Ogunlowo M[2] and Akinwole O.O[3]**

Department of Electrical & Electronic Engineering
The Federal Polytechnic, Ado Ekiti
[1]*ojamesalaba93@gmail.com, [2]jide4tees@gmail.com, [3]akinwole_oo@fedpolyado.edu.ng,

ABSTRACT

The aim of this study is to represent coexistence of harmonics in the power system through an extensive comparison among the different electric bulbs. The Harmonics in the electrical distribution system are the by-products of modern electronics. They are especially prevalent where there are large numbers of nonlinear loads such as compact fluorescent lamp, light emitting diode lamp, personal computers, printers, copiers, hospital equipment, fluorescent lighting and adjustable speed drives. Harmonics do no useful contributions; they degrade the power quality and efficiency in a commercial building or industrial facility. Most people do not comprehend those harmonics have been around for more than 100 years ago. The harmonics at that time were inconsequential and had no detrimental effects. Very often, the operation of electrical equipment may seem normal, but under a certain combination of conditions, the impact of harmonics is enhanced, with damaging results. In this study, we have observed the effects of harmonics and performed a comparison among the four types of electric bulbs which are Light Emitting Diode (LED), Compact Fluorescent Lamp (CFL), Fluorescent Lamp (FL) and Filament Lamp or incandescent lamp. Here, we have evaluated the performance and characteristics of these electric bulbs through experimental set up using Power Logger to evaluate the power quality of the electric bulbs which are common use in the low voltage distribution networks. The results obtained during the experimental analysis exhibit the high number of harmonics produced by LED and CFL bulbs which affirms their contributions to degradation of power distribution networks.

Keywords:lamps, harmonics, power quality, total harmonic distortion.

1. INTRODUCTION

Harmonics are electric voltages and currents that appear on the electric power system because of certain kinds of electric loads. These are the distortion of the utility supplied waveform and are caused by “nonlinear” (distorting) loads, which include motor controls, computers, office equipment, CFLs, light dimmers, televisions and in general, most electronic loads. High harmonics increase lines losses and decrease equipment lifetime. Past to Present, power systems are designed to operate at frequencies of 50 or 60Hz depending on the operating frequency of each country. However, certain types of loads produce currents and voltages with frequencies that are integer multiples of the 50 or 60 Hz fundamental frequency. These higher frequencies are a form of electrical pollution known as power system harmonics[1].

The proliferation of non-linear loads such as Personal Computers, Fluorescent Lamps, Compact Fluorescent Lamps, etc. in commercial buildings has adverse effects on the power quality and the overall performance of distribution networks as these loads inject harmonics into the networks[2]. These adverse effects have been known since the 1980s but the increased concern about in this period is due to the infiltration and popularity of non-linear loads. There is

a need to assess the harmonic behaviour of non-linear loads individually and collectively to determine how this behaviour ties with the power quality of commercial buildings. The increased scrutiny around power quality requirements is due to the sensitivity of equipment of commercial customers as reported by[3] and [4].

Harmonics generated by non-linear loads often cause power quality disturbances such as voltage sags, voltage swells, switching transients, impulses, flickers, notches, etc. [5]. This may cause various technical problems to the devices of customers such as increased heating, maloperation, early aging of devices etc. Poor power quality often results in financial loss to affected customers especially in the industrial and commercial sectors [6].

In this study, our undivided focus is to analyse the characteristics of different harmonic components injected by different electric bulbs to the power system networks. We want to evaluate that which kind of bulb produce huge amount of different harmonic components in the power system and affect the electrical devices of our home appliances.

2. THEORETICAL AND MATHEMATICAL ANALYSIS

The differentiator between linear and non-linear loads is the way the applied voltage relates with the current drawn by the load. The voltage and current of linear loads are sinusoidal and proportional to one another while for non-linear loads either the current, voltage or both are non-sinusoidal and have a non-linear relationship. The non-linear relationship is referred to by [7],[8] and,[9]as harmonic distortion. This linear and non-linear relationship between voltage and current are illustrated by Figure 1a and Figure 1b respectively.

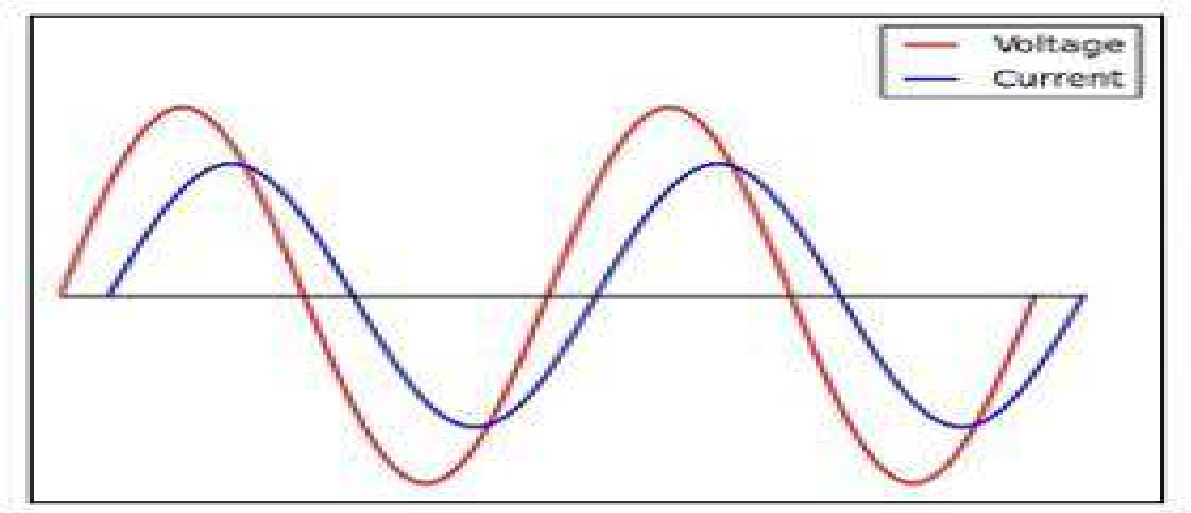

Figure 1 (a): Linear relationship between voltage and current (9).

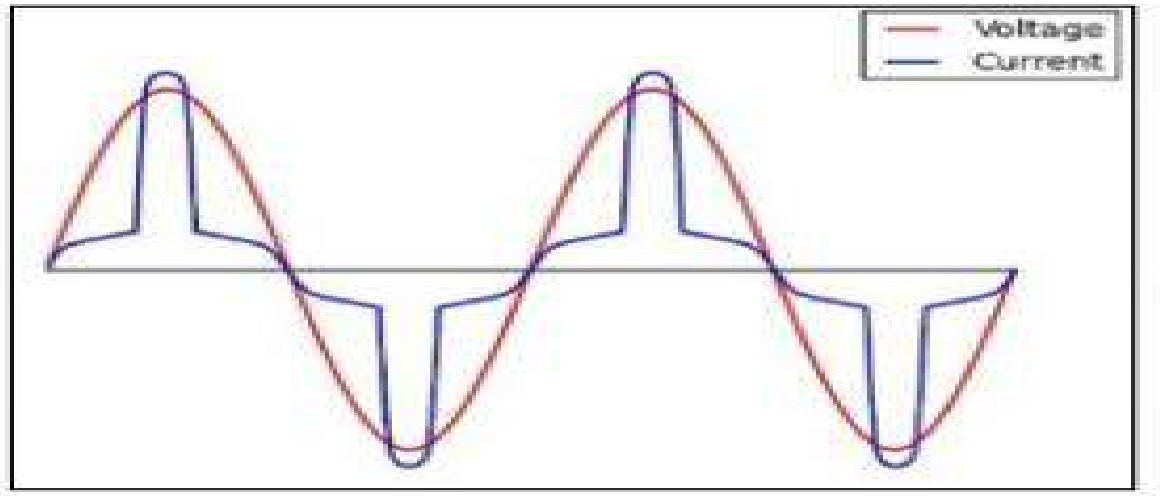

Figure 1 (b): Non-linear relationship between voltage and current (9)

2.1 Harmonic distortion

Harmonics are integer multiples of the fundamental frequency. In Nigeria, the fundamental frequency is 50 Hz, making the 2nd harmonic 100 Hz, the 3rd harmonic 150 Hz, and so on. A distorted waveform results when the waveforms with higher order frequencies are superimposed on the fundamental waveform resulting in a waveform that is no longer sinusoidal.

Even harmonics

Usually, even harmonics exist in small quantities in the power system and are not a great threat under normal operations as they tend to cancel each other out. However, in conditions where equipment malfunctions, large quantities of even harmonics can be generated. This could be exacerbated by harmonic filters in the power system that may excite the resonance of even harmonics. It is shown in[10] that large 4^{th} harmonic currents, generated by rectifiers, flowed in the system that was being analysed as a result of serious resonance and amplification. The 8^{th} and 12^{th} harmonic currents however were minimal and could be attributed to the inductance of the transformer blocking higher order harmonics according to[11] .

Odd harmonics

Odd harmonics, especially triplen harmonics which are odd multiples of the 3rd harmonic (also known as zero-sequence harmonics), are of the greatest concern when analysing the effects of harmonics. It is common for transformers connecting the medium voltage and low voltage to have a Dyn connection. Overheating of transformers due to harmonic currents is a common issue. Contrast to fundamental currents which cancel out in the neutral wire, triplen harmonics add up constructively in the neutral wire. This causes the triplen harmonic current that is in the neutral wire to be three times when compared to the triplen current in each phase which results in overheating of the wire, potential burn off of the wire, and damage to transformers. On the delta side of transformers, triplen currents circulate in the delta connection resulting in overheating of the transformer and additional eddy current losses.

2.2 Harmonic Analysis Methods

The waveforms of both voltage and current associated with nonlinear loads can be obtained at the PCC using appropriate meter such as power quality analyser, spectrum analyser etc.[7]. In the year 1822, Jean Baptiste Fourier[1] postulated that any continuous function with a repetitive pattern can be represented by the sum of the fundamental sinusoidal component, DC component and the higher order sinusoidal components at the multiples of the fundamental frequencies. Harmonic analysis involves the act of calculating the magnitudes and phases of the fundamental and higher order harmonics of period waveforms while the resulting series are known as Fourier series which established the time domain and frequency domain functions.

Fourier Analysis

The common techniques used for Fourier analysis considering the waveform identity, either continuous or discrete signals, are Fourier series, Discrete Fourier Transform and Fast Fourier Transform, these techniques are based on the signals or waveform decomposition or transformation. Any periodic waveform can be decomposed into a Fourier series of DC, fundamental frequency and harmonic terms which contains a sum of simple oscillating functions, namely cosines, sine or complex exponentials.
Considering line current of a waveform represented by a f(t), the decomposition can be done as shown in equation (1).

$$\mathbf{f(t) = \frac{A_0}{2} + \sum_{n=1}^{\infty} [(A_n \cos(n\omega t)) + B_n \sin(n\omega t)]} \qquad (1)$$

Where n = 1, 2, 3, 4, 5, 6, 7…….
A_0 = the average value of the function f (t), A_n and B_n = the coefficients of the series at nth harmonic. Likewise,

$$\mathbf{A_0 = \frac{1}{T}\int_0^T f(t)dt} \qquad (2)$$

$$\mathbf{A_n = \frac{2}{T}\int_0^T f(t)\cos(n\omega t)\,dt} \qquad (3)$$

$$\mathbf{B_n = \frac{2}{T}\int_0^T f(t)\sin(n\omega t)\,dt} \qquad (4)$$

The sine and cosine terms in equation (1) can be converted into polar form to determine the angle using trigonometry function as follows:

$$\mathbf{A_n\cos(n\omega t) + B_n\sin(n\omega t) = \sqrt{A_n^2 + B_n^2} * \frac{(A_n\cos(n\omega t)) + B_n\sin(n\omega t)}{\sqrt{A_n^2 + B_n^2}}}$$

$$= \sqrt{A_n^2 + B_n^2} * \left[\frac{A_n}{\sqrt{A_n^2 + B_n^2}}\cos(n\omega t) + \frac{B_n}{\sqrt{A_n^2 + B_n^2}}\sin(n\omega t)\right],$$

$$= \sqrt{A_n^2 + B_n^2} * [\sin(\theta_n)\cos(n\omega t) + \cos(\theta_n)\sin(n\omega t)] \quad (5)$$

From which trigonometric identity can be applied as follows:

$$\sin(X + Y) = \sin X\cos Y + \cos X\sin Y \quad (6)$$

The resulted polar form is as shown in equation (7),

$$\sqrt{A_n^2 + B_n^2} * \sin(nwt + \theta_n) \quad (7)$$

This implies,

$$\tan(\theta_n) = \frac{\sin(\theta_n)}{\cos(\theta_n)} = \frac{A_n}{B_n} \quad (8)$$

2.3 Harmonic Parameters Formulation in Power System

The most commonly used measure for harmonic analysis is the total harmonic distortion which also determines the distortion factor in the system. If voltage or current signals contains harmonics, the individual harmonic distortion for the signal at any frequency is given as:

$$V_n(\%) = \frac{V_n}{V_1} * 100 \quad (9)$$

$$I_n(\%) = \frac{I_n}{I_1} * 100 \quad (10)$$

Where V_n and I_n represents the voltage and current harmonic of or n respectively while V_1 and I_1 is the voltage and current at the fundamental frequency respectively.

The total harmonic distortion of both voltage and current signals are

$$THD_V = \frac{\sqrt{\sum_{n=1}^{\infty} V_n^2}}{V_1} \quad (11)$$

$$THD_I = \frac{\sqrt{\sum_{n=1}^{\infty} I_n^2}}{I_1} \quad (12)$$

The RMS values of voltage and current can be determine by equations (13) & (14)

$$V_{rms} = \sqrt{V_1^2 * (1 + THD_V^2)} \quad (13)$$

$$I_{rms} = \sqrt{I_1^2 * (1 + THD_I^2)} \quad (14)$$

The apparent power can be resolved using the separation of the RMS current and voltage in fundamental and harmonic terms as shown below[12]

$$S^2 = (V_1^2 + V_h^2) * (I_1^2 + I_h^2) = (S_1^2 + S_N^2)$$

Therefore,

$$S_N = \sqrt{(S^2 - S_1^2)} \quad (15)$$

Where S_N is the apparent power due to harmonics which can also be broken into currents.

2.4 Harmonics Classification

Harmonics are classified according to their frequencies which also determines the sequence and effects of each in a three-phase power system. The classification based on sequence is given in table 1[13]

Table 1: Classification of Harmonics

Harmonics Order	Frequency [Hz)	Sequence	Direction of Rotation	Effects
1, 4, 7, 10, 13, 16, 19..	50,200,350,500...	Positive	Forward	Heating and loss in motors
2, 5, 8, 11, 14, 17, 20..	100,250,400,550…	Negative	Backward	Heating and breaking torque in motors
3,9,12,15,18,21…	150,300,450,600…	Zero	Insignificant	Overloading and Heating of neutral conductor

2.5 Harmonics Distortion Limits

IEEE Standard 519-1992 gives the guidelines for acceptable levels of both voltage and current distortions in power systems network. The acceptable total voltage distortion for voltage level up to 16kV is limited to below 5% while the individual harmonic should not be more than 3%. Other voltage levels and the harmonic limits are shown in table 2 while the current harmonic limits are as shown in table 3.

Table 3: Harmonic Voltage Limits, IEEE Standard 519-1992

Voltage level	Maximum Individual harmonic component (%)	Maximum THD (%)
<69kV	3.0	5.0
69kV<Vn≤161kV	1.5	2.5
>161kV	1	1.5

Table 3: Harmonic Current Limits, IEEE Standard 519-1992

Maximum Harmonic Current Distortion, % of I_L						
Vn≤69kV						
I_{sc}/I_L	h <11	11<h<17	17<h<23	23<h<35	35<h	TDD
<20	4.0	2.0	1.5	0.6	0.3	5.0
20<50	7.0	3.5	2.5	1.0	0.5	8.0
50<100	10.0	4.5	4.0	1.5	0.7	12.0
100<1000	12.0	5.5	5.0	2.0	1.0	15.0
>1000	15.0	7.0	6.0	2.5	1.4	20.0
69kV<Vn≤161						
<20	2.0	1.0	0.75	0.3	0.15	2.5
20<50	3.5	1.75	1.25	0.5	0.25	4.0
50<100	5.0	2.25	2.0	0.75	0.35	6.0

100<1000	6.0	2.75	2.5	1.0	0.5	7.5
>1000	7.5	3.5	3.0	1.25	0.7	10.0
Vn >161kV						
<50	2.0	1.0	0.75	0.30	0.15	2.5
≥ 50	3.0	1.5	1.15	0.45	0.22	3.75
**All power generation equipment is limited to these values of current distortion regardless of actual I_{SC}/I_L						

3. EXPERIMENTAL SET-UP AND MEASUREMENT (METHODOLOGY)

This section presents the methodology used for the power quality measurement of some commonly used electric lamps for residential and commercial buildings as applicable low voltage distribution networks in Nigeria. In this study Light Emitting Diode, Compact Fluorescent, Choke/ballast Fluorescent and Filament bulbs are considered while voltage, current, Active Power waveforms, Total Harmonic Distortions (THDs), and the power factor of each bulb are the parameters considered. All the measurements were carried out in the Power System Laboratory at Department of Electrical and Electronic Engineering of the Federal Polytechnic, Ado- Ekiti using DENT Power Logger with high resolution for effective power quality measurement. Figure 2 and Figure 3 show the schematic diagram and experimental setup of the methodology used.

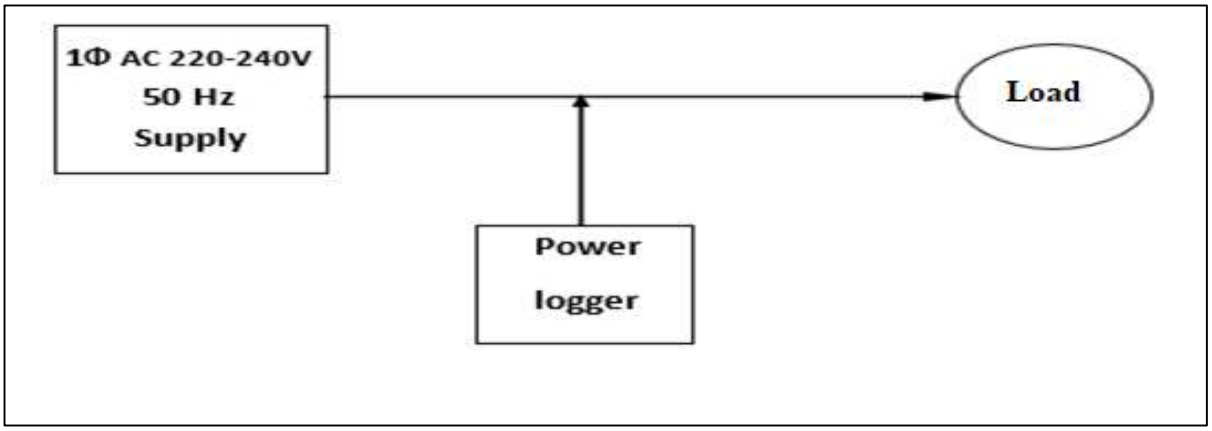

Figure 2: Schematic Diagram for the Experimental Setup

Figure : Experimental setup for power quality measurement with DENT Power logger

4. RESULTS AND DISCUSSION

Following theoretical analysis in Section II, experimental analysis of power quality parameters such as voltage, current, power waveforms, individual harmonics, THDs and power factor of the bulbs are done in this section to validate the pollution of distribution networks through the use of energy saving bulbs if not well monitored and controlled.

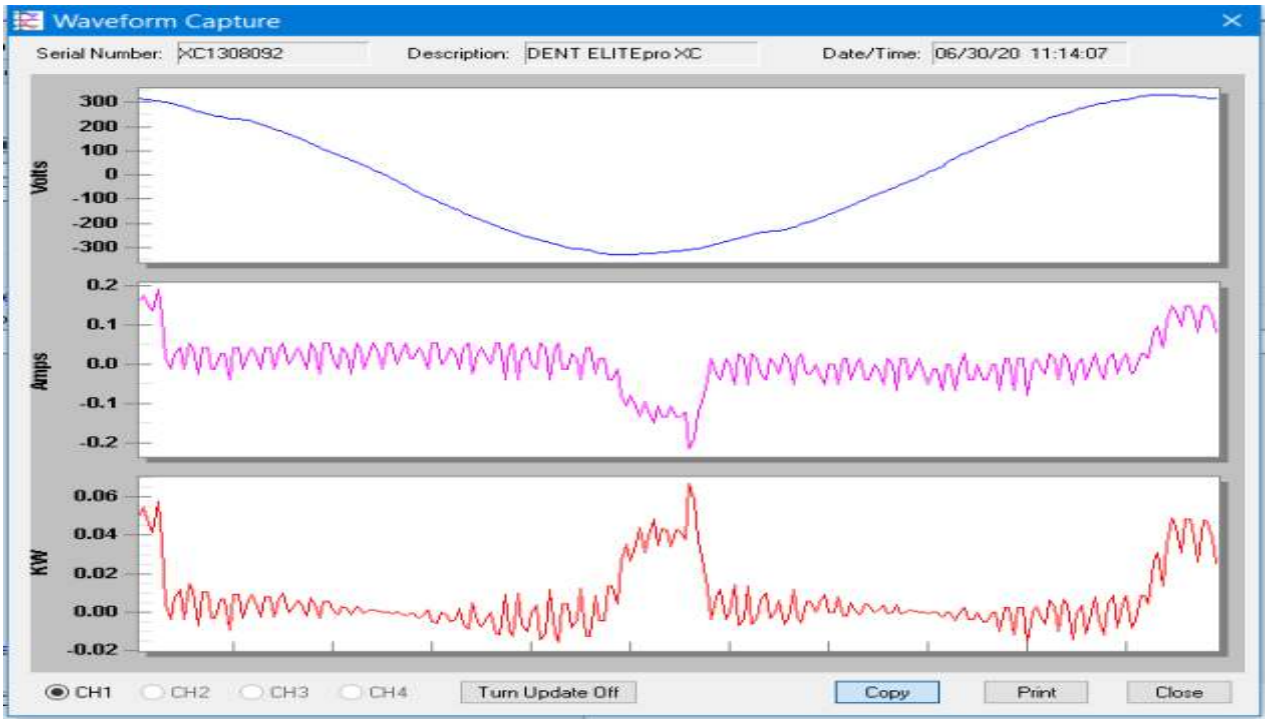

Figure 4: Voltage, Current and Active Power Waveforms of 8W_ LED

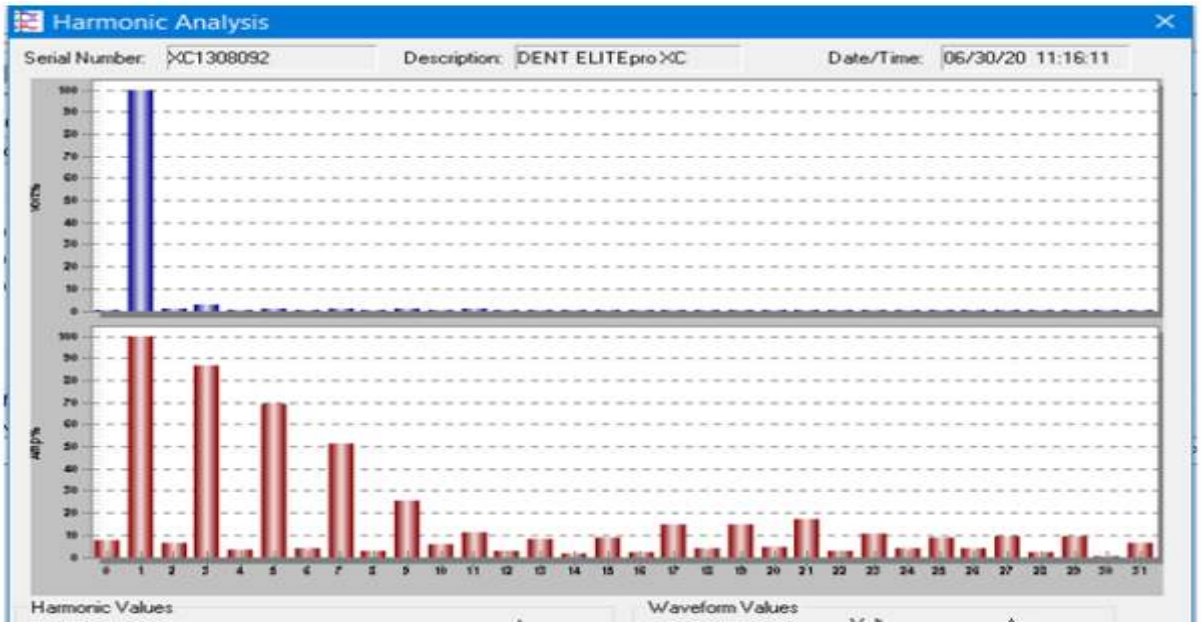

Figure 5: Voltage and Current Harmonics Spectrum of 8W_LED

Light Emitting Diode Lamp: In figures 4 and 5 above, the current and voltage waveforms of LED bulb show the presence of harmonic distortion with decrease in the individual harmonic distortion from 3rd order to 9th order while there is an increase 15th up to 21st harmonics.

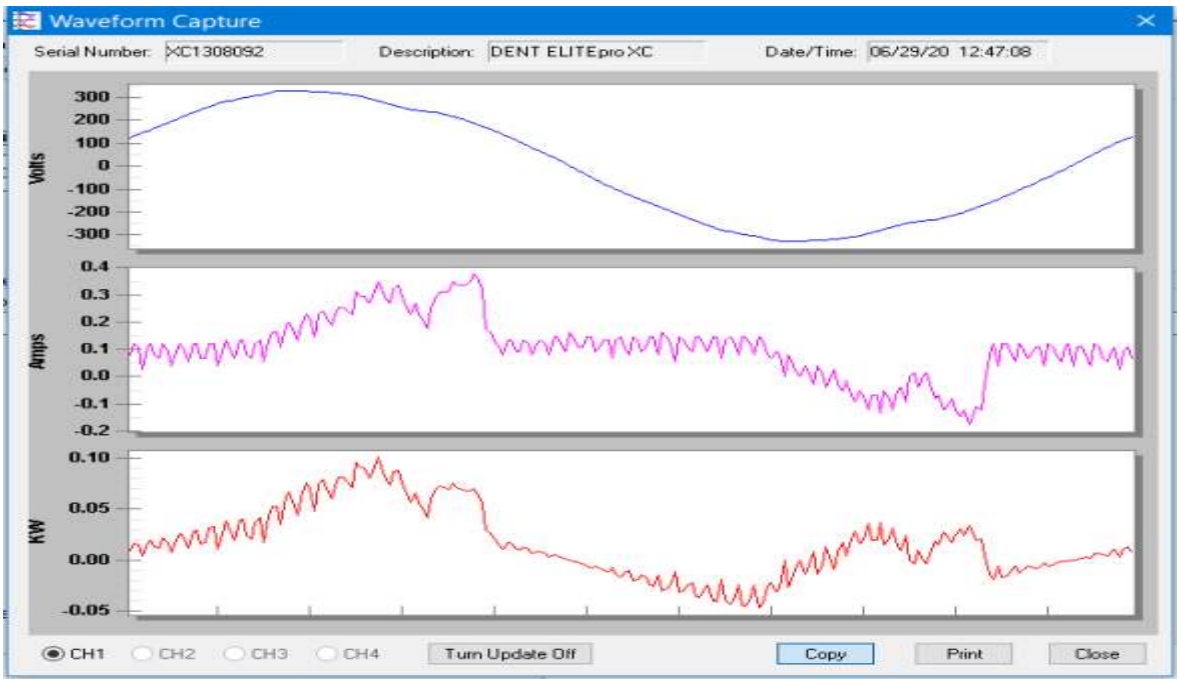

Figure 6: Voltage, Current and Active Power Waveforms of 40W_CFL

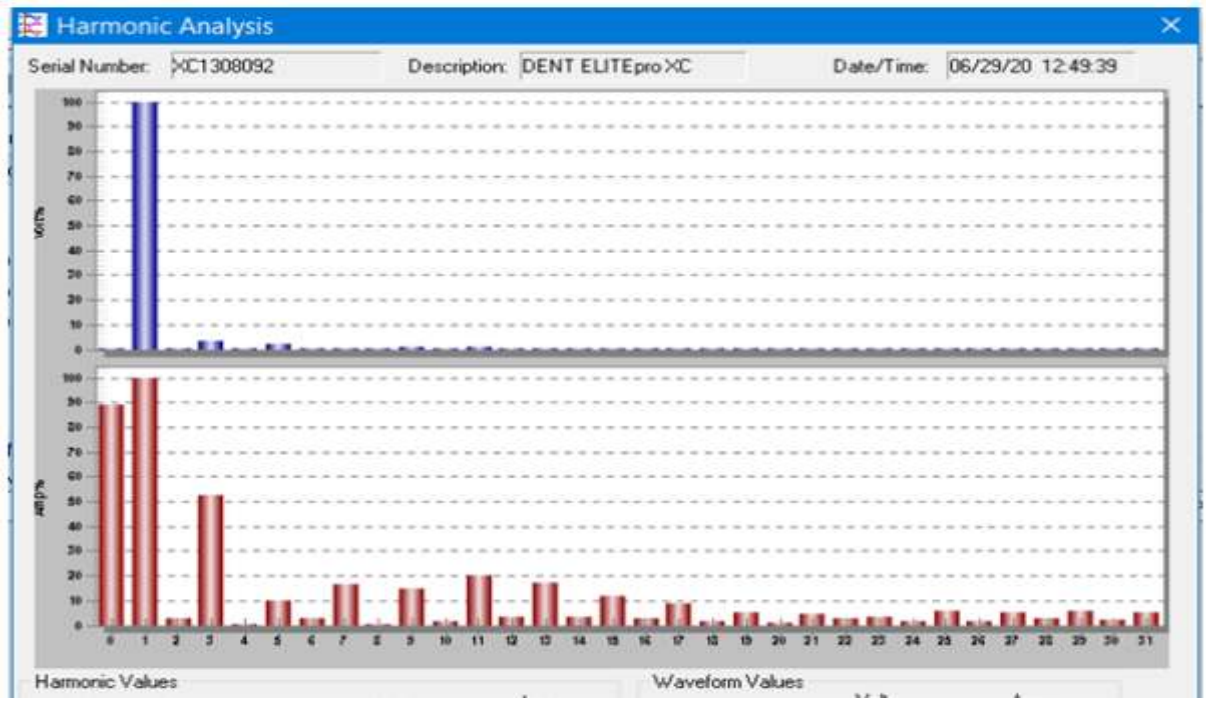

Figure 7: Voltage and Current Harmonics Spectrum of 40W_CFL

Compact Fluorescent Lamp: In figure 6 above, the level of distortion in CFL is on the high due to switch mode power supply embedded in the design which depicts high level of harmonic distortion. There is also a d.c component in the harmonic spectrum shown in figure 7. It is shown further, the presence of odd harmonics from 3rd harmonic order which can lead to pollution of the distribution networks if the usage is not monitored of controlled.

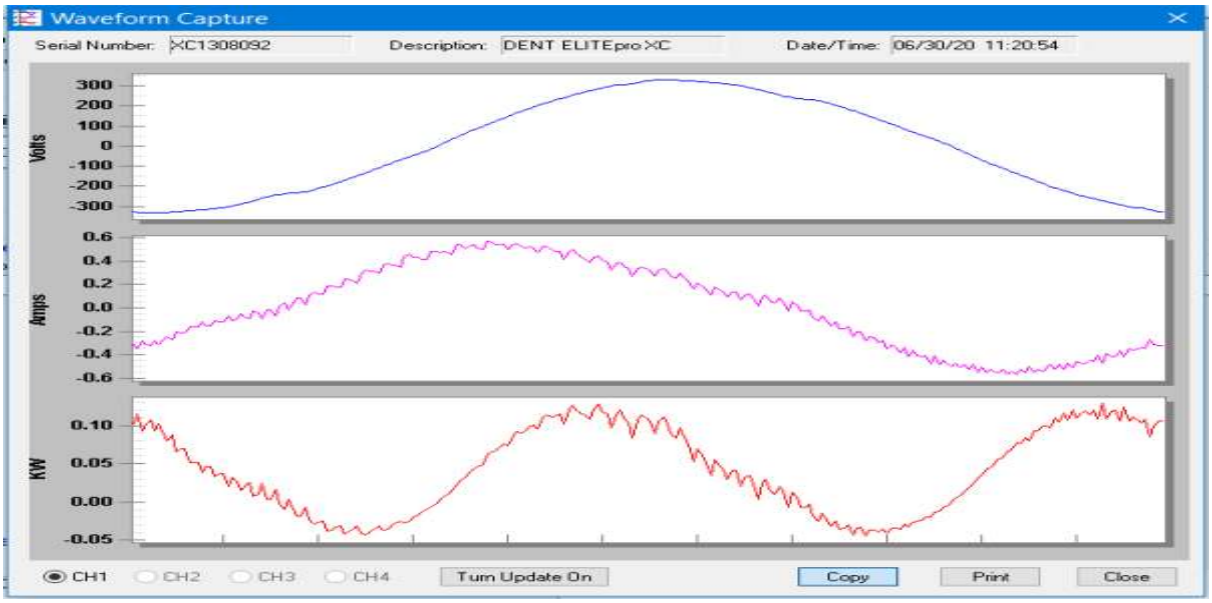

Figure 8: Voltage, Current and Active Power Waveforms of 36W_FL

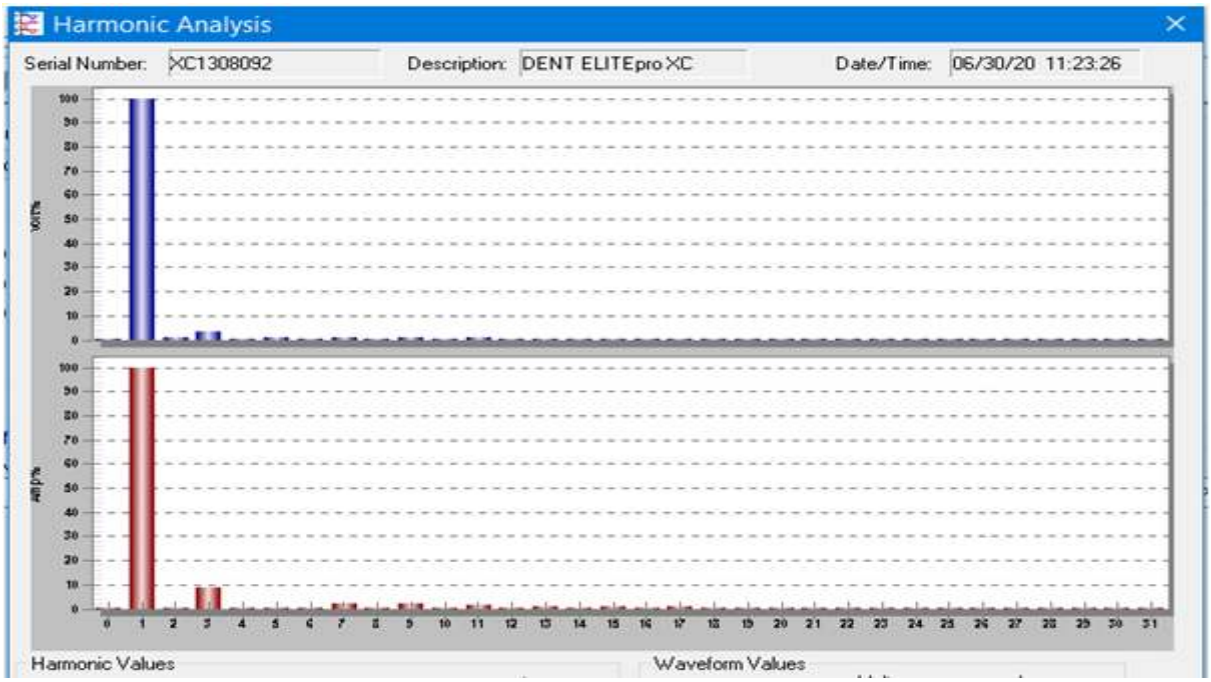

Figure 9: Voltage and Current Harmonics Spectrum of 36W_FL

Fluorescent Lamp: The voltage and current waveforms of a choked fluorescent lamp are shown in figure 8, the current waveform is almost in phase with the voltage waveform which depicts the linearity of the current as compared to LED and CFL bulbs. In figure 9, the harmonic spectrum shows a very small distortion as displayed by less than 10% 3rd harmonics.

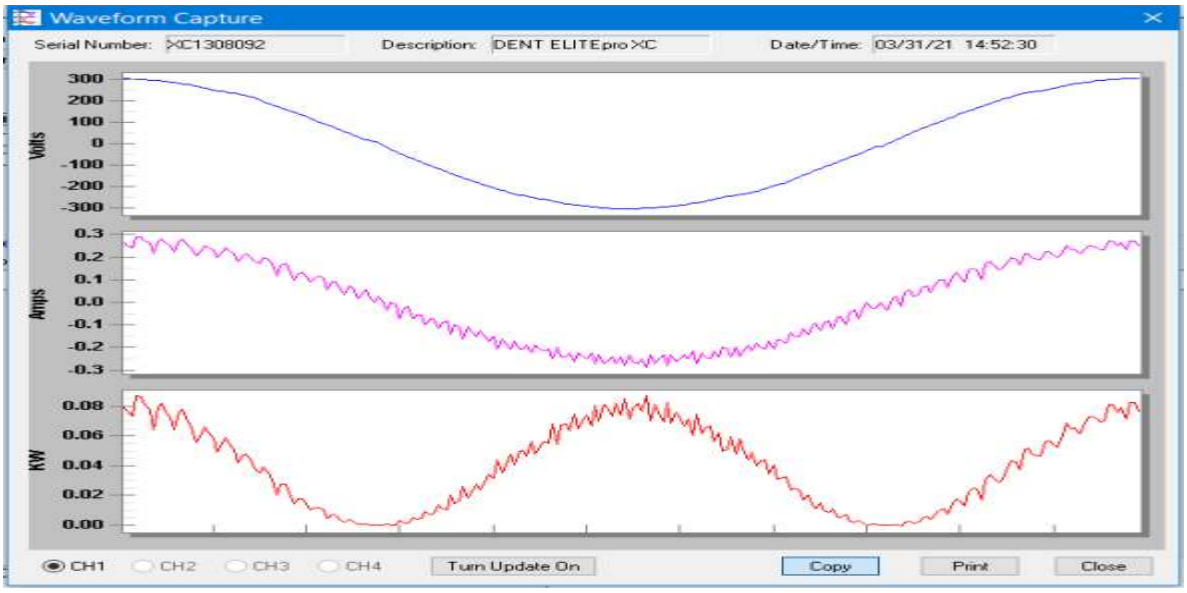

Figure 10: Voltage, Current and Active Power Waveforms of 36W_FL

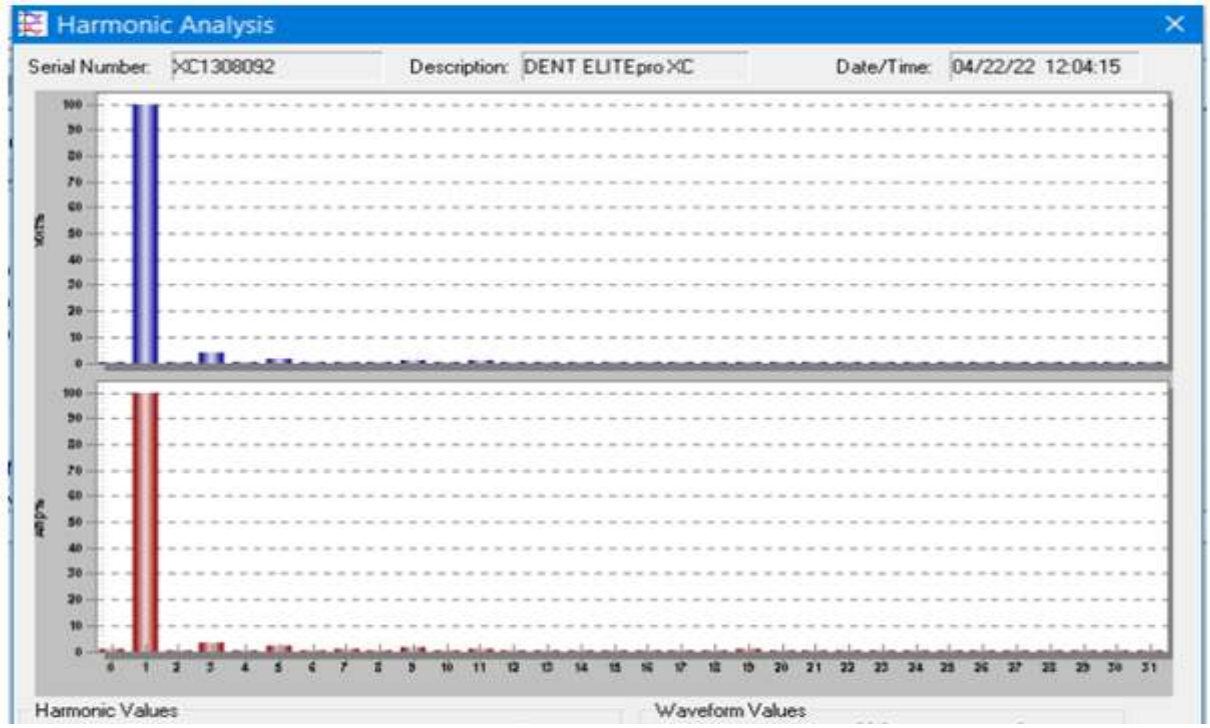

Figure 11: Voltage and Current Harmonics Spectrum of 60W_Filament Lamp

Filament Bulb: As in this bulb, because of its pure resistive in nature, harmonics in this type of bulb is minimum which is close to zero. The unity power factor of these lamps also indicates its zero harmonics. The waveform in figure 10 also depicts that only system frequency is present.

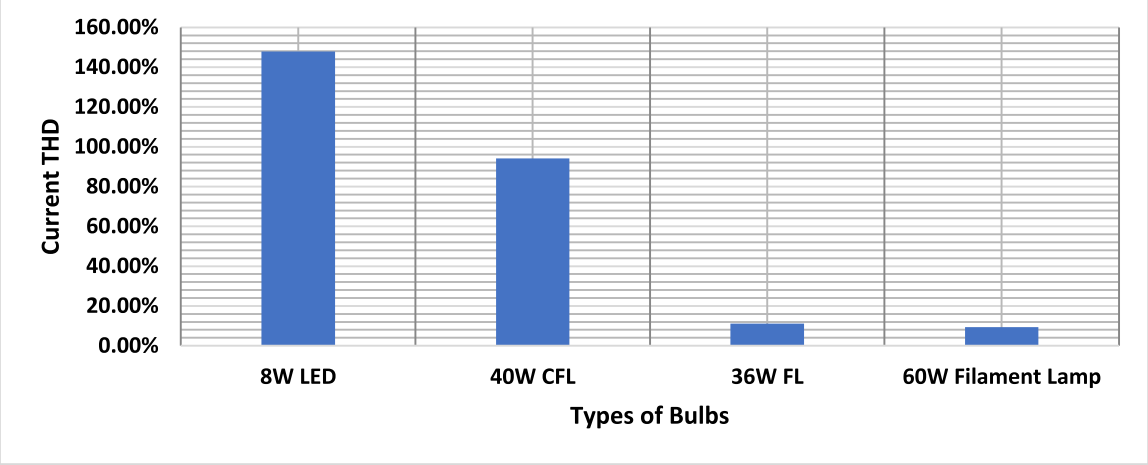

Figure 12: THDs of the Electric Bulbs

THDs: Figure 12 shows the Current THD of LED, CFL, FL and Filament bulb in which LED and CFL have high harmonic distortions of 145% and 92% respectively as shown in figures 4-7. While fluorescent and filament bulbs have little or no distortion which have no dangerous effect on the distribution networks.

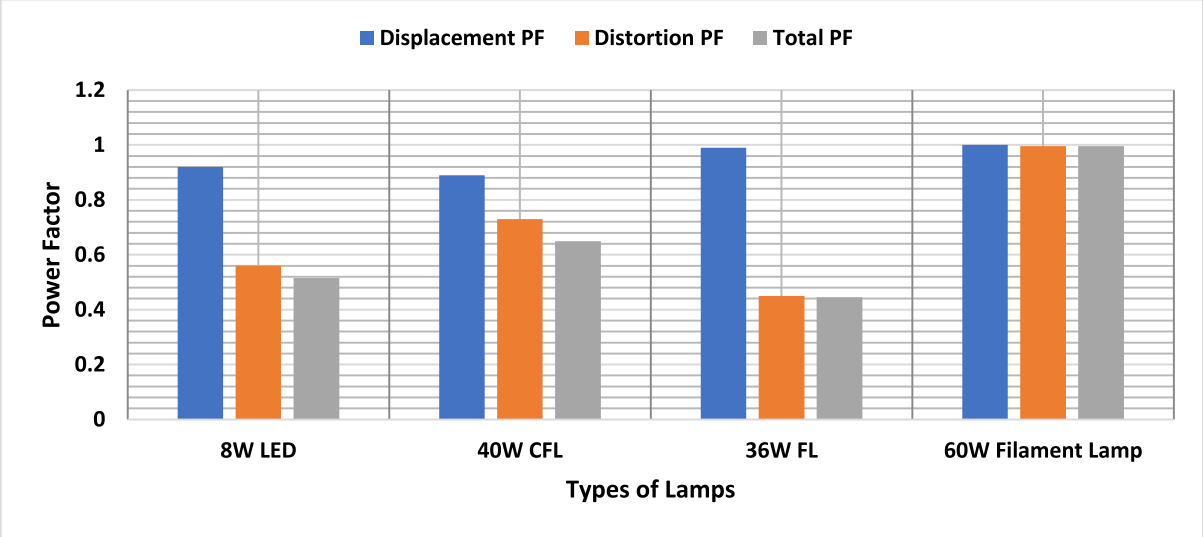

Figure : Power Factor of the bulbs

Power Factor: Figure 13 shows the relationship between the displacement power factor, distortion power factor and the true power factor. In power system analysis, the displacement power factor is the same with true power factor under pure sinusoidal waveforms of voltage and current. As shown in the figure 13, filament lamp maintained that principle but differs in other three bulbs due to harmonic distortions.

5. CONCLUSION

Based on the literature reviewed and experimental measurements of some electric bulbs, commonly used in residential and commercial electrical installation, and the results obtained using a Power logger, it has been shown that energy saving bulbs such as LED and CFL are harmonics injecting loads which affects the overall power quality of the system. These loads are mostly used in the distribution networks feeding residential and commercial sectors as applicable in most of the distribution companies in Nigeria. Hence, there is a need for the distribution companies to monitor and assess the recent power quality issues due to the proliferation of nonlinear loads resulted from energy efficiency measures. In other to improve the power quality and reduce losses in our distribution networks, it therefore recommended that Distribution Companies should ensure adequate and regular power quality assessment of their networks through collaboration with Academic Institutions and there should be proper awareness on power quality issues affecting the distribution networks with proper assessment to be done on electrical installations before adding more energy efficient loads to avoid dangerous pollution of the entire network.

REFERENCES

[1] K. M. Seraphin, "A comprehensive study of Power System Harmonics," University of Johannesburg, Johannesburg, 2013.

[2] P. Puttaswamy and P. Shilpa, "A Review on Power Quality Issues in Power Systems," *International Journal of Industrial Electronics and Electrical Engineering,* vol. 2, no. 10, pp. 64-69, 2014.

[3] J. M. Ghorbani and H. Mokhtari, "Impact of Harmonics on power Quality and losses in Power Distribution Systems," *International journal of Electrical and Electronic Compu Engineering,*vol. 5, no. 1, pp. 166-174, 2015.

[4] R. Herman, C. Gaunt and G. Raubenheimer, "Negative effects of energy-saving, non-linear loads on lv systems: causes and recommendations," *SOUTH AFRICAN INSTITUTE C ELECTRICAL ENGINEERS_ARJ,* vol. 99, no. 01, pp. 32-40, 2008.

[5] K. Anne, S. Wunna and Z. Aung, "Analysis of Harmonic Distortion in Non Linear Loads," in *The Fisrt International Conference on Interdisciplinary Research and Develo* Thailand, 2011.

[6] A. Ojo, K. Awodele and A. Sebitosi, "Power Quality Monitoring and Assessment of a Typical Commercial Building.," in *IEEE AFRICON*, Accra, Ghana, 2019.

[7] J. Arrillaga and N. Watson, Power Ssytem Harmonics, Chichester: John Willey & Sons Ltd, 2003.

[8] C. L. Collocott, "Harmonic Emission of Non-Linear Loads In Distribution Systems & Their Measurements," Department of Electrical Engineering, University of Cape town, Cape town, 2015.

[9] G. Prachi, "Effects of Harmonics on active power flow and apparent power in the power system," in *International conference on emerging trends in Engineering*, Nagpur,India, 2009.

[10] J. Bollen, Understanding Power Quality Problems: Voltage Sags and Interruptions, New York: Wiley-IEEE Press, 2000.

[11] S. Jhampati, J. Chakraborty, S. Lahiri and T. Halder, "Assessment of Power Quality," in *Third International Conference on Computer, Communication, Control and Inform Technology (C3IT)*, Hooghly, 2015.

[12] M. J. Ghorbani and H. Mokhtari, "Impact of Harmonics on Power Quality and Losses in Power Distribution Systems," *International Journal of Electrical and Compute Engineering (IJECE)*, vol. 5, no. 1, pp. 166-174, 2015.

[13] M. P. Rajashekar and Y. R. Udyakumar, "Power Quality Issues in Electrical Distribution Systems and Industries," in *National Conference on recent Advances in control Strategies for integration of distributed Generation sources* , Bangalore, 2016.

[14] B. Adenle, K. Adekusibe and A. Oyedeji, "A Critical Review of Power Quality Issues in Nigeria," Academia, 13 Nov 2014. [Online]. Available: www.academia.edu/26056914. [Accessed 5 March 2020].

[15] A. Batista and K. Awodele, "Assessment of Harmonics Generation on an Off-Shore Mine and Determination of Mitigation equipment," in *IEEE AFRICON*, Nairobi, Kenya, 2009.

[16] M. Abu-bakar, "Assessments for the Impact of Harmonics Current Distortion of Non-linear Load," in *Power System Harmonics Transmission and Distribution Conferenc Exposition*, Latin America, 2008.

[17] R. Dugan, M. McGranaghan, S. Santoso and H. Beaty, Electrical Power Systems Quality, New York: McGraw-Hill, 2004.

[18] IEEE, "IEEE Recommended Practice and Requirements for Harmonic Control in Electric Power Systems, IEE Std – 519 – 2014," IEEE, 2014.

Journal of Engineering, Science, and Technology
ISSN: 2714-2396 | Volume 6, Issue 1

THERMOECONOMIC ANALYSIS OF ALTERNATIVE FUELS ON ROTARY KILN PERFORMANCE OF OBAJANA CEMENT PLANT

Salawu, Abdulrazaq Aliyu,[1] Afolabi, Eyitayo Amos, [1]*and Abdulkareem, Ambali Saka[1]
[a]Department of Chemical Engineering, Federal University of Technology Minna-Nigeria.
*Corresponding author: E-mail: elizamos2001@yahoo.com Phone: +2348105262842

Abstract
A process model for the operation of rotary kiln in the cement production process was developed using Aspen Plus to study the effect of alternative fuels from used tyre, municipal waste (MSW) and sugarcane bagasse on clinker quality, emissions and thermal stability by introducing 5%, 10%, 15%, 20%, 25% and 30% of the alternative fuel mix with coal. The three fuels increased the Lime Saturated Factor (LSF) compared to 100% coal, but the observed values were within acceptable limits. Sugarcane bagasse had the best silica ratio (SR between 2.49458 to 2.49405), with Used Tyre and MSW having a low silica ratio below 1.6. However, the low SRs were complemented by their alumina ratios (ARs). Used Tyre and Sugarcane bagasse can maintain the kiln temperature (1640 ^{0}C to 1690 ^{0}C) up to the reference case. Tyre and MSW can reduce CO_2 emission, but sugarcane bagasse does the opposite with a capacity of up to 9.67 kg/tonne clinker increment in emission at 30% fuel mix. The three alternative fuels considered were found to increase NO_x emissions. Used Tyre was the most preferred alternative fuel due to its ability to reduce CO_2 emission while ensuring thermal stability in exergy efficiency and kiln outlet temperature, coupled with its worldwide availability. However, caution must be employed to monitor its SO_x emissions; hence it should not exceed 20% in the fuel mix to keep SO_x emissions below 310 mg/Nm^3. The alternative fuels were more cost-effective (as higher configurations resulted in lesser costs, particularly in MSW with a cost-saving up to 613.92 $/hr in 30% fuel mix) but less efficient than coal in terms of exergy, with sugarcane bagasse as the potential best (difference of less than 3%). It can be inferred from the results obtained that the development of alternative fuel from blending sugarcane bagasse and coal for a rotary kiln is economical, reduces emissions and feasible.

Keywords: Cement, Kiln modelling, Energy performance, Alternative fuel, Emission.

1.0 Introduction

Cement production involves a mixture of limestone and clay; it requires a kiln temperature of 1500 degrees Celsius [11], [8]. Attaining this high temperature during cement production is possible by burning fossil fuel which is considered expensive [8]. Aside from the high price of fossil fuel, the environmental impact of burning fossil fuel also affects its wide acceptance for industrial application. For instance, study has shown that greenhouse gas and about 900kg of CO_2 are being released into the environment. This is attributed to the high amount of energy needed during the chemical reaction of the raw mix. This is why cement industry is held accountable for about 5–6% of anthropogenic CO_2 emissions. The emission causes about 4% of global warming [12], [6].

It is high time the world looked for sustainable alternatives to the daunting effects of finite fossil fuel. The resources of global fossil fuel, high prices and the damaging effect on our surroundings calls for the more reason to develop alternative fuel that can replace the existing energy for cement production process. This replacement is the fossil fuel. An alternative fuel source can replace fossil fuel in the cement production process. It provides trustworthy solution toward reducing fossil fuel usage and mitigation of pollutant emissions. It can be sourced from industries, agriculture, and municipals [4], [5], [10]. This is further necessitated by the high thermal requirement of the cement production process.

Despite the numerous thermal performance studies on the cement production process, there has been a lack of extensive studies on the thermoeconomic analysis of alternative fuel performance of the cement rotary kiln system, particularly on how the operational parameters of the rotary kiln affect its performance. Minimizing energy cost and environmental effect is the primary goal of cement and concrete production industry. Analytical decision tools are needed in providing vital pieces of information to recognize possible improvement in rational management of raw materials.

Dwindling resources coupled with environmentally unfriendly emissions has necessitated exploring alternative fuels used in the energy-demanding cement industry. Other sources of fuel offer the cement industries the chance to use minimal fossil-fuel derived from CO_2 emissions, reduce fuel costs and add to the conversion of waste streams at a time of increased pressure on landfilling of wastes. However, computer simulation provides the answer to what happens to a cement clinker production process after a switch of fuel.

Problems regarding clinker quality and emission have been related to the initiation of other fuel source in the cement manufacturing process, thus before the employment of the alternative fuel in this complex process, a detailed identification and assessment of all underlying factors must be exhaustively considered. Considering the associated economic risks with alternative fuel experimentation has limited research being conducted to test the cement plant. Alternatively, the process model has been regarded to proffer a realistic solution of testing series of alternatives fuels and forecasting corresponding clinker quality and pollutant emission changes.

Computational fluid dynamics (CFD) is a software package that is use to model majorly the kiln section of a cement production process [1], [3]. The use of Aspen Plus software is a completely different approach which focuses on the clinker chemistry, thermodynamics properties of materials and reaction stoichiometry, this has been reported [7],[16].

Azad Rahman et al; [2], Emad et al; [3] and Miller [9] came up with a model in form of a process of a precalciner kiln system. This was done using Aspen Plus software to bring about the effect of alternative fuels on energy performance and environmental pollutants generally. The other fuels used include; tyre, municipal solid waste (MSW), bone meal (MBM), plastic waste, sugarcane bagasse and meat. Using the cement plant as a reference, the developed energy and mass balance of the system was validated. The clinker's quality was also investigated by the group to determine its effect as an alternative fuel.

The outcome of the test has shown with the use of alternative fuels with a 20% mix in coal can be used to achieve a result that is about 4.4% reduction in CO_2 emissions and up to a 6.4% reduction in thermal energy required.

Research has also proved that other fuel source had a reduced influence on the quality of clinker with an exception of MSW. Generally, MBM can reduce energy requirement and CO_2 emissions; this makes it a better option than others.

From this reported work, it would be derived that economic and exergetic efficiency of alternative fuels was not investigated. Hence, this work would consider the thermo-economic analysis and exergetic efficiency of alternative fuels sources of Obajana cement rotary kiln.

The recent research developed a model for the Kiln of the cement manufacturing process, which was used to simulate the flue gas formation while using selected alternative fuels such as used tyre, Sugarcane baggasses and Municipal Solid Waste (MSW). Aspen Plus-based is the model developed. The model was verified using Obajana Cement Industry's plant data for coal used as the primary fuel in the burning zone. The validated model was run with the three selected alternative fuels, Tyre, MSW and Sugarcane bagasse, to study predictions of changes in emission, kiln environment, clinker quality and cost-effectiveness before the simulation results were used to optimize the usage of selected alternative fuels.
The result of this study will inform the use of locally sourced alternative fuels from wastes in the cement production industry. This kind of study in the cement production industry is unprecedented in Africa. It will add to the body of knowledge on the conversion of waste to wealth while fostering environmental friendliness of the cement production process.

2.0 Methodology

2.1 Extraction of data

Stream composition, temperatures, pressures and flows are all the needed operating data. The instrumentation diagram of the rotary kiln in the Obajana Cement Industry was collected from the plant operator.
The flow diagram was carefully studied to extract all the needed and available information, feed and product need for the simulation of the kiln using Aspen Plus was also collected.

2.2 Modelling

The cement manufacturing process is complex and it includes several endothermic and exothermic reactions. Heat transfer is not an exemption in this process. It is being transferred in the three phases (solid, liquid and vapor) of different materials.
Simulation Aspen Plus was used to develop the process model. Furthermore, it was built in accordance to the reference plant specification. This was achieved using about 6000-day clinker production capacity or tones.
Below are the assumptions made without changing the principles to simplify the model.

1) In two different reactors, the burning zone, the coal and other fuel combustion will occur.
2) The combustion of fuels and the calcination process lead to the production of CO_2.
3) Fuel combustion lead to the generation of NO_x from the kiln.
4) In the clinker formation process, ash is involved. From the ash analysis of coal and alternative fuel.
5) To facilitate pyroprocesses, all the clinker formation reactions in the kiln took place in three separate reactors.
6) Throughout the entire model, air linkages were not considered.

Redlich Kwong Soave-Boston Mathias (RKS-BM) property method was selected for the suitability for coal and solid fuel combustion. All thermodynamic properties use the Redlich-Kwong-Soave (RKS) cubic equation of state with the Boston-Mathias (BM) alpha function for all its process.
Throughout the simulation, the MCINCPSD sub stream (MIXED, CISOLID and NC streams) with particle size distribution option was used. The feed to the kiln contained conventional part and all fuels were considered non-conventional.
HCOALGEN and DCOALICT attribute was used in the proposed model based on the elemental analysis of fuelsto calculate enthalpy and density respectively. This is for coal and selected alternative fuels.

Equilibrium and non-equilibrium equations can be used to generate a realistic output. Different reactor blocks were chosen for the process model.
Due to the introduction of alternative fuels all the output data regarding the composition of clinker and the stack gas provides vital information about any possible changes due to the introduction of alternative fuels in the system. Collected plant data was used to validate the model from clinker composition and pollutant emission perspective.
The exergoeconomic assessment were performed by the Specific exergy costing method (SPECO) to decide the potential enhancements in its efficiency and cost-viability.

2.3 Model equations

There is a need for the power in the rotary kiln to be balanced. Therefore, the average temperature of the walls was used in the mode.
The following equations for the gas, and solid walls, respectively [15] written.

$$Q = m_i Cp_i \Delta T_i \quad (1)$$

Where m_i($i$mass flow rate in kg/s), Cp_i($i$specific heat capacity in kJ/(kg·°C)), ΔT_i(i temperature change according to°C), Q (heat in kJ) is, and $m_i$replaced by equation two:

$$m_i = \rho_i v_i A_i \quad (2)$$

Where ρ_i(i density in kg·m^3), v_i(i speed in m/s), A_i(i surface area in m^2). Therefore, the temperature in the gas phase transport equations are:

$$A_g C_{pg} \rho_g v_g \frac{\partial T_g}{\partial z} = \beta_1 (T_w - T_g) + \beta_2 (T_w - T_g) + Q_{comb} \quad (3)$$
$$A_g C_{pg} \rho_g v_g = \rho_i v_i A_i$$

where T_w (wall temperature by °C), Tg(gas temperature in °C), Ts(solid temperature in °C), β_1 (heat transfer coefficient between the wall and the gas in W/°C), β_2 (transfer coefficient between the solid and the gas temperaturein W/^{0}C), Q_{comb}(combustion heat in W), v_g(gas velocity in m/s), ρ_g(average gas density of 0.85 kg/m3),$\partial T_g/\partial z$ (gas temperature change over the elements in °C/m), C_{pg}(gas specific heat capacity of 1173.8 kJ/kg/°C)and A_g(of gas per m^2) and $v_g$obtained from the following equations:

$$v_g = \left(\frac{m_f + m_a}{A_g \rho_g}\right) \quad (4)$$

Where m_f (fuel mass flow rate) and m_a (air mass flow rate) is:

$$A_g = \frac{r_i^2}{2}(\rho - sin\rho) \quad (5)$$

Where r_i (radius of the kiln according to m) and p (surrounded by a solid angle 3π/2) and the solid phase are:

$$A_s C_{ps} \rho_s v_s \frac{\partial T_s}{\partial z} = \beta_2 (T_g - T_s) + \beta_3 (T_w - T_s) + A_s Q_c \quad (6)$$

Where β_3 (heat transfer coefficient between the wall and solid in terms of W/^{0}C), Q_c(heat of reaction in terms of W), v_s(solid velocity in m/s), ρ_s(solid density of 890 kg/m3), $\partial T_s/\partial z$ (solid temperature changes over the elements in °C/m), Cp_s(specific heat capacity of solid 1089.97 kJ/kg/°C) is, As (solid surface in m^2) and $v_s$calculated from the following equations:

$$v_s = \frac{\dot{m}_s}{A_s \cdot \rho_s} \quad (7)$$

$$A_s = \frac{r_1^2}{2}(2\pi - p + \sin p) \quad (8)$$

2.2 Process simulation and description

The modeled Kiln in the simulation environment of Aspen Plus Software is as shown in Figure 1 below.

Journal of Engineering, Science, and Technology
ISSN: 2714-2396 | Volume 6, Issue 1

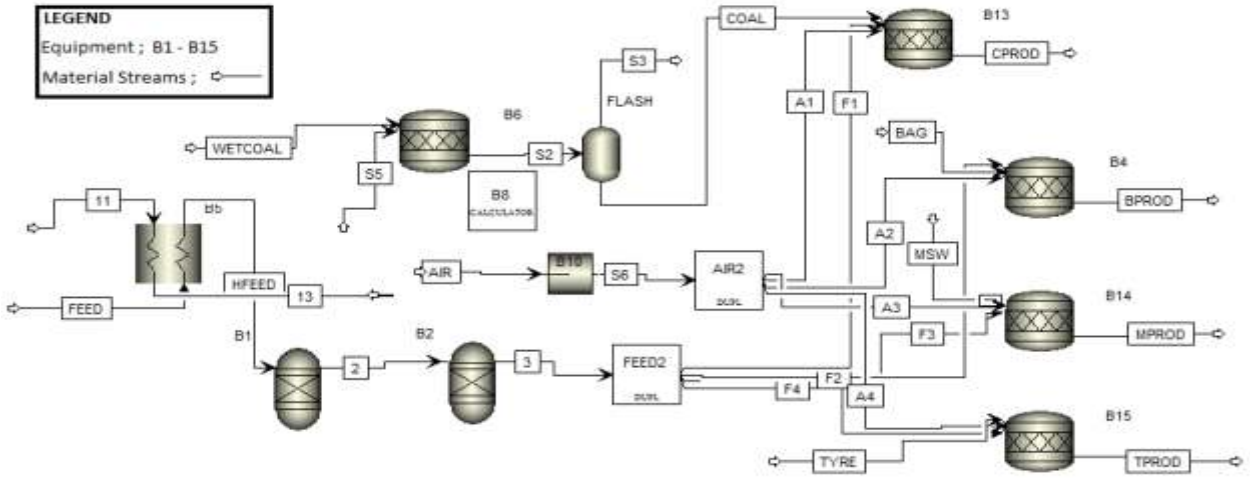

Figure 1: Converged Model of Rotary Kiln System (Aspen Plus v8.0)

A conventional stream containing feed to the kiln section was passed through a heat exchanger train B5 to raise the feed to a reaction temperature of 850 ^{o}C. The hot product of the heat exchange (HFEED) was then passed into two sets of RGibbs reactors B1 and B2, operating at 1000 ^{o}C and 1400 ^{o}C, respectively, where reactions such as the formation of alite and belite took place. The product of the reactors (Stream 3) was passed into a Duplicator block FEED2, which was used to duplicate stream three into four streams (F1 – F4) that served as feed to four RSTOIC reactors (B4, B13, B14 and B15). Wet coal (WETCOAL), a nonconventional stream of raw coal, was treated with nitrogen gas (Stream S5) in an RSTOIC reactor B6. A calculator block (B8) was used to actuate the coal drying process, and the product (Stream S2) was passed into a separator (FLASH) where the nitrogen gas and water were flashed off from the top (Stream S3), and the treated coal (COAL) from the bottom was sent as fuel to block B13; one of the four RSTOIC reactors. Air (AIR) at 70 ^{0}C and 1 bar were passed to a compressor block B10, and the outlet stream (S6) was sent to a Duplicator block AIR2, which was used to duplicate stream S6 into four streams (A1 – A4) that respectively supplied air for combustion reactions that took place in the RSTOIC reactors. Having served one of the RSTOIC reactors (B13) with fuel (COAL), air (A1) and clinker feed (F1), the system represented the existing process in the understudied plant. The product stream of the reaction was named “CPROD”. The three remaining RSTOIC reactors were served with alternative fuels. A non-conventional stream with the composition of bagasse fuel (BAG) was introduced to the reactor block B4, which had air (A2) and clinker feed (F2) also attached to it. The product stream of block B4 was named “BPROD”.

Similarly, streams with nonconventional components of MSW and TYRE were respectively served as fuels to RSTOIC reactor blocks B14 and B15. The reactor block B14 had air (A3) and clinker feed (F3) also attached to it, and the product stream was named “MPROD”. Reactor

block BI5 also had a supply of clinker feed (F4) and air (A4) with its product stream called "TPROD".

3.0 Results and Discussion

This paper reports the Thermo-economic analysis of alternative fuel usage on rotary kiln performance of Obajana cement plant using Aspen plus simulation software. Therefore, the validation of simulated results needs to compare to plant data of coal measured in kg/kg clinker. Observed results from the simulation were compared with plant data and presented in Table 1. In 1 kg of clinker, the significant difference was 0.0097 in the composition of CaO (in oxide form) and 3.9783 (wt. %) in C_3S composition. Also, a difference of 1.2501 was observed in the Lime Saturation Factor (LSF). These observations confirmed that the developed model in Aspen Plus is an accurate representation of the studied plant as variations are within limits that do not affect the clinker quality. The plant's emission data were not available; thus, that simulation was compared with acceptable limits and reported by a similar cement plant. Lesser emissions were observed in the simulation than the plant data, except in SO_2, where the emission was 4.542 gm/kg tonne higher. This value is still within the acceptable limits. The disparity could be attributed to the choice of the thermodynamic model.

Table 1: Validation of simulation results with plant data using 100% coal as a fuel source

Variables	Plant Data	Simulation	Difference
Clinker (Oxide Form)			
CaO	0.598	0.5883	0.0097
SiO_2	0.19	0.1892	0.0008
Al_2O_3	0.058	0.0503	0.0077
Fe_2O_3	0.035	0.0328	0.0022
MgO	0.0045	0.006	0.0015
Clinker (Compound Form)			
C_3S	62.435	66.4133	3.9783
C_2S	14.7327	12.9318	1.8009
C_4A	10.734	9.0484	1.6856
C_4AF	12.098	11.6065	0.4915
Clinker (Quality)			
Lime Saturation Factor	72.5063	73.7564	1.2501
Alumina Ratio	1.6571	1.5335	0.1236
Silica Ratio	2.043	2.2768	0.2338
Emissions			
CO_2(kg/tonne clinker)	977	825.976	151.024
NO_x(gm/tonne clinker)	2200	2139.5	60.5
SO_2(gm/tonne clinker)	170	174.542	4.542

3.1 Alternative Fuels Performance

The introduction of a used tyre and MSW in the fuel mix increased the LSF compared to coal only (represented by 0 % with a value of 79.1077). This increase was optimum at 20 %

alternative fuel mix for both with 86.3407 and 86.3387 for used tyre and MSW respectively, as a further increase of the alternative fuel in the combination above this level brought about no noticeable change, due to saturation of the combustion reaction. In contrast, the introduction of bagasse alternative fuel resulted in a decrease in the LSF. This decrease was continuous until the highest mix of 30%, with a value of 78.1351. LSF indicates the amount of unacceptable free lime present in the clinker [14]; hence lesser values are more appreciable. This implies MSW had the best performance in this regard.

The introduction of 5% alternative fuels in the fuel mix resulted in a decrease in the value of AR from 1.2281 observed in 100% coal to a value of 1.1314 for bagasse and 1.1094 for both MSW and used tyre. The values for MSW and used tyre remained the same despite varying configurations remaining same up to a composition of 25% alternative fuel in the fuel mix but further reduced to 1.1092 and 1.1093 respectively for used tyre and MSW at 30% fuel mix. As for bagasse, a steady decrease in AR was observed with each increment of 5% Bagasse in the fuel mix, resulting in a value of 1.1349 with the introduction of 30% fuel mix. Though all the values observed in the various configuration of the alternative fuels fall within the acceptable limit of 1 to 4 for Portland cement [14], bagasse was considered to have the best performance in this regard since it was further from the baseline among the three alternative fuels. The introduction of 5% alternative fuels in the fuel mix resulted in a decrease in the value of SR from 2.5860 observed in 100% coal to a value of 2.4946 for bagasse and 1.4541 for both used tyres and MSW. However, higher configurations above 5% of the alternative fuels did not bring about a noticeable change in SR. Preferred SR ranges for Portland cement is between 2.0 to 3.0 [14] hence bagasse had the best performance in this regard. This finding is similar to a recent report that observed bagasse has a good SR compared to plastic and some other alternative fuel due to its relatively low Al_2O_3 content [2].

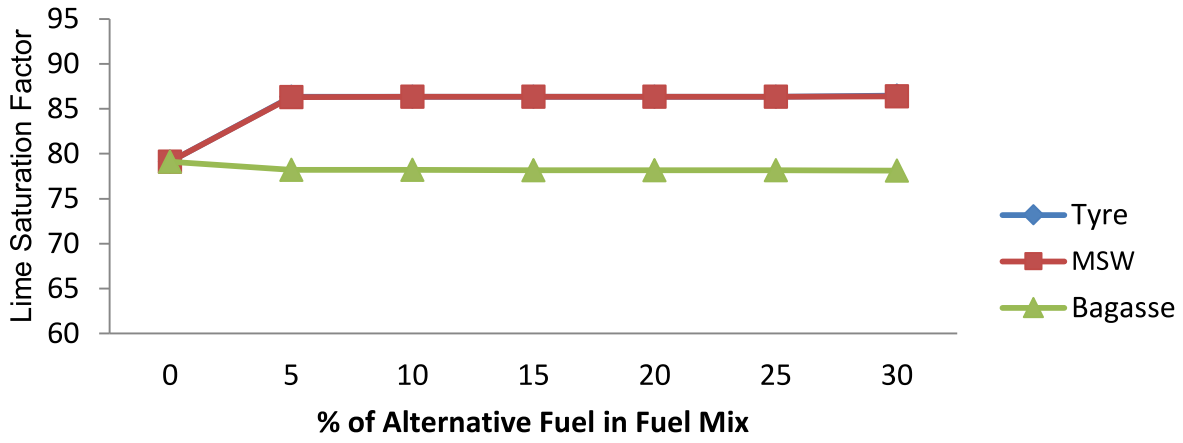

Figure 2: Lime Saturation Factor of Alternative Fuel in Fuel Mix

3.2 Environmental performance

An environmental assessment of the use of alternate fuel in the fuel mix was carried out to inform the ecological friendliness of the alternative fuels. The introduction of a used tyre and MSW in the fuel mix decreased CO_2 emission compared to coal only (represented by 0 % with a value of 825.98). This decrease was optimum for a used tyre at 20 % alternative fuel mix with a value of 817.434 kg/tonne clinker. The reduction in CO_2 emission with a higher configuration of MSW in the fuel mix was steady all through, and the opposite was observed with a steady increase in emission with higher configurations of bagasse. MSW had the best potential to

reduce CO_2, and the used tyre came close. However, bagasse increased emission close to the acceptable limit of 900 kg/tonne clinker; hence it should not be used above 25% mix to ensure environmental friendliness.

One of the excellent options to lower CO_2 emission up to 4.7% is the use of MSW. This is achieved by replacing thermal energy needed of about 30%; a higher amount of fuel is required to keep the production amount near to the reference case because MSW has a lower energy requirement [2].

The introduction of a used tyre and MSW in the fuel mix decreased CO_2 emission compared to coal only (represented by 0 % with a value of 825.98). This decrease was optimum for a used tyre at 20 % alternative fuel mix with a value of 817.434 kg/tonne clinker. The decrease in CO_2 emission with a higher configuration of MSW in the fuel mix was steady all through. The opposite was observed with a steady increase in emission with higher configurations of bagasse. MSW had the best potential to reduce CO_2, and the used tyre came close. However, bagasse increased emission close to the acceptable limit of 900 kg/tonne clinker; hence it should not be used above 25% mix to ensure environmental friendliness.

MSW was found as the best option to reduce CO_2 emission up to 4.7% while substituting 30% of the thermal energy requirement. MSW has a lower energy content which implies that a higher amount of fuel is required to keep the production amount near the reference case [2].

Introduction of bagasse and used tyre in the fuel mix slightly increased NO_x emissions from 890.001 mg/Nm^{3}observed in 100% coal to 891.704 mg/Nm^{3}and 891.406 mg/Nm^{3}respectively for bagasse and used tyre at 5% fuel mix. The slight increment in emission observed with higher configurations of the fuel mix was sustained till 30% at a value of 897.78 mg/Nm^{3}and 891.941 mg/Nm^{3}respectively for bagasse and used tyre. A more pronounced increase in NO_x emissions from 890.001 to 941.712 mg/Nm^{3}at 5% fuel mix was observed in the case of MSW. This marginal increase was steady and resulted in the emission of 1032 mg/Nm^{3}and 1156.96 mg/Nm^{3}at 15% and 30% fuel mix, respectively. This high value (compared to reference 100% coal) is an indicator for carefulness in the use of MSW as an alternative fuel; hence, it should not be used above 25% mix. Though used tyres in fuel mix brought about a slight increase in NO_x emission, it is relatively the best in these regards. MSW potentially reduces CO_2 emissions. An opposite scenario was observed in the case of NO_x emission with a 29.5% increase in the stack gas, and all the selected alternative fuels were found to increase the NO_x emission [2], [17].

SO_x emission increased with the introduction of used tyres and MSW in the fuel mix. However, this increase is more pronounced in used tyres than MSW, proven by an increase from 281.102 mg/Nm^{3}observed in 100% coal to 279.306 mg/Nm^{3}and 291.322 mg/Nm^{3}respectively for MSW and used tyre at 5% fuel mix. The slight increase in emission observed in MSW was steady and resulted in the emission of 283.398 mg/Nm^3, 284.295 mg/Nm^{3}and 285.35 mg/Nm^{3}at 10%, 20% and 30% fuel mix, respectively. A similar but more marginal trend was observed in a used tyre, which resulted in SO_x emission of 295.072 mg/Nm^3, 307.069 mg/Nm^{3}and 316.273 mg/Nm^{3}at 10%, 20% and 30% fuel mix, respectively. In a bid to ensure SO_x emission below the marked 310 mg/Nm^3, it is recommended that the used tyre should not exceed 20% in the fuel mix. In contrast to observations in MSW and used tyres, the introduction of bagasse in the fuel mix brought about a notable decrease in SO_x emission. This is evident in the observation of SO_x emission of 273.142 mg/Nm^3, 261.754 mg/Nm^3 and 248.696 mg/Nm^{3}at 10%, 20% and 30% bagasse fuel mix. Evidently, bagasse showed the best potential for SO_x emission. SO_2 emission

remained almost constant for the case of MSW. Due to the sulfur content of the tyre MSW produced about 11% more SO_2 than the reference case [2].

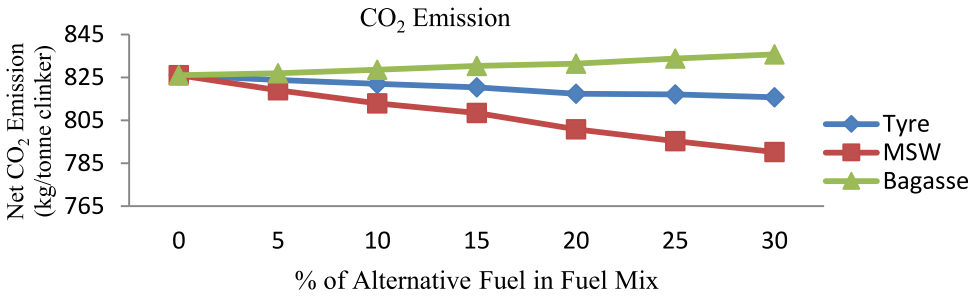

Figure 3: Net CO_2 Emission of Alternative Fuel in Fuel Mix

3.3 Thermal stability

Though sugarcane bagasse showed some potential for keeping the kiln outlet temperature at an acceptable value of 1687 ºC at 5% fuel mix, the used tyre was able to maintain the reference temperature of 1689 ºC at 5% fuel mix while MSW notably dropped the kiln outlet temperature to 1669 ºC. Though there was a marginal decline in the temperature with higher configurations, the used tyre maintained the reference temperature even at the highest configuration (30 % fuel mix) considered at 1688.5 ºC. Sugarcane bagasse had a drop of 2 ºC with each increment of 5% in the fuel mix which resulted in acceptable temperatures of 1685 ºC, 1681 ºC and 1677 ºC at 10%, 20% and 30% fuel mix, respectively. The notable drop in the kiln outlet temperature of MSW was steady through the configurations, resulting in 1639 ºC, 1589 ºC and 1549 ºC at 10%, 20% and 30% fuel mix, respectively. Used tyre performed best in this regard and sugarcane bagasse came close, MSW, however, did not show good temperature profile, hence should not be introduced in the fuel mix beyond 15% with an outlet temperature of 1609 ºC to ensure the kiln outlet temperature does not go below 1600 ºC in order not to change the clinker chemistry.

According to the result obtained from the simulation, kiln temperature was markedly low for the case of MSW, change the clinker chemistry apart from bagasse. All other three alternative fuels can maintain the kiln temperature up to the reference case [2].

3.4. Exergy efficiency

Exergy efficiencies decreased with the introduction of alternative fuels, resulting in an efficiency of 75.5% for bagasse and 72.7% for both used tyres and MSW at 5% fuel mix, compared to 82.5% efficiency observed in 100% coal. Higher configurations of alternative fuels brought a marginal reduction in efficiency in the three alternative fuels, resulting in efficiencies of 75.3%, 72.5% and 72.4%, respectively, for sugarcane bagasse, used tyre and MSW at 10% fuel mix. At 30% fuel mix, efficiencies of 74.3%, 71.8% and 71.6% were respectively observed for bagasse, used tyre and MSW. Sugarcane bagasse was the most efficient of the three alternative fuels considered. However, the other two had a good performance as well. Table 2 shows the results of exergy efficiency at different configuration

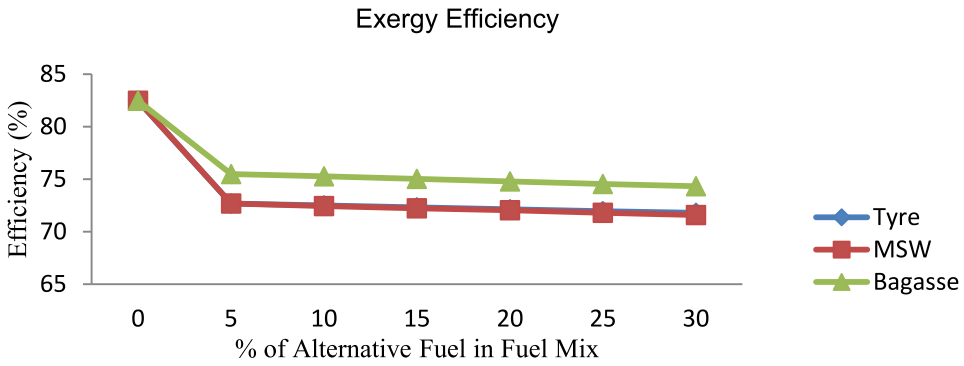

Figure 4: Efficiency (%) of Alternative Fuel in Fuel Mix

3.5 Energy Costing

Energy costing regarding alternative fuels usage in cement plants will enable us to minimise cost and maximise profit by cutting down the cost of conventional fuels usage. This research shows that the cost of fuels decreased with alternative fuels, resulting in $1411.40 for sugarcane bagasse and approximately $13952 for both used tyres and MSW at 5% fuel mix, compared to $14350.02 observed in 100% coal. Higher configurations of alternative fuels brought a marginal reduction in cost in the three alternative fuels. However, the three alternative fuels were cost-effective (with MSW having the potential to save 613.92 $/hr in 30% fuel mix). Table 2 shows the results of fuel cost at different configurations.

Table 2: Cost Analysis of Coal and Alternative Fuel at different Configurations

Component	Exergy (KJ/h)	Exergy (KW/h)	Costing ($/h)	Efficiency (%)
0 % Fuel Mix				
Coal	430500751.10	119583.54	14350.02	82.46
5 % Fuel Mix				
Bagasse	423582101.60	117661.69	14119.40	75.49
MSW	418434063.40	116231.68	13947.80	72.68
Used Tyre	418547583.20	116263.22	13951.59	72.70
25 % Fuel Mix				
Bagasse	418291522.50	116192.09	13943.05	74.55
MSW	413332289.50	114814.52	13777.74	71.79
Used Tyre	414338829.60	115094.12	13811.29	71.97
30 % Fuel Mix				
Bagasse	416965171.20	115823.66	13898.84	74.32
MSW	412083088.40	114467.52	13736.10	71.57
Used Tyre	413308574.50	114807.94	13776.95	71.79

4.0 Conclusions

In the cement manufacturing, a process model was used for the operation of rotary kiln. Aspen Plus was used in the study of energy performance, and the effect of other fuels on clinker quality,

emissions, thermal stability and cost effectiveness. Used tyre, municipal solid Waste (MSW) and sugarcane bagasse were the three alternative fuels used.
The model confidence was established with the aid of Obajana plant data, literature data, and acceptable limit. The model was validated with reference cement plant data, and the validated model was run for the selected alternative fuels. In the reference condition, it was noticed that selected alternative fuels had a minimum influence on clinker quality except for MSW. MSW was particularly capable of reducing CO_2 emissions while sugarcane bagasse increased it. Though the three alternative fuels were found to be cost-effective (with MSW having the potential to save 613.92 $/hr in 30% fuel mix), used tyre was found to be the best option due to its ability to reduce CO_2 emission while ensuring thermal stability both in terms of exergy efficiency and kiln outlet temperature, coupled with its worldwide availability.

References

[1] Ariyaratne, W.K.H.; Malagalage, A.; Melaaen, M.C.; Tokheim, L. (2015). CFD modelling of meat and bone meal combustion in a cement rotary kiln—Investigation of fuel particle size and fuel feeding position impacts. Chem. Eng. Sci. 123, 596–608

[2] Azad Rahman, Mohammad G. Rasul, M.M.K. Khan and Subhash C. Sharma (2017) Assessment of Energy Performance and Emission Control Using Alternative Fuels in Cement Industry through, a Process Model.

[3] Emad B., Gholamreza Z., Haslenda H., (2012). 'A novel design for green and economical cement manufacturing', *Journal of Cleaner Production*, 22, 60-66.

[4] Fryda, L.; Panopoulos, K.; Vourliotis, P.; Kakaras, E.; Pavlidou, E. **(2007).** Meat and bone meal as secondary fuel in fluidised bed combustion. Proc. Combust. Inst., 31, 2829–2837.

[5] Greco, C., G. Picciotii, R.B. Greco, & G.M. Ferreira (2004). Fuel Selection and Use Chap. 2.5 in *Innovations in Portland Cement Manufacturing*. Skokie, Illinois: Portland cement association.

[6] Greer, W.L. (2004). A Qualitative Examination of the Control of Major Gaseous Pollutants Generated in Portland Cement Kilns. (Proceedings of the A and WMA's 97th Annual Conference and Exhibition; Sustainable Development: Gearing up for the Challenge, Indianapolis, in, June 22-25).

[7] Hokfors, B. (2014). Phase Chemistry in Process Models for Cement Clinker and Lime Production. PhD. Thesis, Thermal Energy Conversion Laboratory, Department of Applied Physics and Electronics, UMEA University, Umeå, Sweden.

[8] Jackson, P.J. (1998). Portland Cement: Classification and Manufacture. Chap. 2 in *Lea's Chemistry of Cement and Concrete*. 4th ed. London: Arnold.

[9] Miller, F.M. (2004). Raw Mix Design Considerations. Chap. 2.2 of *Innovations in Portland Cement Manufacturing*. Skokie, Illinois: Portland Cement Association.

[10] Mokrzycki, E., A. Uliasz-Bocheńczyk, & M. Sarna. (2003). Use of Alternative Fuels in the Polish Cement Industry. *Applied Energy* 74, (1-2), 101-111.

[11] Rahman, A.; Rasul, M.G.; Khan, M.M.K.; Sharma, S. (**2015).** A recent development on the uses of alternative fuels in the cement manufacturing process. Fuel, 145, 84–99.

[12] Rodrigues, F.A. and Joekes, I. (2011). Cement industry: Sustainability, challenges and perspectives. Environ. Chem. Lett., 9, 151–166.

[13] Price, L. (2008); "Potentials for Energy Efficiency Improvements in U S Cement Industry", *Journal of Energy,* Vol. 25, pp.1169 – 1214.

[14] Taylor, H.F.W. Cement Chemistry, 2nd ed.; Thomas Telford Publishing: London, UK, 2004.Torres E.A.,

[15] Yunus, A. C, (2010), Thermodynamics- An engineering approach 9th edition

[16] Zhang, S. (2011). Aspen Plus-based simulation of a cement calcined and optimisation analysis of air pollutants emission. Clean Technol. Environ. Policy, 13, 459–468.

[17] Ziya, S. M. (2012): 'Research on exergy consumption and potential of total CO_2 emission in the Turkish cement sector', *Energy Conversion and Management*, 56, 37–45.

Journal of Engineering, Science, and Technology
ISSN: 2714-2396 | Volume 6, Issue 1

INFLUENCE OF OPC:PS:CS TERNARY BLEND ON SOME ENGINEERING PROPERTIES OF CONCRETE

Bilkisu Danjuma[1]*and Ibrahim Shuaibu[2]
[1]Department of Civil Engineering Technology, Nuhu Bamalli Polytechnic, Zaria, Kaduna
[2]Department of Civil Engineering, Kaduna Polytechnic, Kaduna
***Correspondence Author Email Address: bdanjuma14@nubapoly.edu.com**
Phone: 08133806987

ABSTRACT
In order to reduce the carbon footing of the cement industry in concrete production, this research investigated the possibility of using a ternary blended cement composed of ordinary portland cement, palm kernel shell ash and coconut shell ash in concrete. The experimental procedure involves employing a mix ratio of 1:2:4 at constant water to binder ratio of 0.63 in casting ternary concrete cubes with varying OPC: PS: CS ash ratios of 100:0:0, 97.5:1.25:1.25, 95:2.5:2.5, 92.5:3.25:3.25, 90:5:5 and 85:7.5:7.5 under research laboratory conditions. Test results show that the workability of the fresh ternary blended concrete diminishes with increase in percent substituted pozzolanic ash using the slump test. At day 7, all the pozzolana containing concrete cubes exhibited early strength compared to the regular concrete, while at 28 days, all the PS: CS ash partly supplemented concrete displayed inferior compressive strength in comparison to the regular concrete. The 2.5% to 10% ternary blended concrete cubes yielded an average of 19. 67N/mm^2 compressive strength which is very close to the target compressive strength of 20N/mm^2, hence 10% is the optimal in producing light weight concrete. Chemical, other mechanical and durability studies are recommended for sustainable green concrete production.

Key words: OPC: PS: CS, Ternary Blend, SCC, Percent substitution

1. INTRODUCTION

For decades, the quest for the innovation of suitable cementitious resources to partially or even totally replace the conventional cement rages on, by both the Civil/Structural as well as the material engineers in order to principally reduce its carbon footing. Agricultural waste(Rice husk ash, corn cob ash and others), industrial waste (Fly ash, ground granulated blast furnace slag, silica fume etc.), and urban waste (cast-off concrete, glass, rubber tyres, plastics, papers and other recovered materials) have been used world-wide as Supplementary Cementitious Constituent (SCC) in the greening of concrete Liew, Sajobi & Zhang [1].
Several investigations have been carried out the world over, through the years in other to find out the possibility of the use of supplementary materials partially or wholly in place of cement in concrete, mortar and sand-crete block making.Binary, ternary and quaternary cements have been introduced as the binder structure in concrete production to reduce the use of Portland cement, improve, modify and balance workability, durability, strength and economy, Yurdakul, Taylor, Ceylan, & Bektas [2]. Due to the economic implications of using sophisticated industrial SCC, the most generally and freely accessible material used in the least developed part of the world, is the agricultural based SCC, Akhionbare [3]. The SCC is otherwise known as pozzolanic material. According to Neville [4], the merits of the use of pozzolanas in conjunction with Ordinary Portland Cement (OPC) include: improvement in workability, water retention, sulphate resistance, alkali aggregate resistance; decrease in bleeding; release of low heat of hydration and superior lasting strength in addition to economy. Protection or conservation of the environment is one other merit that cannot be over emphasized.

Blended Concrete denotesthe part substitution of cement (usually OPC) with one or more pozzolans in concrete production.According to Hameed & Aleyas [5], a ternary blended concrete is developed when dual supplementary cementitious materials are used as part substitution of cement in concrete while a binary blended concrete is composed of a mono-supplementary cementitious material and other concrete constituents. Agreeing with Blezynski, Hooton, Thomas & Rogers [6], huge quantities of mono-SCC (binary blends) may be detrimental to concrete, e.g. protracted setting time and others, depending on the chemical properties of the SCC employed and other variables. In researches where more than two combinations of pozzolanas are blended, the type is called quaternary concrete [7] [8] & [9].

Reviewing some of the researches on binary and ternary concrete, it was documented that:
According to a research carried out by Oyedepo, Olantori & Akande [10], to determine the performance of coconut shell ash and palm kernel shell ash as partial replacement for cement in binary concrete. Their results showed that 20% part substitution of the individual ashes led to a compressive strength suitable for lightweight concrete. However, the highest compressive strength is obtained from the coconut shell ash at 10% replacement. Investigations conducted by Adeala, Olaoye &Adeniji [11], on the effect of coconut shell ash on fresh and hardened concrete properties which include: workability, water absorption and compressive strength, results showed that concrete containing 10% of coconut shell ash has the least water absorption rate, increase in the percent substitution of the ash in the mix led to a stiffer mix (decrease in workability). XRF analysis indicated that the coconut shell ash belongs to class F pozzolanic group. 5-15% part replacement of coconut shell ash with OPC was recommended for average weight production of concrete. In undertaking an experimental program to determine the effect of water-to-binder ratio, air content, and type of cementitious materials on fresh and hardened properties of binary and ternary blended concrete, Yurdakul *et. al* [2] found out that ternary blends trailed the developments of their individual materials. Binary and ternary mixtures containing Class C fly ash and slag cement exhibited higher compressive strength than the regular mixture.

The surface resistivity and shrinkage outcomes of binary and ternary mixtures were equal to or better than the regular combination. They recommended additional tests on other mechanical and durability properties of the different blends. Ghrici, Kenas & Said-mansour [12], investigated the effect of combining silica fume on the mechanical properties and durability of cements containing natural pozzolana, test results confirm that the use of ternary cements contributes to the enhancement of strength at an initial phase. Improved resistance to sulphate and acid attacks and low chloride ions permeation likewise enhanced durability. Obute *et. al.*[9], studied, a ternary mixture of OPC, Cassava Peel Ash (CPA), and Rice Husk Ash (RHA) which were used as the cement in concrete production. The concrete mix was prepared to set CPA at 5% for all combinations while the RHA was replaced at 0 to 25% of the total blend. With a 0.65 water/binder ratio, an optimal strength was attained at 20% substitution of CPA (5%) and RHA (15%).

The part substitution of cement with CPA – RHA in concrete also clearly influencedthe concrete's water absorption characteristics. Summarizing the experimental investigations on Strength characteristics of concrete containing fly ash and micro silicaternary blends in the last decade, Harishav, Mukesh & Sohit [13], stated that most of the studies were of the view that the materials (fly ash and micro silica) are thoroughly safe for use in any environment and they complement each other in blends. Saleh *et. al.*[14], reported the laboratory study to establish the prospect of using Palm Oil Fuel Ash (POFA) and Rice Husk (RH) in developing green unfired bricks where 2% - 10% of POFA and 1% - 5% RH were used in brick production. Addition of POFA was intended to lessen the cement usage and RH was meant to be part substitution of sand in the blend. Their result showed that adding POFA and RH led to the reduction of the density of the bricks while the compressive strength also decreases in comparison to the conventional brick.

It can be concluded from the literature above that numerous researches involving binary and ternary blends had been performed experimentally in order to determine some mechanical and durability properties of concrete, which revealed that the ternary blends are superior to the dual combinations.

One of the Author's in this research reported a study on the use of binary blends of palm oil husk ash and coconut shell ash, with cement individually in green concrete production, where Danjuma & Amamat [15] found out that their binary blend of palm oil husk ash indicated a compressive strength close to that of their regular concrete at 28 days while the coconut shell ash blend did not measure up. Hence, the idea of a ternary blend was born. Envisaging the possibility of a synergistic combination where the ternary mixture/blend properties will be superior to that of the binary blend. It is hoped that this will minimize the demerit of any of the individual constituents and in the same vein maximize their collective strengths.

The focus of this research is to determine the effect of a ternary blended cement comprising Ordinary Portland Cement, Palm-kernel Shell ash and Coconut Shell ash(OPC: PS: CS) used at various levels of substitution of the components,on the workability and compressive strength of concrete and suggest an optimum amount of the ternary cement to be used for concrete production

2. MATERIALS AND METHODS

2.1 MATERIALS

The materials used for this experimental work are: Cement, Palm kernel shell ash, coco nut shell ash, Sand, gravel, and water; with the deliberate exclusion of an admixture, hence, a fairly high water binder ratio of 0.63 was adopted to make the mix suitably workable.

Cement

In this study, the Ordinary Portland Cement (OPC) type 1(42.5N), produced by Dangote Cement Limited, Obajana, being one of the Nigeria largest cement producer and as such easily accessible in almost every part of Nigeria was used for all the mixes required. This cement conforms to the requirements of the British Standard Code, [16]. To prevent the cement from being exposed to moisture and hardened before usage, it was kept in air tight packages and stored inside the laboratory store.

Palm-kernel Shell ash (PS ash)

The palm kernel shell burnt to ash in this research work was obtained from Zaria city, Zaria Local Government Area of Kaduna State, Nigeria. Though Zaria does not locally grow palm fruits, but the oil, fruits and kernels are in abundance because it is a metropolitan area that enjoys trade between the northern and southern part of Nigeria. The ash was sieved using sieve number 200 (75µm) in order to make sure it is of suitable uniformity and only ash particles that pass through sieve was used in the concrete preparation.

Coconut Shell ash (CS ash)

The coconut shells were obtained from a coconut seller in Zaria metropolitan area, Zaria local Government Area of Kaduna state. It was sun dried for 4 days, in order to reduce its moisture to the barest minimum and burned thoroughly in open air. The dust retrieved from the burning was sieved using sieve number 200 (75µm) and then collected for use.

The palm kernel shell ash (PS ash) and coconut shell ash (CS ash) were then blended in equal proportion (i.e. in same ratio 1:1) to produce the PS: CS ash used in the study.

Fine aggregates, coarse aggregates and water

The Fine Aggregate used was sourced from Gobirawa community in Zaria, Kaduna state, Nigeria. It was thoroughly washed with water to reduce the level of impurities and organic matter, and later sun dried. The fine aggregates (sharp sand) particle sizes ranges from 0.10mm-6.0mm in diameter which conforms to the requirements of BS 1881-108 [17]. The gravel was obtained from Danmagaji along Kano-Kaduna express-way, Zaria, Kaduna state Nigeria having a maximum size of 20mm which also conforms to [17]. The water used for the study was obtained from a borehole close to the material's laboratory of School of Engineering, Nuhu Bamalli Polytechnic, and Zaria. The water was clean and free from any visible impurities. It suitability was based on BS 882 [18] requirements.

2.2 METHODS

The various tests carried on the materials used for the experiment are: sieve analysis for fine aggregate and pozzolanes (ash), aggregate impact value test, aggregate crushing value test., cement soundness, Initial and final setting time of cement and ash mixture, etc.

Mix proportions

The total amount of materials needed for each mix was determined in accordance to BS 3148:1993 [19] by the assumption of light weight concrete of density 2000kg/m^3. For the purpose of this study, a concrete cube of 150 x 150 x 150mm was produced under laboratory condition. The mix ratio used was 1:2:4 (one-part cement to two parts of sand to four part of coarse aggregate) at constant water cement ratio of 0.63. The ternary concrete was casted using varying OPC: PS: CS ash ratios of 100:0:0, 97.5:1.25:1.25, 95:2.5:2.5, 92.5:3.25:3.25, 90:5:5 and 85:7.5:7.5 respectively, i.e. 8 cubes for each percent substitution. The 100: 0: 0 served as the regular (control) sample for the study. To prevent deficiency due to waste, compaction and bulking of aggregates, 10% was permitted on the materials. The concrete materials used for each batch of eight cubes is as shown in Table 1.

Table 1: Concrete Materials for Production of a Batch of Eight Cubes

Concrete Materials (Kg)	PS:CS 0%	PS:CS 2.5%	PS:CS 5%	PS:CS 7.5%	PS:CS 10%	PS:CS 15%
Cement	9.60	9.36	9.12	8.88	8.64	8.16
PS:CS ash	0.00	0.24	0.48	0.72	0.96	1.44
Fine Aggregate	18.60	18.60	18.60	18.60	18.60	18.60
CoarseAggregate	38.00	38.00	38.00	38.00	38.00	38.00
Water	5.96	5.96	5.96	5.96	5.96	5.96
Water/Binder	0.63	0.63	0.63	0.63	0.63	0.63

Mixing process

Hand mixing was adopted in producing the samples as it is possible to make concrete on a small scale without a concrete mixer. Hand mixing may be advantageous when considering that the amount of concrete required is not much though it may limit production and not always be thorough.The blendingfor each batch was done on the floor. All the materials were weighed precisely prior to blending. The surface of the floor was moistened before putting the materials to minimize water losses through the floor. Fine aggregate, coarse aggregate, PS: CS ash and cement were placed on the floor accordingly and mixed well with a shovel before water was poured and mixed thoroughly. Slump test was then undertaken on the fresh mix in order to determine the workability of the concrete. Workability is one of the primary characteristics of any concrete material; for practical purposes, it largely indicates the ease with which a blended concrete can be controlled from the mixer to its final compacted form. Its main characteristics are consistency, mobility and compact-ability. The slump test is widely used due to its simplicity amongst others, to determine workability; its values depends to a large extent on the concrete constituent materials. In the absence of admixtures, such as super-plasticizers, pozzolanic cement blends demands high water to binder ratio for their concretes to be reasonable workable.

Production of Concrete and Curing

48 moulds of (150 x 150 x 150) mm were used in concord with BS 8500 [20]. They were lubricated with engine oil in order to reduce friction and enhance removal of cubes from the moulds. They were then filled with concrete in three layers and each layer was tamped 25 times. The moulds containing the cubes were left for 24 hours under the laboratory temperature for the cubes to set before removing the moulds. Plate I shows the process of concrete production. The cubes were removed after 24 hours and were taken to curing tank were they were totally immersed in water as shown in Plate II

Plate I: Concrete Production

Plate II: Curing

The most important engineering property of concrete is its compressive strength. It is the maximum compressive load it can sustain for each unit area, in concrete constructions. It is generally affected by type of cement, mix proportions, modes of compaction and curing circumstances.

The compressive tests of the hardened, cured concrete cubes were undertaken in accordance to [21] as captured in Plate III

Plate III: Compression Testing Machine

3. RESULTS AND DISCUSSION

The pattern of variation of the slump value of the concrete blends with part substitution of ashes is as shown in Figure 1, it can be seen that the workability of the concrete with the part substitution of cement decreases with increase in percent substitution. According to Neville [4], any slump value ranging from 15 to 30 is low, so all the slumps are very low also BS 12390-3 [22] classifies all the slump value between 10 and 40 as S1. This may be attributed to the larger porous particles of the PS:CS ash supplement as documented by [22] [23] & [24], hence, the mixes with such supplements due to higher specific surface, need more water to be workable.

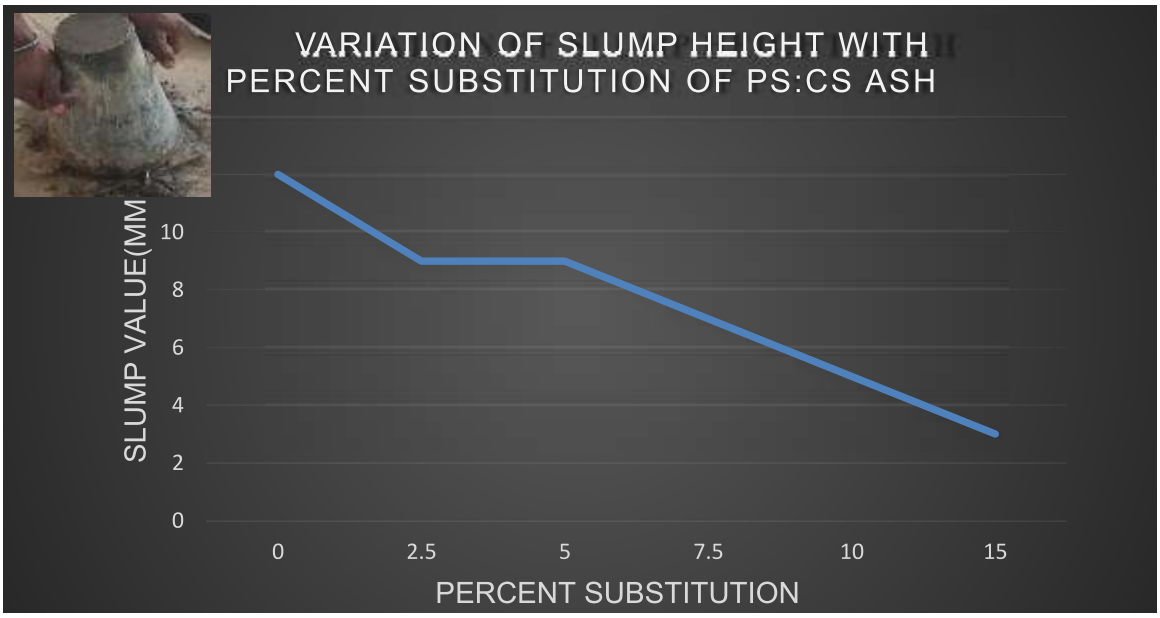

Figure 1: Variation of Slump Value with Percent Substitution in the OPC: PS: CS Concrete

The weight of each cured cube and the average compressive strength for all substitution is depicted in Table 2 and Figure 2

Table 2: Average weight and Compressive Strength at Curing ages

Percent Substitution (%)	Average Weight of each Cured Cube (Kg)				Average Compressive Strength (N/mm^2)			
	7days	14days	21days	28days	7days	14days	21days	28days
0	8.23	8.71	8.66	8.63	10.10	20.70	18.90	27.90
2.5	8.25	8.64	8.43	8.56	18.20	18.50	25.30	20.60
5	8.40	8.45	8.34	8.43	15.80	23.40	16.60	19.40
7.5	8.52	8.29	8.33	8.30	11.50	22.10	16.40	13.30
10	8.45	8.20	8.28	8.30	13.70	20.10	17.20	19.00
15	8.18	8.10	8.25	8.30	12.20	11.00	16.10	15.70

Generally, the pattern of compressive strength development is as shown in Figure 2. At day seven, all percentages of substitution showed significant early strength development than the regular (0% substitution) concrete. This has been the pattern with agricultural pozzolanic materials used in partial substitution and could be of advantage especially in structures where early strength development is required as recognized by Ogunwemimo, Salami & Familusi [25], this, they stated could be ascribed to the pozzzolana acting as void filler during hydration; thus, positively affecting the early age strength gained.

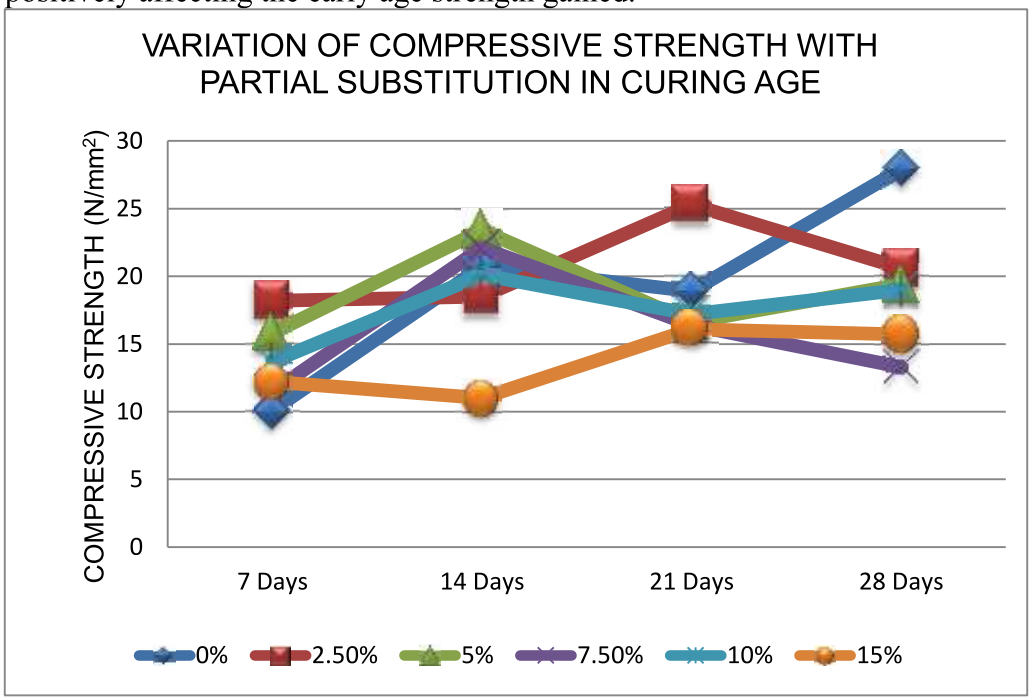

Figure 2: Variation of Compressive Strength with Curing ages at different PS: CS Part Substitution.

Also all percentages of substitution yielded an increase in strength at day fourteen with the exception of 15 per-cent substitution whose compressive strength dropped. At twenty-one days

all substitutions saw a decrease in compressive strength, with the exception of 2.50per-cent and 15per-cent substitutions that increased. At 28days only the regular exceeded the targeted strength of 20N/mm^2 with a compressive strength of 27.9N/mm^2 while 2.5, 5, and 10 per-cent partial substitution followed closely with an average of 19.67N/mm$^{2.}$ According to Danjuma & Amamat [15], the reduction in compressive strength of the part substituted concrete may be due to a low proportion of Calcium Oxide in the PS ash, and low calcium oxide and silicate oxide in CS ash, because the dual oxides are the main components of OPC cement and are principally answerable for its strength progression.

So, as the cement content is gradually substituted by the ash, the amount of cement for hydration is reduced, therefore, the strength of the concrete declines. This implies that PS: CS ash fractional replacement of a maximum of 10per-cent could be used as a SCC of cement in concrete successfully, especially lightweight concrete. The decrease in strength observed at 28 days should not be considered as a drawback in the use of pozzolanic blended cements as it has been documented by other researchers such as Olowe & Adebayo [24], that beyond 28 days, their strengths even exceeds those made from of the regular OPC cement.

The researchers attributed the strength gain to the continuation of cement hydration or the reaction of the pozzolana with lime or even the slowing of rate of hydration allowing the development of heavier hydrates of strength enhancing C_2S. Jonida *et. al*. [26], attributed the later age strength gain in pozzolanic concrete to the reaction of SiO_2 present in the pozzolana with free lime $Ca(OH)_2$ acquired through cement hydration in an additional reaction as time passes to form calcium silicate hydrate (C-S-H).

4. CONCLUSION AND RECOMMENDATIONS

The workability of the fresh ternary blended concrete decreases with increase in percent substituted pozzolanic ash.

At 7 days all the pozzolana containing concrete exhibited early strength compared to the regular Concrete

At 28 days, all the P S: CS ash partly replaced concrete displayed lower compressive strength in comparison to the regular concrete

The least amount of the ternary cement for usage in concrete is 2.5% while the optimum amount is 10%

More research and development in order to better understand the chemical and other mechanical properties of such ternary cements and their concretes should be undertaken. Such mechanical tests may include: tensile strength, corrosion and abrasion resilience; drying shrinkage, microstructure etc.

Longstanding studies on the development of strength as well as durability aspect of concrete containing ternary mixtures and other green concrete is necessary.

ACKNOWLEDGEMENT

The Authors do acknowledge the contribution of the Technologists of the Civil Engineering Materials Laboratory in carrying out the laboratory tests.

REFERENCES

[1] Liew, K.M, Sajobi, A. O. and Zhang, L. W. 2017. Green Concrete Prospects and Challenges.*Construction & Building Materials*

doi:10.1016/j.conbuldmat.2017.09.008

[2] Yurdakul, E.,Taylor, C., Ceylan, H. and Bektas, F. 2014. Effect of Water-to-Binder Ratio, Air Content, and Type of Cementitious Materials on Fresh and Hardened

Properties of Binary and Ternary Blended Concrete. doi: 10.1061/(ASCE)MT.1943-5533.0000900.

[3] Akhionbare, W.N. 2013. A Comparative Evaluation of the Application of Agro - Waste as Construction Material. *I.J.S.N.*, VOL.4 (1).141-144 ISSN 2229 – 6441 141.

[4] Neville, A. M. 2011. *Properties of Concrete*. (5th ed.). London: Longman Scientific and Technical Publishing

[5] Hameed, A.S.& Aleyas, B. 2016.Experimental Investigation on Properties of Binary and Ternary Blended High Strength Concrete using Silica Fume and Bagasse Ash. *International Journal of Engineering Research & Technology (IJERT)* 5(09), ISSN: 2278-0181 http://www.ijert.org

[6] Bleszynski, R., Hooton, R. D., Thomas, M. D. A., and Rogers, C. A. 2002. Durability of Ternary Blend Concrete with Silica Fume and Blast-Furnace Slag: Laboratory and Outdoor Exposure Site Studies. *ACI Mater. J.*, 99(5). 499–508

[7] Patel, N., Dave, R., Modi, S., Joshi, C., Vora, S. and Solanki, M. 2016. Effect of Binary and Quaternary Blends on Compressive Strength. *International Journal of Civil Engineering and Technology.* 7(5), 242–246.

http://www.iaeme.com/IJCIET/issues.asp?JType=IJCIET&VType=7&IType=

[8] Datok E. P, Ishaya A. A, Bulus A. D. & Amos, N. G. 2018. An Investigation of the Behaviour of Binary and Ternary Blends of Binding Materials in Concrete. *Scien tific Research Journal (SCIRJ)*, 4(03) 89 ISSN 2201-2796 www.scirj.org

[9] Obute, J. O., Akin, O. O., Amartey, Y. D. and Ejeh, S. P. 2021. Effects of the Partial Replacement of Cement with Cassava Peel Ash and Rice Husk Ash on Concrete. *CJET* 5(1) 20-28 http://journals.covenantuniversity.edu.ng/index.php/cjet

[10] Oyedepo, O.J., Olanitori, L.M. and Akande, S.P. 2015. Performance of Coconut Shell Ash and Palm Kernel Shell Ash as Partial Replacement for Cement in Concrete. *J. Build. Mater. Struct.* 2: 18-24. http://journals.oasis-pubs.com

[11] Adeala, A.J., Olaoye J.O & Adeniji A.A. 2020. Potential of Coconut Shell Ash as Partial Replacement of Ordinary Portland Cement in Concrete Production. *International Journal of Engineering Science Invention (IJESI)*, Vol. 09(01). 47-53

[12] Ghrici, M., Kenai, S. and Said – Mansour, M. 2007. Mechanical Properties and Durability of Morta and concrete Containing Natural Pozzolana and Limestone Blended cements. *Cement &Concrete Composites*. 29,542-549.

[13] Harishav, Mukesh,P. & Sohit, A. 2017. An experimental Investigation on Strength Properties of Concrete Containing FA and MS as Partial Replacement of Cement: An Overview. doi: 10.9790/9622-0707012428

[14] Saleh, A.M., Rahmat, M.T., Mohd Yusoff, F.N. and Eddirizal N.E. 2014. Utilization of Palm Oil Fuel Ash and Rice Husks in Unfired Bricks for Sustainable Construction Materials Development. http://dx.doi.org/10.1051/matecconf/2014150103

[15] Danjuma, B. and Adeyemi, O. A. 2020. Evaluation of the Compressive Strength of Green Concrete Incorporating Ashes for Sustainable Concrete Production. – In Association of Professional Women Engineers of Nigeria National Conference: Dynamics of Engineering Education for Sustainable Economic Development. (Vol. 37, pp. 1-9).

[16] British Standards Institution (1996). BS 12: *Specification for Portland cement*. London: BSI.

[17] British Standards Institution. (1983). BS 1881-108: *Testing Concrete: Method for Making Test Cubes from Fresh Concrete*. London: BSI.

[18] British Standards Institution 1992. BS 882: *Specification for Aggregates from Natural Sources for Concrete*. London: BSI.

[19] British Standards Institution. BS 3148:1993. *Method of test for water for making concrete (including note on the suitability of water)*. London: BSI British Standards Institution. 2002.

[20] BS 8500. *Concrete- Complimentary British Standard to BS EN 206-1. Part 1: Method of Specifying and Guidance for the Specifier; Part 2: Specification for Constituent Materials and Concrete*. London: BSI.

[21] British Standards Institution. 1983. BS 1881-108: *Testing Concrete: Method for Making Test Cubes from Fresh Concrete*. London: BSI.

[22] British Standards Institution. 2000. BS 12390-3: *Testing Concrete: Method for Determination of Compressive Strength of Concrete Cubes*. London: BSI.

[23] British Standards Institution. 2000. BS EN 206 – 1: *Testing Concrete: Method for Determination of Slump*. London: BSI.

[24] Olowe, K. O.1. & Adebayo, V. B. 2015. Investigation on Palm Kernel Ash as Partial Cement Replacement in High Strength Concrete. *SSRG International Journal of Civil Engineering (SSRG-IJCE)* 2 (4) 45-53. www.internationaljournalssrg.org

[25] Ogunwemimo, I. O., Salami, L. O. and Familusi, A. O. 2019. Evaluation of Palm Kernel Shell as a Partial Replacement for Coarse Aggregate in Concrete. *Journal of New Trends in Civil Engineering*, 1(2). 001-004

[26] Jonida, P., Ahmed, A., John, K. and Fraser, H. 2018. Palm Oil Fuel Ash as a Cement Replacement in Concrete. *Mod App Matrl Sci*. 1(1). doi: 10.32474/ MAMS.MS.2018.01.000102

Journal of Engineering, Science, and Technology
ISSN: 2714-2396 | Volume 6, Issue 1

COMPARATIVE STUDY OF AMERICAN CONCRETE INSTITUTE (ACI) AND COUNCIL FOR THE REGULTION OF ENGINEERING IN NIGERIA (COREN) MIX DESIGN MANUALS

* Joseph Oluwatosin Funke [1], Agenyi, Yakubu Akwu [2], Ayoola Johnson Oluwaseyi [3], and Ibrahim Madiyat Oniya [4]

[1,] Department of Civil Engineering, Kogi State Polytechnic, Itakpe Campus, Nigeria.
[2] Department of Civil Engineering, Federal University of Technology, Minna, Nigeria
[3, 4]Department of Minerals and Petroleum Resources Engineering, Kogi State Polytechnic.
[1] Corresponding Author's Email: victoryarrival@yahoo.com

ABSTRACT

COREN mix design method for Nigeria and ACI method are both based on the basic principles and empirical relations, developed after substantial experiments of locally available materials. However, some minor differences are seen in the quantities of the material used for mix proportion, which includes the cement,aggregate (fine and coarse)and water content which attributes to the variation in strength of concrete. In ACI method, the quantities of fine aggregateswere calculated, while the reverse is the case in COREN mix design method. The results indicate that the COREN method of mix design requires higher cement content than ACI method, and the water/cement ratio is higher in ACI method compare to COREN mix method. Although, the coarse aggregate content in COREN mix method is higher than the ACI mix method, from correlation and deviation between design and actual strength, it shows that COREN mix method is reliable and its meet the 25Mpa strength requirements than the ACI mix method.

Keywords: *ACI Mix Method, COREN Mix Method, Ordinary Portland Cement, River Sand, Gravel.*

1.0 INTRODUCTION

Concrete is a material similar in shape and appearance to natural limestone rock but formed by artificial binding together of natural or artificial stone with sand, cement and water [1]. The water cement ratio is usually the governing factor that determines the strength of concrete, other factors such as mix ratio, aggregate grading and quality or type of cement also play significant role to determine the strength of concrete. Due to the significant of mix ratio, mix design is usually done prior to the production of concrete [2].

Development of infrastructure has become the number one priority in the world particularly for developing countries like Nigeria, this has been jeopardized by increase in the price of conventional building materials including cement which is one of the major ingredients used in concrete production and has inevitably put inflationary pressure on the economy as construction materials become more expensive [3]. In designing a concrete mix, the primary objective is to select suitable constituent materials and determine their required amounts in order to produce concrete of specific characteristics and properties as economically as possible [4], [5].

Generally, concrete mix design includes two main steps: Selection of the main components suitable for the concrete (cement, aggregate, water, and additives) and determination of more economical mix ratios to fulfill performance and efficiency requirements [6]. Many international methods of mix designs have been developed by different countries such as American concrete institute (ACI), British Standard (BS) methods, India Standard (IS) which will not give the same strength if used in another area as a result of the difference in the properties of materials locally available in the country.

Concrete mix design is a process of specifying the proportion of ingredients (cement, aggregates, sand and water) required to meet anticipated properties of concrete in both fresh and hardened states [5], [7]. Concrete mix design is a well-established practice around the world. All developed countries, as well as many developing countries, have standardized their concrete mix design methods.

ACI and COREN are mostly based on empirical relations, charts, graphs, and tables developed as outcomes of extensive experiments and investigations of locally available materials. All of those standards and methods follow the same basic trial and error principles [1]. In 2017, the Council for the Regulation of Engineering in Nigeria, **COREN**, present the concrete mix design manual for Nigeria, thus, the scope of this study is to compare ACI and COREN recommended mix design guidelines [8].

The scope of this work is to compare ACI concrete mix design method and COREN concrete mix design guidelines which involves determination of the physical properties of aggregates, determining the proportions of the materials in both mix design methods and the determination of the compressive strengths. The scope of this work is limited to absolute volume and concrete mixdesign for compressive strengths less than 40MPa.

2.0 LITERATURE REVIEW

Fresh or hardened concrete behaviour depends basically on the characteristics of its components and the relationship between them. Therefore, obtaining a concrete with certain properties depends fundamentally on the concrete mix design [4],[6]. Generally, concrete mix design includes two main steps:

a. Selection of the main components suitable for the concrete (cement, aggregate, water, and additives).
b. Determination of more economical mix ratios to fulfill performance and efficiency requirements [6].

Currently, there are many international methods locally approved for mix designs such as American Concrete Institute (ACI) and British Standard (BS) methods.Some of the prevalent concrete mix design methods are:

a) ACI Mix Design Method,
b) USBR Mix design practice,
c) British Mix design Method, and
d) ISI Recommended guidelines.

Some research works have been carried out which gives some basic ideas about comparison of BIS (Bureau of Indian Standards) and ACI(American Concrete Institute) method of concrete mix design. Deepak [9], investigated the comparison of BIS (Bureau of Indian Standards) and ACI (American Concrete Institute) methods ofconcrete mix design.However, both methods are built on the basis of some basic principles and empirical relations but some minordifferences exist between them. M25, M35 and M45 grades of ordinary strength, medium strength and higher strength were chosen. 27cubes specimens (15 cm sides) and 27cylindrical specimens (15 cm diameter, 30 cm height) were prepared by BIS and ACI concrete mixdesign methods respectively.

These specimens were tested after 7days, 14 days and 28 day of curing. Materials (ordinary portland cement, coarse aggregates of 10mm and 20mm, natural river bed fine aggregates, sika viscocrete 4005 and water) quantities (M25, M35 and M45) required formanufacturing one cubic meter concrete by both methods were calculated numerically under codal provisions. Some

differences werefound in quantities calculated by both methods. Major differences were noticed in compressive strengths of specimens made by bothmethods. It was also noticed that cracked specimens of both methods show a great similarity in their cracking pattern.
Greatersimilarities were found between the shapes of brokenspecimens after 28 days compressive strength test. It was alsoobserved that M25 samples collapse by gentle crushing. M35samples and M45 samples get fractured by sudden brittlefracture. It was also observed that the shape of brokenspecimens changes with respect to increase in strength.

Nataraja [10],examined the procedure ofcalculating the material quantities of both methods and drewan idea that in case of ACI method, fine aggregate should be calculated after calculating the coarse aggregate content. Healso found that as the strength requirement increases, the sandrequirement goes on decreasing due to the relative low grade of available cement at the time in India and also due to limited research data during the time of research.

Singh and Verma [11],suggested that thehighest amount of aggregates should be used in BIS method and least in ACI method. For M25 grade the BIS method shows avast increment in the split tensile strength as compared toM20 and achieved highest strength among the rest of themethods.Generally, the behavior of M20 in terms ofmechanical properties of concrete wasbetter than that of the M25, the performance ofconcrete designed for ACI method was useful forthis grade of concrete.
Deepa [12], carried outcompressive strength of concreteusing different mix design methods and reported that the fine aggregate content in ACI is morethan the BIS method of concrete mix design. He also observed that in BIS method of concrete mix design the coarseaggregate content is more than that of ACI method.

3.0 MATERIALS AND METHODS

3.1 Materials

For the purpose of this research the materials used includes; ordinary portland cement, river sand, gravel of 20 mm size and water. The ordinary portland cement used in this study was obtained from a mini depot in Minna, Niger State,while the river sand and gravel were obtained from a supplier at kpakungu road in Minna, Niger State. The water used was obtained from the tap, it was colourless, odourless and free from organic materials.

3.2 Methods

The tests carried out are;

i. Sieve analysis test (determination of the particle size distribution).
ii. Specific gravity
iii. Bulk density
iv. Slump test
v. Compressive strength test of concrete cubes

3.2.1 Sieve analysis

This test is a method of separation of soil into fractions based on the particle size. It expresses quantitatively the proportion by mass of various sizes of particle present in a soil. Material retained in the number 4 sieve (4.75mm) is considered as coarse aggregate; material passing in the number 200 sieve (75μm) is considered as fine aggregate and is referred as micro-fines [8].

3.2.2 Specific gravity

The determination of specific gravity test was carried out according to BS 1377 (2016). It is the ratio between the unit mass of solid particles and water. Determination of the volume of a mass

of dry sample particles was obtained by placing the soil particles in a glass density bottle filled completely with the desired distilled water.
The density bottle and the stopper were weighed to the nearest 0.001g (M_1). The air-dried soil was transferred into the density bottle. The bottle content and the cover were weighed as M_2. Water was then added just enough to cover the soil; the solution is gently stirred to remove any air bubble, the bottle was then filled up and covered, wiped dry and weighed to the nearest 0.001g (as M_3). The bottle was subsequently emptied and filled completely with water, wiped dry and weighed to the nearest 0.001g (M_4). The specific gravity was calculated using equation (3.1).

$$G_s = \frac{M_2 - M_1}{(M_4 - M_1) - (M_3 - M_1)} \quad (3.1)$$

where:
G_s is the specific gravity
M_1 is the weight of density bottle (g)
M_2 is theweight of density bottle and dry sample (g)
M_3 is theweight of bottle, sample and water (g)
M_4 is theweight of bottle and water only (g)

3.2.3 Slump test
Slump test is one of the tests used in the determination of workability of fresh concrete, to ensure the fresh concrete is in adequate consistency for placement.

3.2.3.1 Casting of concrete cubes
The fresh concrete was poured into a lubricated metal moulds in three layers of 50mm, each layer was compacted using the tempering rod by distributing the strokes in a uniform manner in the mould for each of the three layers (35 strokes per layers). The concrete surface was marked for easy identification and allowed to set for 24 hours before demoulding of the concrete cube which was then immersed in water in the curing tank in accordance to BS1881: part 108: 1989.

3.2.3.2 Curing of Concrete Cubes
Curing is the process of keeping concrete moist which promotes hydration in concrete. All concrete requires curing in order for cement hydration to proceed and also to allow for development of strength, durability and other mechanical characteristics [13]. All cubes were submerged in water for 28 days in the curing tank.

3.2.4 Bulk density test
Bulk density is the total mass of soil per unit total volume of soil. A bulk density of 2400 kg/m^3 was used as recommended by COREN for all mixes using normal weight aggregates. The fine and coarse aggregate content are determined by obtaining the proportion of fine aggregate in the total aggregate content.

3.2.5 Compressive strength test
The capacity of the concrete to withstand axially directed load is determine by compressive strength. The compressive strength test was carried out to determine the maximum load the concrete cube can withstand before failing. All concrete requires curing so as to allow for development of strength, durability and other mechanical characteristics [11], [13]. All cubes were submerged in water for 28days in the curing tank. The compressive strength was determined from concrete cubes obtained and tested for 28 days. The concrete cube was tested to
.

determine its compression strength which is an important property of the hardened concrete which was determined by a compressive strength test on the cured concrete cubes.This test was carried out to determine the consistency, wetness or fluidity of fresh concrete.

3.3 Mix Design

The mix designs were carried out in accordance with COREN concrete mix design manual (2017) and ACI 211 (2002). Concrete mix design is the procedure by which the proportions of constituent materials are suitably selected so as to produce concrete, satisfying all the required properties for the minimum cost.

3.2.3 Determination of water cement ratio

Concrete strength depends on its water cement ratio, as cement requires water for the hydration of cement to take place. It is generally accepted as a rule ofthumb that every 1% increase in quantity ofwater added reduces the strength of concrete by 5% (COREN), [8].
Water/cement ratio was determined using the equation of strength verse water/cement graph (Figure 3.1) and Table 3.1 for grade 32.5 cement for ($0.3 \leq r \leq 0.9$).

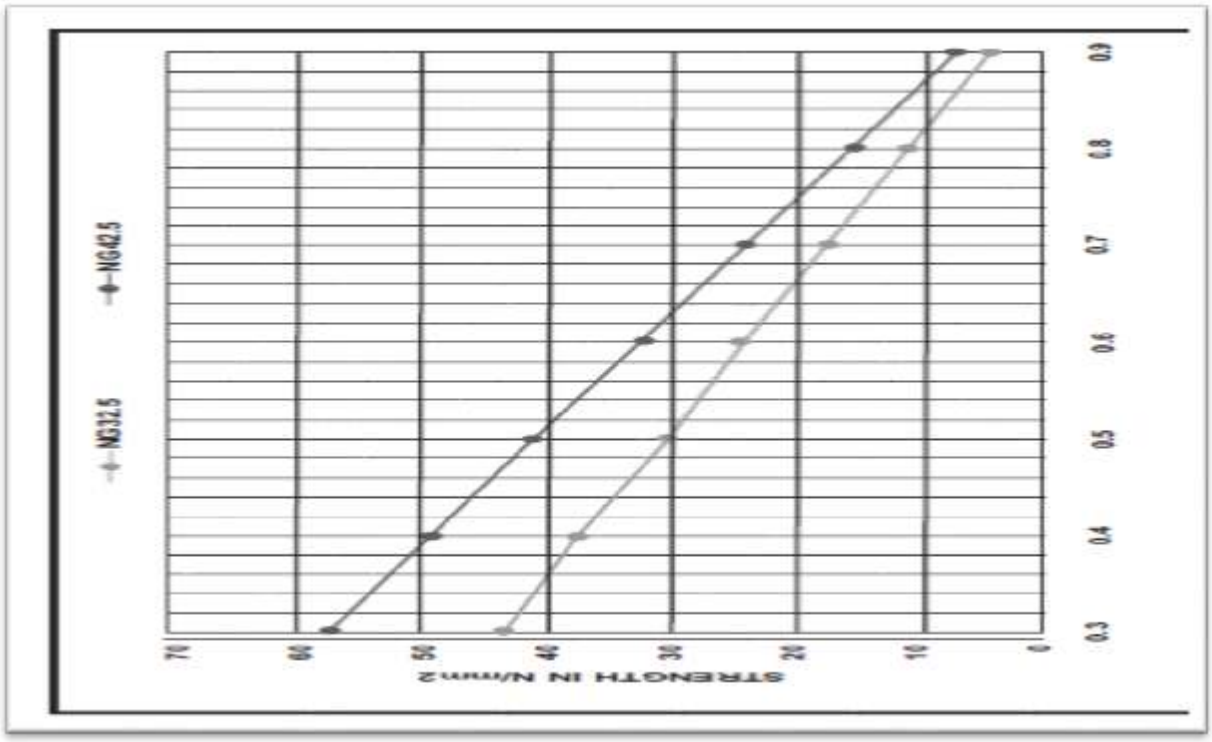

Figure 3.1: Strength versus Water Cement ratio for Nigeria cement (COREN, 2017).
Table 3.1: Relationship between Water Cement Ratio and Mass

	Water-Cement Ratio	
Compressive strength at 28 days (N/mm^2)	Non-air entrained concrete	Air entrained concrete

40	0.42	–	
35	0.47		0.39
30	0.54		0.45
25	0.61		0.52
20	0.69		0.60
15	0.79		0.70

Source; ACI211.1-91 [11].

3.2.3 Determination of water content

In concrete the water content largely depends on the type and maximum size of concrete to give a required workability. The range of slump recommended according to COREN manual was used while the approximate free water contents required to give various levelsof workability according to ACI[14], was also used.

3.2.4 Determination of aggregate content

To determine the total aggregate content, an estimate for density of the fully compacted concrete was knownfrom the tests carried out, a density value of 2400kg/m^{3}was recommended for use for all mixes using normal weight aggregates. The fine and coarse aggregate content are determined by obtaining the proportion of fine aggregate in the total aggregate content.

4.0 RESULTS AND DISCUSSIONS

4.1 Laboratory Results

Fineness modulus is the summation of the cumulative percentage mass retained on sieve 4.75mm to 150µm divide by 100. Fineness modulus of 3 was obtained for the sieve analysis carried out for the fine aggregate. The sieve analysis test is presented on Table 4.1 and the particle size distribution curve is shown on Figure 4.1.

Table 4.1: Sieve Analysis Test for Fine Aggregate

S/N	Sieve size	Mass retained (g)	Percentage mass retained (g)	Cumulative Percentage mass retained (%)	Percentage mass passing (%)
1	12.5mm	-	-	-	100
2	8.0mm	-	-	-	100
3	4.75mm	13.90	2.78	2.78	97.22
4	2.36mm	47.10	9.42	12.20	87.80
5	1.18mm	131.70	26.34	38.54	61.46
6	600µm	134.30	26.86	65.40	34.60
7	300 µm	82.20	16.44	81.84	18.16
8	150 µm	61.70	12.34	94.18	5.82
9	75 µm	4.90	0.98	95.16	4.84

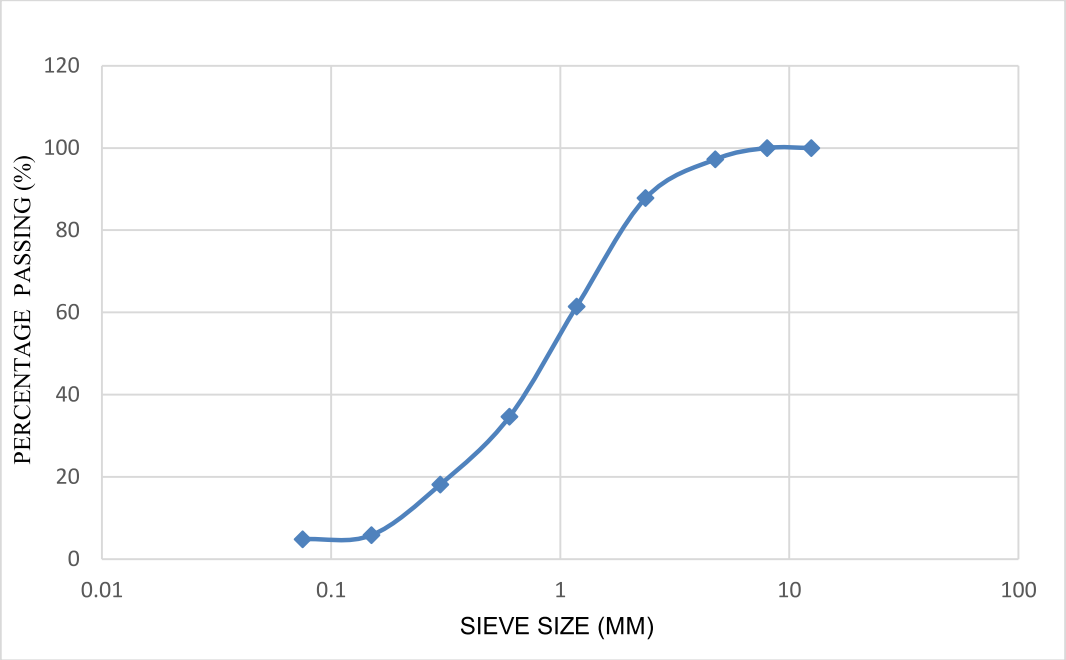

Figure 4.1: Particle size distribution curve

The specific gravity obtained for test carried out for fine and coarse aggregate are 2.67 and 2.68 kg/m^3 respectively according to IS:10262 [16], and it is within the range required for aggregates[15], [16]. The bulk density results obtained for fine aggregate from compacted and uncompacted aggregates are 2.75kg and 2.5kg respectively. While the bulk density results for coarse aggregates (compacted and uncompacted) are 2.71kg and 2.45kg respectively. This is why a concrete that is hardened or stronger than necessary for its intended use is not economical, and one that is not strong enough can be dangerous. The higher the cement content, the greater the tendency of shrinkage cracks.

4.2 Slump Test

4.2.1 COREN:A slump of 120mm was obtained from the mix design carried out which is in the range of 60mm-180mm as recommended in COREN GUIDE for a water content of 235.

4.2.2 ACI:A slump of 140mm was obtained from the mix design carried out which is in the range of 150mm-175mm as recommended in ACI CODE for a water content of 216.

4.3 Compressive Strength

The target mean strength for COREN is 25.52, while for ACI is 25.00 N/mm^2. The strength was determined for 3 days, 7 days and 28 days respectively. There was a rapid increase at 28 days (27.92N/mm^2) [17], [18], which meets up with COREN mix design method, while ACI does not meet with the requirements of ACI mix design method at 28 days. Table 4.2 indicates the compressive strength of concrete cubes obtained for the two mix design methods carried out and Figure 4.2 shows the compressive strength of concrete using ACI and COREN guide.

Table 4.2: Summary of the Compressive Strengths and Mix Proportions

Mix Design Method	Characteristic Strength (N/mm^2)	Target Mean Strength	3days Mean Strength	7days Mean Strength	28days Mean Strength	Mix Proportion
COREN	20	25.52	14.99	19.80	27.92	1:1.5:2.8
ACI	20	25.00	13.12	15.22	23.39	1:2.8:3.1

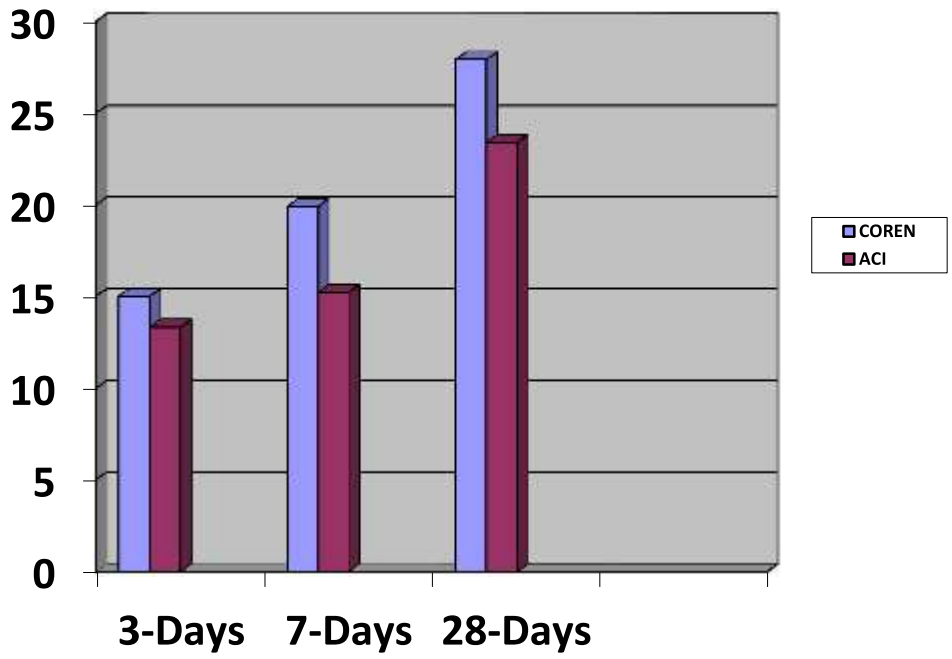

Figure 4.2: Compressive strength of concrete using ACI and COREN guide

4.4 Similarities between COREN and ACI Mix Design Method

COREN and ACI methods of mix design are based on empirical relations that are derived in different countries based on the available local materials within. Tables 3.1 which shows the relationship between water cement ratio and mass and Figure 3.1 graph which shows the relationship between strength and water cement ratio for Nigeria cement are used during the design process and selection of materials through a logical means for the determination of the target mean strength and ingredients.

The determination of cement content of both methods is based on the relationship of two perimeters: W/C and the cement content are derived separately and independently. Workability of both methods is determined using slump test.
Workability is used to measure the degree at which a fresh concrete can flow, this allows for ease of compaction and placing of the concrete. The result obtained shows that COREN and ACI mix proportion are of high workability.

4.5 Differences between COREN and ACI Mix Design Method

The differences between COREN and ACI mix design method is presented on Table 4.3 and Table 4.4. Water-Cement ratio (W/C) in the ACI method is determined with the combination of two parameters: the target strength and the concrete type (air or non-air entrained) which is obtained from Table 3.1 While W/C ratio for COREN is obtained from Figure 3.1. Coarse and fine aggregate content for ACI method is obtained without knowing the absolute volume of the fine aggregate.

Table 4.3: Mix Design Calculated for $1m^3$ of Fresh Concrete

Ingredients	ACI (N/mm^2)	COREN (N/mm^2)
Water(kg)	210.66	224.33
Cement(kg)	305.30	393.50
Fine aggregate(kg)	854.84	590.36
Coarse aggregate(kg)	946.26	1101.1
Water/cement ratio	0.69	0.57

Table 4.4: Analysis of 28-Days Compressive Strength

Target Strength (N/mm^2)	Average Strength (N/mm^2)		Strength Deviation (N/mm^2)	
	ACI	COREN	ACI	COREN
25	23.39	27.92	-1.61	2.91

CONCLUSIONS

This research work was carried out to compare ACI and COREN mix design method using materials of the same properties to determine the strength of concrete cubes cast and cured for 3,7 and 28 days.
The following conclusions were drawn:

1. It was observed that the ACI mix method requires higher water content than COREN mix to be able of have a workable concrete.
2. COREN mix design gives higher strength development than ACI mix.
3. Concrete made using ACI mix design can be of low strength.
4. More quantity of cement is required in the use of COREN as compared to ACI mix.

Therefore, COREN mix design method should be used in the proportioning of concrete mix.

RECOMMENDATIONS

The following recommendations are made:

1) COREN mix design method should be used in the proportioning of concrete mix.
2) Mix design such as USBR Mix design practice, British Mix design Method, and ISI Recommended guidelines IS, should be compared with COREN mix design

REFERENCES

[1] E. Mezie, "Concrete Mix Design Based on COREN Mix Design Manual". https//mycivillinks.com/2021/07/09/concrete-mix-design-based-on-coren-mix-design-manual. 2021.

[2] M. A. Salau, andA. O. Busari, "Effect of Different Coarse Aggregate Sizes on the Strength Characteristics of Laterized Concrete".*2nd International Conference on Innovative Materials,Structures and Technologies* IOP Publishing IOP Conf. Series: Materials Science and Engineering 96 (2015) 012079 doi:10.1088/1757-899X/96/1/012079, 2015.

[3] S.M.Auta,A. Uthman, S. Sadiku, T.Y. Tsado and A. J Shiwua. "Flexural Strength of Reinforced Revi-brated Concrete Beam with Sawdust Ash as a Partial Replacement for Cement". *Construction of Unique Buildings and Structures*,2016, pp. 31-45.

[4] M. Abdulahhi. "Effects of Aggregate Type on Compressive Strength of Concrete". *International Journals of Civil and Structural Engineering.*vol. 2, pp. 791-800, 2013.

[5] C. H. Aginam, C. A. Chidolue and C. Nwakire."Investigating the Effects of Coarse Aggregates Types on the Compressive Strength of Concrete". *International Journal of Engineering Research and Applications, vol. 3,* pp. 40-44, April 2013.

[6] S. A. Hakim,M. K. Jamal, and S. E. Ali, "New Concrete Mix Design Approach". *2nd International Sustainable Building symposium* (ISBS), pp. 367-372, 2015.

[7] C. H. Aginam,S. N. Umenwaliri andC. Nwakire, C. "Influence of Mix Design Methods on the Compressive Strength of Concrete". *Journal of Engineering and Applied Science.* Asian Research Publishing Network (ARPN). 2013, http://www.arpnjournals.com

[8] Council for the Regulation of Engineering in Nigeria (COREN), (2017). "ConcreteMix Design Manual." COREN 2017/016/RC.

[9] K. Deepak, K. Ankush, K. Praveen,and B. Neeraj, "Comparative Study of ACI and BIS Methods ofConcrete Mix Design and Demonstration ofCracking Pattern of Concrete Specimens". *International Journal of Science and Research (IJSR*)ISSN (Online), pp. 2319-7064, 2017.

[10] M. C. Nataraja, and D. Lelin, "Concrete MixProportioning as Per IS 10262:2009 - Comparison withIS 10262:1982 and ACI 211.1-9S".*The Indian ConcreteJournal*.2010.

[11] S. Ravinder,and S. K. Verma, "Comparative Study ofM20 and M25 Grades of Concrete by ACI, DOE and BISMethods of Mix Design Using CrushedAggregate".*International Journal of Scientific Researchand Management (IJSRM),* vol. 5, pp. 6377-6383, 2015.

[12] A. S. Deepa, "Compressive Strength of Concreteusing Different Mix Design Methods".Vol. 4, 7th ed. ISSN - 2249-555, 2014.

[13] A. R. Akeem, A. S. Aliu and J. E. Amaka J.E, "Effect of Curing Methods on Density and Compressive Strength of Concrete". *International Journal of Applied Science and Technology*. vol. 3, pp. 55-64, 2013.

[14] ACI Committee 211, (Re-Approved in 2002), "Standard Practice for Selecting Proportions for Normal, Heavyweight and Mass Concrete". American ConcreteInstitute, USA. Re-approved 2002.

[15] A. M. Neville, "Properties of Concrete Fifth Edition". Pearson Education Limited Edinburgh Gate Harlow Essex CM20 2JE England, 2011.

[16] Bureau of India Standard, "Indian Standard ConcreteMix Proportioning– Guidelines",(First Revision) IS-10262:2009, New Delhi, India

[17] I. L. Aminul, "Mix Design of High-Performance Concrete Materials". *National Institute of Technology, vol.* 14, pp. 429-433, 2013.

[18] A. Annadurai1,and A. Ravichandran, "Development of Mix Design for High Strength Concrete with Admixtures". *Journal of Mechanical and Civil Engineering* (IOSR-JMCE) vol. 10, pp. 22-27, May 2014.